Titre: Title:	A driver model with supervision aspects
Auteur: Author:	Saéd M. Ehsani
Date:	1998
Type:	Mémoire ou thèse / Dissertation or Thesis
Référence: Citation:	Ehsani, S. M. (1998). A driver model with supervision aspects [Thèse de doctorat, École Polytechnique de Montréal]. PolyPublie. https://publications.polymtl.ca/8683/

UNIVERSITÉ DE MONTRÉAL

A DRIVER MODEL WITH SUPERVISION ASPECTS

SAÉD M. EHSANI

DÉPARTEMENT DE GÉNIE MÉCANIQUE

ÉCOLE POLYTECHNIQUE DE MONTRÉAL

THÈSE PRÉSENTÉE EN VUE DE L'OBTENTION

DU DIPLÔME DE PHILOSOPHIAE DOCTOR

(GÉNIE MÉCANIQUE)

JUIN 1998

UNIVERSITÉ DE MONTRÉAL

ÉCOLE POLYTECHNIQUE DE MONTRÉAL

Cette thèse intitulée:

A DRIVER MODEL WITH SUPERVISION ASPECTS

Présenté par: EHSANI Saéd M.

en vue de l'obtention du diplôme de: Philosopiae Doctor

a été dûment acceptée par le jury d'examen constitué de:

M. FORTIN Clément, Ph.D., président

M. GOU Michel, M.Sc.A., membre et directeur de recherche

M. TÉTREAULT Mario, Ph.D., membre et codirecteur de recherche

M. PIEDBOEUF Jean-Claude, Ph.D., membre

M. ROUSSELET Jean, Ph.D., membre

Dedication

In the name of God,
Lord of Life and Wisdom

To my parents,
who educated us through faith and discipline,
by being our examples of love and humanity
and providing us all essential supports.

Acknowledgment

My first appreciation go to professors Michel Gou and Mario Tétreault for their support, their time and the attention that they provided in debating and revising chapters of this thesis as well as the submitted papers. I also owe them a second thanks for the chance they granted me to express my opinion. Of the many people whom I have been associated with at "École Polytechnique de Montréal," I would especially thank professors El-Kébir Boukas, R.M. DeSantis and Ahmad Hemami.

Among all my friends, I would particularly mention Ph.d. students Pascal Bigras for his helpful discussions and technical advices, Jean-Pierre Kenné for the encouragements he gave me, and psychology student Bernadette Masson for her boundless moral support and her selfless assistance.

I add the final thanks to the members of the jury, especially, the president professor Clément Fortin for his positive and comprehensive attitude through the after defense correction process.

Résumé

Dans un Système de transport intelligent (ITS), le développement des lois de commande d'un véhicule qui suit une route sans intervention humaine nécessite la modélisation des comportements d'un conducteur qui sont classés en trois niveaux : Commande, Supervision et Définition.

- La Commande est le niveau le plus bas et sa responsabilité est d'atteindre la vitesse désirée tout en gardant le véhicule à l'intérieur des limites géométriques de la route et sur le trajet désiré. Ce niveau modélise les comportements compensatoires d'un conducteur.
- Certains comportements intelligents du conducteur humain jouent un rôle important dans la conception d'un système de commande fiable et efficace capable de remplacer le conducteur dans sa tâche. Ces types de comportements font partie du niveau de Supervision, un niveau plus élevé, qui supervise certains paramètres critiques et qui définit et modifie les valeurs désirées du niveau de commande si nécessaire.
- L'itinéraire de la route ainsi que la définition des limites géométriques et de la vitesse se font par le niveau de Définition.

Cette thèse porte principalement sur le développement du niveau de commande permettant éventuellement d'intégrer les niveaux supérieurs. Cette recherche nécessite l'étude de la cinématique et de la dynamique des véhicules routiers, ainsi que l'étude des lois de commande du correcteur. Elle comporte trois étapes de développement qui ont fait l'objet de publications dans des revues scientifiques.

La première étape consiste à développer un correcteur non linéaire basé sur un modèle dynamique d'un robot mobile de type véhicule automobile (car-like). Plusieurs travaux ont déjà été réalisés sur la commandabilité des robots mobiles de type omnidirectionnel. En s'inspirant de ces travaux et en faisant ressortir la différence entre la cinématique de ces deux types de robot, la méthode de la linéarisation par retour d'états a été appliquée, tout en assurant la stabilité de la dynamique interne. Cette dynamique inobservable existe pour tous les systèmes mobiles ayant un contact rigide et sans glissement entre la surface de roulement et la roue (centre instantané de la vitesse nulle). Dans cette étape, les sorties du système de commande sont la vitesse du robot et son rayon de courbure.

La deuxième étape consiste à améliorer le contrôle latéral du robot, c'est-à-dire commander la position (les coordonnées X-Y) du robot dans un système de référence cartésien. Contrairement aux robots omnidirectionnels, la réalisation de cette étape est impossible pour un point de commande attaché au corps principal du robot de type véhicule automobile. Ce problème fut contourné en commandant la position d'un point attaché aux roues de direction. Comme à l'étape précédente, ce deuxième système de commande est basé sur un modèle

dynamique non linéaire du véhicule et développé avec la méthode de linéarisation par retour d'états.

Dans les méthodes classiques de commande des robots, les entrées du système sont des trajectoires désirées (les valeurs désirées en fonction du temps). L'utilisation de cette méthode pour développer le niveau de commande complique la réalisation du niveau de supervision puisque la modification des valeurs désirées en cours d'exécution s'avère difficile étant donné la nécessité de recalculer toutes les trajectoires désirées. La troisième partie de ce travail consiste donc à développer un système de commande où la vitesse du robot est commandée indépendamment de sa déviation latérale par rapport à un trajet désiré. En définissant la déviation latérale comme étant la distance entre la position d'un point du véhicule et son trajet désiré, une erreur latérale dépendant seulement des caractéristiques géométriques du trajet désiré est obtenue. Avec cette nouvelle approche, les entrées du niveau de commande ne sont plus des trajectoires. Cela rend la modification des valeurs désirées plus facile et permet éventuellement l'intégration des aspects intelligents d'un conducteur humain dans notre modèle de conducteur qui est l'élément de base d'un ITS.

Abstract

In an Intelligent Transport System, for a vehicle which follows a path without the presence of a human driver, the control law development requires the modeling of the human driver behavior. A driver behavior are classified in three different levels: Control, Supervision, and Definition.

- Control level is the lowest level with the responsibility of reaching the desired speed and maintaining the vehicle on the path. This level models driver compensatory reactions.
- Some of the driver intelligent activities which play a role in the modeling of the driver behavior are realized at the Supervision level. This level is placed above the control level and it defines and modifies the control level desired values.
- The itinerary, road geometric limits and speed limits are defined at the Definition level.

In this thesis the focus is on the control law developments for the control level, which requires an analysis on the kinematics and dynamics of ground vehicles. The research has been carried out in three steps which resulted in three publications given in appendices A, B and C.

The first step consists in developing a control law based on a dynamic model of car-like mobile robots. The controllability of omnidirectional mobile robots has been vastly studied before. Taking advantage of these studies, the kinematic differences between these two mobile robot families have been pointed out. Input/Output Feedback Linearization (I/OFL) method has been used to develop the first control law commanding a car-like robot speed and its instantaneous curvature.

In the second step, the objective is to complete the vehicle lateral control. But, the I/OFL cannot be realized for the Cartesian coordinates of any point attached to the vehicle main body, however it is possible for a point attached to the front steerable tire. Similar to the first step, the nonlinear dynamic model has been used for the controller design.

Conventionally, the control of robots is based on inputs of desired trajectories, which are functions of time. The approach is not a convenient choice for the structure of our control level. Hence, in the third step, the lateral control law has been developed using a geometric lateral-offset as the system input instead of the conventional desired trajectories. This input removes the time dependence of lateral inputs and the vehicle speed control becomes independent from the vehicle lateral control. As a result, the supervision level can modify the control level inputs (desired values) which is an essential element for the integration of the driver intelligent activities at the supervision level.

Condensé en français

Contexte

Dans un système véhicule/conducteur/route, le véhicule automobile et la route représentent les deux éléments construits par les êtres humains. Le véhicule est un système dynamique à plusieurs degrés de liberté avec des contraintes géométriques (holonomiques) et de vitesse (non holonomiques). Une route est un trajet quasi planaire défini par des caractéristiques géométriques. Le conducteur humain, qui doit guider le véhicule entre les limites de la route, se présente comme l'élément le plus imprévisible de ce système. Le conducteur a une responsabilité très importante quant à la sécurité routière. Comme les véhicules d'aujourd'hui sont mieux conçus, les erreurs humaines demeurent la première cause des accidents mortels dans notre système de transport. Cette réalité nous amène à considérer le remplacement partiel ou complet du conducteur par un système de pilotage automatique. En plus d'améliorer la sécurité routière, le but de la recherche sur un ITS (Intelligent Transport System) est d'augmenter la productivité du réseau de transport.

Les comportements d'un conducteur sont une combinaison de ses réactions compensatoires et de ses activités intelligentes. Les corrections de la déviation latérale et de l'erreur sur la vitesse sont catégorisées parmi les réactions compensatoires d'un conducteur. La tendance actuelle est de modéliser ces types de réactions par des correcteurs classiques qui ont des

performances et une fiabilité reconnues pour la commande des systèmes dynamiques linéaires et non linéaires. Toutefois, le manque de flexibilité de leur structure complique leur application dans un système véhicule/conducteur/route. La littérature montre que certaines des activités intelligentes d'un conducteur humain telles l'adaptation à la dynamique de son véhicule, l'anticipation sur la forme future de la route et la prédiction de l'état futur de son véhicule jouent un rôle important dans la correction de la déviation latérale et la commande de la vitesse du véhicule.

La réalisation d'un modèle de conducteur qui considère les réactions compensatoires ainsi que les activités intelligentes d'un conducteur humain, nécessite une division des tâches en trois niveaux : commande, supervision et définition. Le niveau de commande réalise les réaction compensatoires d'un conducteur et il a la responsabilité d'annuler la déviation latérale et l'erreur sur la vitesse. Certains auteurs ont combiné les activités intelligentes du conducteur avec ses réactions compensatoires dans un seul correcteur. Ils ont ainsi obtenu des correcteurs complexes avec certaines limites d'application.

Le niveau de supervision vérifie certains paramètres critiques et définit les entrées du niveau de commande. Lorsqu'un conducteur suit un chemin, il analyse la configuration (position et orientation) de son véhicule par rapport à la route et prend des décisions en utilisant ses connaissances et son expérience. Dans le but de maintenir la validité de son raisonnement, le conducteur supervise les conditions ayant menées à une prise de décision. Il doit par conséquent adapter ses décisions avec le changement des conditions. Une façon de réaliser

cette adaptation est de modifier les valeurs désirées du niveau de commande avec le niveau de supervision. Ce niveau réalise certaines activités intelligentes du conducteur et il active seulement si une des valeurs désirées requiert une modification ou un des paramètres sous sa supervision atteint sa valeur critique. Le comportement d'un tel niveau de supervision est discret.

Le niveau de Définition choisit l'itinéraire et définit les limites géométriques de la route de même que la vitesse maximale.

L'objectif principal de cette recherche est de concevoir un système de commande continu qui est assez robuste aux variations discontinues et non fréquentes de ses valeurs désirées. Ce type de système de commande (correcteur) sera compatible avec le niveau de supervision et il permettra une intégration facile des caractéristiques intelligentes d'un conducteur. La démarche pour atteindre cet objectif a été réalisé en trois étapes. La première étape consiste à étudier la cinématique et à développer un nouveau modèle dynamique des robots mobiles de type véhicule automobile de même qu'à concevoir un correcteur avec la méthode de la linéarisation par retour d'états. Le développement d'un système de commande qui corrige la position de ce type de robot représente la seconde partie de cette recherche. La troisième étape consiste à commander la vitesse du robot indépendamment de sa déviation latérale, grâce à une nouvelle définition géométrique de cette déviation. Ces trois étapes sont détaillées respectivement dans les annexes A, B et C.

Correcteur adaptés aux caractéristiques d'un robot de type véhicule automobile

Cette section introduit les deux premiers articles, soit "Kinematics, Dynamics and Control of a Car-like Mobile Robot" présenté à l'annexe A et, "Looking Ahead Path-tracking of a Car-like Mobile Robot" fourni à l'annexe B. Pour développer le correcteur du niveau de commande, on a besoin d'un modèle dynamique simplifié du véhicule. Un modèle complet, qui pourrait prendre en compte presque tous les comportements d'un véhicule, est trop complexe pour être utilisé dans la conception d'un correcteur. Un modèle plus adéquat retient seulement les mouvements planaires du véhicule qui influencent significativement la commande latérale et la correction de la vitesse du véhicule.

Dans le contexte d'un ITS, le modèle dynamique le plus approprié pour la conception d'un système de commande est celui d'un robot mobile de type véhicule automobile ayant des caractéristiques similaires aux voitures de tourisme d'aujourd'hui. Le modèle doit représenter un véhicule dirigé par une roue avant et pouvant être entraîné par une traction avant ou par une propulsion arrière. Dans la littérature, il existe aussi des robots mobiles de type omnidirectionnel qui ont les roues arrières actionnées indépendamment. Ce type de robot est conçu pour avoir une bonne manoeuvrabilité. Dans le contexte des ateliers flexibles (FMS), la commande de ce type de robot a été beaucoup étudiée. Ces travaux nous ont amené à étudier les comportements cinématique et dynamique de ces deux types de robots dans le but de trouver les différences qui influencent la conception du système de commande (annexe

A). Pour l'étude de la cinématique, le lien entre les vitesses cartésiennes (espace de la tâche) et les deux vitesses de l'espace d'articulation est défini par la matrice jacobienne.

Pour un robot mobile de type véhicule automobile, la variation de l'angle de direction, qui est une des vitesses d'articulation, n'influence pas les vitesses angulaire et linéaire du corps principal du robot. Cette cinématique restreinte produit une colonne de zéro dans la matrice jacobienne. Ce problème de singularité n'existe pas dans le cas des robots mobiles de type omnidirectionnel puisque la vitesse de chaque roue influence la vitesse angulaire ainsi que la vitesse linéaire du corps principal du véhicule dans l'espace cartésien.

Connaissant les différences entre la cinématique des deux types de robots, un modèle dynamique non linéaire a été développé pour un robot mobile de type véhicule automobile. Ce modèle est non linéaire et simule les comportements dynamiques importants d'un véhicule dans ces mouvement planaires. Il reproduit les effets d'inerties et l'accélération centrifuge ainsi que le couplage entre la dynamique de la direction et celle de la traction (annexe A) ou de la propulsion (annexe C). Ce modèle dynamique a été utilisé comme base pour la conception des systèmes de commande non linéaires de tous mes travaux. Les entrées de ce modèle dynamique sont les couples de traction et de direction.

À l'annexe A, tout comme pour mes autres travaux, le système de commande est réalisé en utilisant la méthode classique de linéarisation par retour d'états. Les contraintes non holonomiques étant une partie inséparable d'un système mobile sans glissement, la

dynamique des contraintes n'est pas observable. L'étude sur la stabilité de cette dynamique interne est nécessaire à la conception d'un correcteur non linéaire basé sur cette méthode.

Dans le développement de notre premier système de commande, la vitesse du véhicule et le rayon de courbure instantané du robot ont été choisis comme les sorties commandées. Avec ces sorties, la vitesse du véhicule est commandée directement, et le problème de singularité dans la matrice jacobienne est éliminé. Les principales contributions dans cette étape sont le développement d'un modèle dynamique non linéaire avec les caractéristiques citées et la conception d'un système de commande invariant dans le temps pour un robot mobile de type véhicule automobile qui assure la stabilité de la dynamique interne et qui réalise le contrôle longitudinal (vitesse) du véhicule. Les détails mathématiques et les résultats de simulation pour cette partie de travail sont donnés dans l'article présenté à l'annexe A.

Ce premier système de commande ne fournit pas toutes les performances désirées sur le niveau de commande de notre modèle de conducteur. En contrôlant le rayon de courbure, on commande indirectement l'orientation du véhicule. Toutefois, sa position dans un système de référence cartésien n'est pas commandée. Advenant une perturbation sur la position du robot, le système de commande est incapable d'éliminer la déviation latérale.

L'objectif du second article (annexe B) est d'éviter ce problème en commandant la position du robot dans un système de référence newtonien. La principale contribution scientifique de ce travail est le développement d'un correcteur qui permet de commander les coordonnés

cartésiennes d'un robot de type véhicule automobile, selon un système de référence newtonien. Pour éviter le problème de singularité, on commande les coordonnés X-Y d'un point à une certaine distance de l'avant du véhicule et qui se déplace avec les roues de direction. En contrôlant les variations des coordonnés cartésiennes de ce point de commande, la dérivée de l'orientation du véhicule est également commandée étant donné la présence des contraintes non holonomiques. Les détails mathématiques et les résultats de simulation sont donnés dans l'article présenté à l'annexe B.

Les deux approches proposées précédemment comportent certains avantages et inconvénients. La première approche a l'avantage de commander la vitesse du véhicule d'une façon indépendante. Cela facilite l'intégration des aspects de supervision, mais la commande latérale n'est pas complète. Dans la deuxième approche, la position du véhicule est bien contrôlée, mais le système ne commande pas directement la vitesse du véhicule. Il est difficile de réunir ces deux avantages dans un seul système de commande sans être obligé de poser des contraintes telle la linéarité du trajet. Pour ne pas rendre trop complexe la structure du système de commande, nous avons choisi de garder le même nombre d'entrées et de sorties. Puisque le véhicule possède deux entrées et qu'il est préférable de commander indépendamment la vitesse du véhicule, la commande latérale doit être réalisée par un seul paramètre de sortie n'influençant pas la vitesse du véhicule.

Conception d'un système de commande avec une déviation latérale géométrique

Dans un système de transport intelligent, l'objectif principal de commande est la poursuite d'un trajet géométrique (garder le véhicule sur la route) à une vitesse désirée. La modification de cette vitesse ne dépend pas seulement de la position du véhicule sur ce trajet. Elle dépend aussi des conditions de la route, le trafic, le type de véhicule, l'accélération latérale du véhicule, etc. Cela justifie le besoin de commander la vitesse indépendamment de la position du véhicule. Dans les deux premières approches, les entrées du système sont des trajectoires désirées qui représentent le trajet désiré en fonction du temps. La responsabilité du système de commande est donc de suivre une position donnée à chaque instant. L'utilisation d'une trajectoire comme entrée du système amène une dépendance entre la commande de la vitesse du véhicule et la correction de la position.

Pour éviter cette dépendance, cette thèse propose une commande latérale qui corrige une erreur latérale géométrique obtenue par la projection de la position du véhicule sur le trajet (annexe C). Contrairement aux approches classiques utilisant des trajectoires, dans le système de commande basé sur une erreur latérale géométrique, l'entrée de la correction latérale est indépendante du temps. Cette nouvelle approche sépare la commande de la vitesse de la correction de l'erreur latérale, et facilite l'intégration des activités intelligentes d'un conducteur à l'intérieur du niveau de supervision. Cet aspect géométrique du système de commande est une contribution scientifique importante et intéressante dans un ITS.

Une interprétation intuitive peut clarifier l'idée du correcteur géométrique par rapport aux systèmes de commande basés sur des trajectoires désirées. La stratégie de commande par trajectoire peut être comparée à la poursuite d'un véhicule virtuel qui suit un trajet à une vitesse donnée. Dans cette stratégie, si le robot mobile est en arrière du véhicule virtuel tout en étant sur le trajet désiré, le système de commande, qui compare la position instantanée du robot avec celle du véhicule virtuel, interprète cette distance comme une erreur de position et envoie une commande d'accélération pour annuler l'erreur. Cette commande d'accélération produit une variation de la vitesse. Si l'objectif est de rester entre les limites de la route à une vitesse désirée, cette variation sera interprétée comme une erreur de vitesse. Ainsi les deux parties du système de commande (correcteur latéral basé sur une trajectoire désirée et correcteur de vitesse) agissent de façon contradictoire. Par contre, dans le concept d'un correcteur avec une déviation géométrique, cette erreur ne se génère pas puisque l'erreur latérale sera une distance entre la position actuelle du robot et le trajet désiré. Ainsi, il n'y aura pas de contradiction entre les deux parties du système de commande.

Le système de commande géométrique ne requiert plus une génération de trajectoires en fonction du temps. Cela allège la structure du système de commande, enlève la réaction contradictoire à l'intérieur du correcteur et permet de commander indépendamment la vitesse et l'erreur latérale. Les détails mathématiques, la projection géométrique et les résultats de simulation sont donnés dans l'article scientifique donné à l'annexe C. Ce dernier système de commande offre les caractéristiques recherchées qui permettent d'intégrer les aspects de supervision à un modèle de conducteur.

Table of Contents

List of Figures

List of Principal Symbols

n_i : unite vectors of the Newtonian reference frame N.

a_i : unite vectors of the reference frame A presenting the principal axis of inertia.

b_i : unite vectors of the reference frame attached to the massless body B.

c_i : unite vectors presenting the front virtual-tire principal axis of inertia (body C).

d_i : unite vectors presenting the rear virtual-tire principal axis of inertia (body D).

q_i : i^{th} generalized coordinates of the car-like mobile robot in figure 3.1.

C_r : car-like mobile robot instantaneous pivot center.

R^* : car-like mobile robot instantaneous radius of curvature.

T_{ab}, T_1 : torque applied from body A to body B, the 1^{st} degree of freedom (steering) torque.

T_{bc}, T_2 : torque applied from body B to body C, the 2^{nd} degree of freedom (steering) torque.

e_1 : geometric lateral-offset.

e_1^A : geometric lateral-offset from the straight line segment of the desired path.

e_1^B : geometric lateral-offset from the circular segment of the desired path.

e_2 : speed error

x_i : state variables

t : vector of steering and traction torques, T_1 and T_2, respectively.

Z^{-1} : inverse of decoupling matrix.

v : vector of linear commands

ψ : vector of nonlinear terms

List of Abbreviations

ITS	: Intelligent Transport System
IVHS	: Intelligent Vehicle Highway System
I/OFL	: Input/Output Feedback Linearization
FMS	: Flexible Manufacturing System
FDW	: Front Wheel Drive
RWD	: Rear Wheel Drive
AWD	: All Wheel Drive
AVCS	: Advanced Vehicle Control System
OCM	: Optimal Control Model
FSLQ	: Frequency Shaped Linear Quadratic
c.g.	: center of gravity
d.o.f.'s	: degrees of freedom

List of Appendices

Introduction

Research on the Vehicle/Pilot/Environment system consists of a vast variety of concepts and covers a great amount of works from different branches of science and engineering. The word vehicle can address any mobile system which has one or several degrees of freedom (d.o.f.'s). Here, the vehicle is a Front Wheel Drive (FWD), a Rear Wheel Drive (RWD) or an All Wheel Drive (4WD) Car, the pilot is a human driver, and the environment is a road, thus, our working frame becomes a Car/Driver/Road system. Both cars and roads are designed and built by humans and usually have invariant and predictable characteristics, while the driver behavior are affected by many factors such as fatigue, age, experience, intelligence, etc. These special characteristics, of a human driver, portrays him as the unpredictable element of the Car/Driver/Road system, and also as the cause of a majority of fatal accidents. In order to increase the safety of the surface transportation system, the Advanced Vehicle Control Systems (AVCS) is the research branch that seeks to increase the driver perception of his environment, for example, detecting obstacles in vehicle blind spots and warning the driver. This branch aims to equip vehicles with devices or systems to provide a safer transportation.

Although vehicles are better equipped and drivers have more complete driving courses, the human driver is still the first cause of most fatal accidents. This bitter reality enhance the necessity of understanding the driver control behavior in order to design a sort of intelligent

autopilot system which may replace the human driver control responsibilities. Applying this advanced technology to the operation of the surface transportation systems, aims to, improve transportation productivity, enhance road safety, maximize the use of existing roads and reduce adverse environmental effects. Hence, research toward an Intelligent Transportation System (ITS), in particular an Intelligent Vehicle Highway System (IVHS), is among the major initiatives of government, industry and academia.

I.1 Human Driver Compensatory Reactions

Since the goal of this research is to find a Driver Model which can model a human driver behavior during a driving task, the first step is to understand how the driver makes decisions when he[1] is driving his car on a road. Thus, it is important to understand how an experienced driver selects the path and modifies the vehicle speed on the road. Driver's intelligent appears through the decision making process toward setting the desired values, i.e. driver receives information from environment (ex. weather and road condition, the road turns, etc.) as well as from his vehicle (ex. vehicle speed, dashboard information, noises, vibrations, etc.). By analyzing these information, an experienced driver defines the path to follow (the desired path) and chooses the appropriate speed (desired speed). Driver compensatory reactions or the driver automatic reactions are defined to envelop the traction and steering commands that he performs to maintain the vehicle on the desired path and to achieving and

[1] "Him" is used here for simplicity of writing and addresses both sexes.

stay on the desired speed. Meanwhile, he keeps supervising these reactions, what gives him the ability of modifying the previously defined desired values. If there is any change in the conditions under which the desired values are defined or if any of supervised parameters such as lateral acceleration approaches their critical values, the experienced driver adapts his driving pattern to this new condition.

I.2 Driver Intelligence and Path Tracking (Supervision)

Path tracking is the battery of the driver compensatory reactions in order to cancel the error between the controlled parameters and the associated desired values. Our tendency is to model these reactions by recent servo regulators which have shown their performance and their reliability on the control of many linear or nonlinear dynamic systems. Taking advantage of the power of modern controllers, they can well simulate the drivers compensatory reactions, indeed, they can model the tasks of the control level. However, their need to the desired trajectories, as the inputs time-dependent functions, limits their direct application to this concept, i.e. the car/driver/road system.

Previous work in this field reveals that some of the driver's intelligent activities play a role in the lateral and speed control of vehicles. Driver's adaptation to the vehicle dynamics and road condition, driver's anticipation on the future road turns, and driver's prediction of the future state of the vehicle are frequently discussed in the literature. When a driver is

following a path, he uses his intelligence to supervise his driving manner, in fact, a human driver is not just an error compensator he is an intelligent path tracker.

A human driver makes his decisions by analyzing the situation using his knowledge and his experience. Even after the decision is made, an intelligent driver supervises the condition under which the decision has been made in order to maintain his decision validity. If the condition is changed, the given decision, i.e. the chosen desired values, may not be valid anymore and must be modified for the new condition. The supervision can be either a preventive action or a global verification of conditions.

The place of driver intelligent activities in the existing driver models has not yet been defined. Some authors tried to integrate driver intelligent activities and compensatory reactions in one controller using the classical theory of linear or nonlinear control but the result was controllers with complex mathematical structure even for simple kinematic vehicle models (Peng et al., 1989). Some others defined the control problem only by driver compensatory reactions without considering driver intelligent activities. Anyhow, we also believe that driver intelligent activities should be modeled in order to have a complete driver model, but it should be placed on a higher level than the compensatory reactions. The supervision level modifies the desired values for the control level and requires the compatibility of this level, in which driver compensatory reactions are modeled, with the supervision level.

A simple example can show the necessity of having a supervision level in the structure of the proposed driver model with supervision aspects. Let's assume that in the presence of a good visibility and normal road condition, a driver is guiding his vehicle between the geometrical limits of a road. Suddenly there is a change in an environmental condition which has been under supervision during the control execution; for example rain starts falling. An experienced driver knows intuitively that under this new condition a high lateral acceleration may cause the vehicle to skid. The preventive reaction of an experienced driver is thus to reduce the car speed, (modification of the desired speed). Besides, because of slippery road conditions, the driver becomes more conscious of his lateral steering commands. In other word, for the same path tracking the driver defines a new driving pattern by modifying his speed and his manner of steering.

In this example, road condition and visibility are changed, none of them can be a direct input of the control level. Hence, supervision is done on different parameters than outputs of the control level by which simulates driver compensatory reactions. In this example, the driver new decisions would be respectively speed reduction and/or performing smoother steering commands to stay within the road adhesion limit and thus far from skidding risk. This new decision can be realized by changes in the desired speed and the control level settling time. From this example it is seen that although the driver does not control the lateral acceleration explicitly, he supervises it very carefully.

I.3 From Human Decision Making to Design of Control Level

In the above explanations, two different levels have been introduced in order to model the human driver decision making process. A control level that realizes driver compensatory reactions and a supervision level that supervises parameters and applies the modification on the desired values if it is necessary. The third one, a Definition level must also be added also to solve the navigation problem.

Figure 1.1 shows how a driver makes his decisions in a Car/Driver/Road system (Lefebre et al., 1992), (Saridis, 1985). The definition level carries out a general analysis of all receiving information and defines the itinerary with the general limits of the roads and speed limits and send them to the supervision level. Off-line decisions before a driver starts moving his vehicle, i.e. road navigation, are made in this level. The selection and determination of exact desired path and speed, the critical values for parameters under supervision and the obstacle avoidance are examples of supervision level responsibilities. This level modifies the desired values if need be, which means that it has a discontinuous nature. The control level receives the desired values (path and speed) from supervision level and the actual values from the vehicle. The responsibility of the control level is to cancel the lateral-offset of the vehicle from the desired path and to ensure that the vehicle speed is as close as possible to its desired value in a continuous manner.

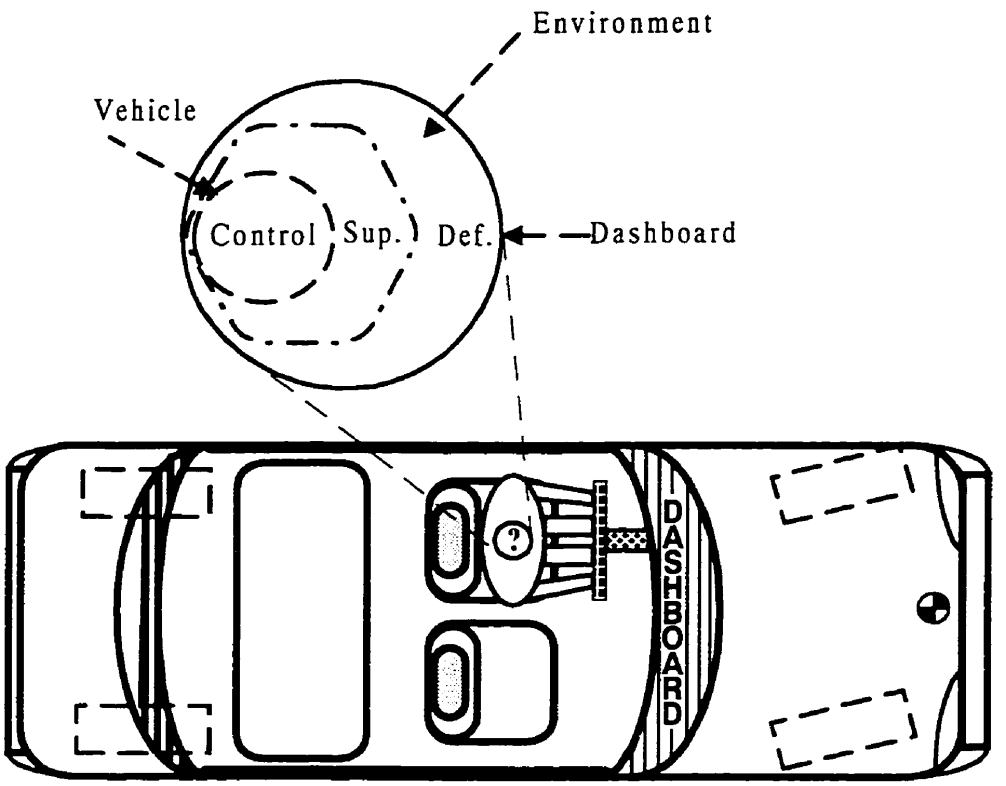

Figure 1.1 Decision making levels: Definition, Supervision and Control.

Our main research objective is to develop a driver model which is able to reproduce, as closely as possible, the behavior of a human driver. Our focus is on the control level design considering its essential compatibilities with the supervision level. Since the vehicle dynamics is a continuous system, the goal is to achieve a continuous control level which is robust enough to discontinuous but non frequent changes of the desired values. This objective is realized in three steps:

A) the development of a compact vehicle dynamic model with the state space representation, which includes the generally neglected steering dynamics, in addition with the realization of an independent speed control which ensures the exponential convergence of errors to zero and the stability of the so called internal dynamics.

B) the design of a zero-error tracker which is based on the developed vehicle dynamic model and which has a simple and time-invariant linear structure after the application of the Input/Output Feedback linearization on a steerable virtual point in front of the vehicle,

C) the design of a geometric lateral-offset tracker and an independent speed controller to be used in the control level and in order to form a compatible structure with both discontinuous commands of the supervision level and the continuous feedbacks of the vehicle dynamics. In this scheme, the conventional time-dependent desired trajectories can be replace by the geometric characteristics of the path and the modifiable desired speed at any time.

The theoretical explanations and simulation results of these steps are presented respectively in the papers of appendices A, B and C. In the next chapter, a literature survey is carried out on the driver models. Chapter 4 presents the synthesis of these three paper results and explains why the research has been conducted towards them. The papers given in appendices contains the essential details and the continuity between them is explained in chapter 4. Chapter 6 concludes on the results of the research and suggests some future work.

Chapter 1

Literature Survey

To realize the research objective, the literature survey has been done for vehicle models, driver models and controllers which partially fulfill driver control behavior. The general literature survey here describes the history and the diversity of approaches. Also a technical literature survey is performed at each of the appendices and on the specific subject for which a paper has been submitted.

1.1 Vehicle Models

This section presents a review of complete vehicle models in which vehicle dynamics with several d.o.f.'s, mechanics of tire pneumatics, vehicle suspension characteristics, etc., has been discussed. The complete vehicle models cannot be used for feedback control design because of their time-consuming calculation and their need for a huge amount of information. Although, from a control-point of view, such complete models are too complex to be useful in the design of an efficient controller, they present an overview of ground vehicle characteristics, measurable and non measurable variables as well as the complexity of the dynamic system on which the driver model should be applied.

General principles of non guided ground vehicles have been discussed in (Ellis, 1969) and (Wong, 1978). As mentioned by Wong, the interaction between the vehicle and the ground is important to the study of vehicle performance, handling, and ride, because aside from aerodynamic inputs, other forces and moments affecting the motion of ground vehicles are applied through the tire contact patch. Some theoretical and experimental studies on the dynamic properties of tires have been shown in (Clark, 1981), and a model to be used in vehicle dynamic handling has been given in (Bakker et al., 1984). Readers who are interested to this subject are also addressed to literatures such as (Mastinu et al., 1992) and (Szostak et al., 1986). Anyhow, studying the tire dynamics is beyond our objective, i.e. modeling the human driver reactions and its supervision aspect.

Allen et al. (Allen et al., 1986) have presented a modeling procedures to identify the directional handling characteristics of ground vehicles over the full maneuvering range. The authors have measured many dynamic responses of the vehicles to show the usefulness of the method for a variety of possible inputs, such as sinusoidal steer frequency sweep in turn. In another work (Allen et al., 1987), they have presented a detailed nonlinear-time-domain dynamic model and a considerable effort was devoted to ensure its validity. Interesting factors of this model are the use of a complete pneumatic tire model and the study of vehicle transient responses to the large inputs which take the vehicle into the limit performance maneuvering regions. Significant insight can be gained into the consequence of the tire force saturation which is a base for evaluating performance limits.

Obviously, the role of the suspension design is important for the vehicle dynamic transient response, especially, when cornering and braking acceleration are considered in maneuvers. The effect of the suspension design on the stability has been studied in (Naleczz 1987) on a model similar to the one used in (Allen et al., 1987). A computer code generator is used in (Sayers) to compare the simulation run speed of the above model to some other existing vehicle models, models with four to ten d.o.f.'s. It is concluded that the simulation responses of the six d.o.f.'s models is close enough to the one with the ten d.o.f.'s and the vehicle model dynamic responses does not change significantly by adding more d.o.f.'s.

Based on simplified vehicle models with linear equations of motions, vehicle lateral and longitudinal behavior during normal driving (Cornell, 1968), (McRuer et al., 1997), (Takasaki et al., 1977) or on emergency avoidance maneuvers (Billing, 1977), (Maeda et al., 1977) have been previously studied and controllers have been designed from these linear models. Major disadvantages of these simplified linear models is that they cannot model coupling effects between traction and steering dynamics.

1.2 History of Driver Models

This section introduces a survey on efforts carried out by pioneers to model human driver behavior. They defined different terminologies to explain their approaches. Let us define a Driving Task as one complete movement from one permanent stable state to another state such as a complete lane change or a left-hand turn. Although there is no clear distinction

between drive lateral and longitudinal control behavior, originally this distinction came from the driver efforts for controlling his vehicle perpendicular or along its longitudinal axis, respectively. The study of longitudinal control behavior of a driver leads generally to the problem of vehicle speed control (Fenton et al., 1991), (Fenton et al., 1974), (Garrott et al., 1982). Meanwhile, the basic purpose of vehicle lateral control has been elaborated in (McRuer et al., 1997) as the selection of the appropriate pathway (desired path), establishing and maintaining of the car on the specified pathway even in the presence of disturbance and, reducing path error (lateral-offset) in a stable, well damped rapidly responding manner. The problem of vehicle lateral control has been discussed at length in the literature. These works, for modeling driver lateral control reactions, can be summarized into the classes of: quasi-linear models, feedback models with feed forward, preview-predictor models, and models with nonlinear feedback. The former class may be used for the existing vehicle longitudinal (speed) control as well.

1.2.1 Quasi-Linear Models

Perhaps, the first series of driver models were the crossover pilot models (McRuer et al., 1965), (McRuer et al., 1974), (McRuer et al., 1968) which present trials for understanding driver compensatory reactions. These models are based on the classical theory of linear systems to which human delay, which is a non linear function, has been added. The crossover models (figure 2.1) are based on the fact that the human pilot has the capability of adjusting or equalizing his behavior so that the close-loop characteristics fulfill the basic conditions

required for any good feedback control system. Then, the describing function of the open-loop driver/vehicle system is given as:

$$Y_{ol}(j\omega) = Y_p Y_c \approx \frac{\omega_c e^{-j\omega\tau_e}}{j\omega}$$

where

Y_p and Y_c : are respectively the pilot and vehicle transfer functions.

ω_c : is the crossover frequency.

τ_e : is the human delay.

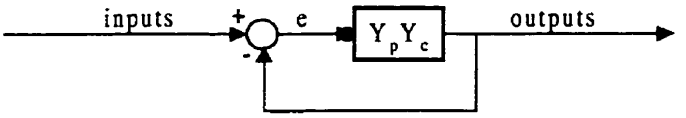

Figure 2.1 Crossover models of a pilot/car system

This quasi-linear model is matched with the experimental data around the crossover frequency except for a discrepancy in the low-frequency phase match. This discrepancy has almost no effect in the performance and stability of the predicted pilot/vehicle model. Here, like in every tracking problem, the art of optimal control has been employed to form the Optimal Control Models (OCM). Hess (Hess, 1987) compared the performance of an OCM to the simple crossover models and concluded that both model results are quite acceptable especially around the important crossover region.

McRuer (McRuer et al., 1968) explains the describing function $|Y_pY_c|$ as follows: "The describing function is written in terms of the frequency operator ($j\omega$) instead of the general Laplace variable ($s = \sigma - j\omega$) to emphasize that it is strictly valid only in the frequency domain with continuous inputs, and should not be used to compute the system response to a deterministic input such as a step." This is an obstacle in the perspective driver model application. Also, the above quasi-linear models are helpful in studying driver compensatory reactions in vehicle lateral control and are not suitable for modeling human driver behavior because the given describing function includes both driver and vehicle models.

1.2.2 Feedback Models with Feed-forward

The literature supposes that a human driver performs his driving task using both guidance and control compensatory reactions. Practically, these reactions are joined together and it is hard to find a clear distinction between them. However, Donges (Donge, 1978) and McRuer et al. (McRuer et al., 1997) modeled them in two respective submodels. They defined the guidance as the driver first rapid reaction when he is in front of a driving task, and the control as the following reactions that he performs to correct the remaining errors. This idea formed a class of driver steering model with one feedforward and one or several feedbacks.

The general characteristics of models in this class is that major driver commands are realized by a feed-forward and added to the feedback commands which has the responsibility of

stabilizing the vehicle on the pre-defined trajectory. Hence, the driver guidance and control reactions are carried out by two respective submodels. The guidance submodel generates a feed-forward command that varies if there is any change in the desired trajectory. If the vehicle dynamics is negligible and if everything is ideal, this command is sufficient to guide the vehicle through the road. Since there is no ideal case, the control submodel is previewed to cancel the residual errors after applying the guidance command. In figure 2.2, Donges (Donge, 1978) incorporated driver anticipation, which is one of his intelligent activities, in the guidance submodel by adding a lead to the feed-forward command.

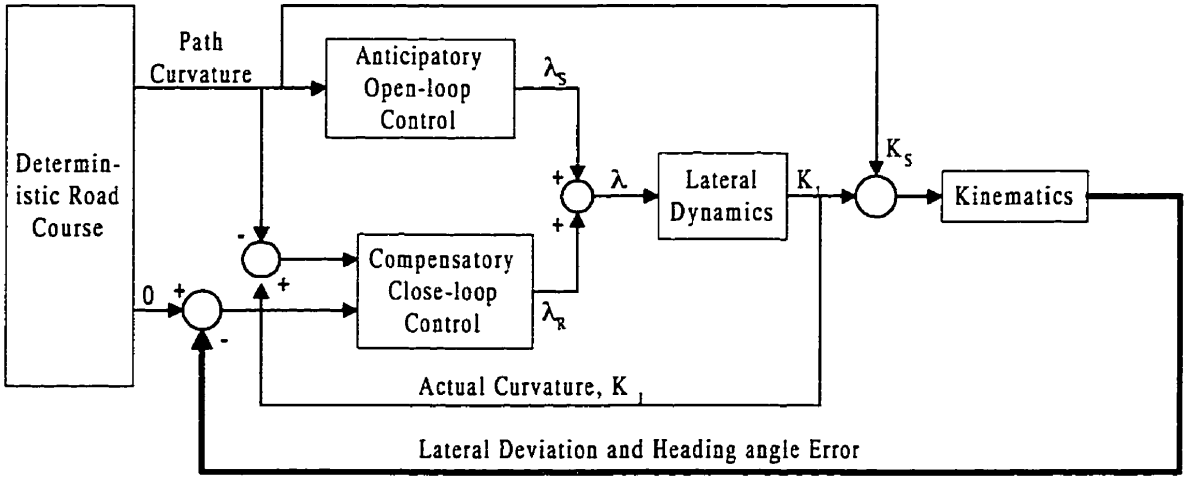

Figure 2.2 Structure of a driver model with guidance and control submodels.

This notion, i.e. the use of guidance and control submodels, has also been followed by other authors. Billing (Billing, 1977) modeled the driver steering reactions for normal and severe maneuvers and validated his model by simulation. Other researchers (Hessburg et al., 1991), (Peng et al., 1993) implemented the conventional PID controller on the control submodel and

achieved acceptable tracking results. Advantages of these models are that they are simple, comprehensive, and accounts well for driver behavior and also their structure are easily applicable for the purpose of vehicle lateral control.

Differences between models of this class are mainly in the design of control submodels and less attention has been paid to the guidance submodels. Ehsani et al. (Ehsani et al., 1995) figured out a major problem of this class. They showed that a contradictory behavior exists between the commands generated by the two submodels. They argued that this contradictory behavior can be removed by realizing the driver anticipation in the desired trajectory definition instead of adding a lead into the feed-forward.

1.2.3 Preview-Predictor Models

The preview-predictor models are designed based on the predictive behavior of a human driver which is another driver intelligent activities. Pioneers of this class believed that the driver predictive reaction is required to compensate the system responding delay. This delay is in the nature of every dynamic system and a human driver recognizes it by experience. Considering the fact that a driver somehow predicts future events in order to perform his present reactions, the preview-predictor control strategy can be another solution for the vehicle lateral control. Kroll (Kroll, 1970) and Garrott et al. (Garrott et al., 1982) are among the pioneers of these models. Figure 2.3 shows how prediction is used to generate several lateral errors. Garrott et al. developed a closed loop driver model based on the given models

in (Donge, 1978), (Kroll, 1970) and (McRuer et al., 1997). Their predictive command is obtained by the weighting summation of the lateral deviation errors on the predicted points.

Mac Adam (Mac Adam, 1980) introduced a technique for synthesizing close-loop control of linear time-invariant systems. This technique is obtained by minimizing a defined preview output error which can be the lateral deviation of the vehicle from the desired trajectory in the context of steering control. He applied his technique to the automobile path following problem (Mac Adam, 1981). This effort resulted in a satisfactory tracking behavior, both in simulation and application, for a smooth lane change case. This technique did not attract the attention of other researchers in this field mostly because of its mathematical complexity.

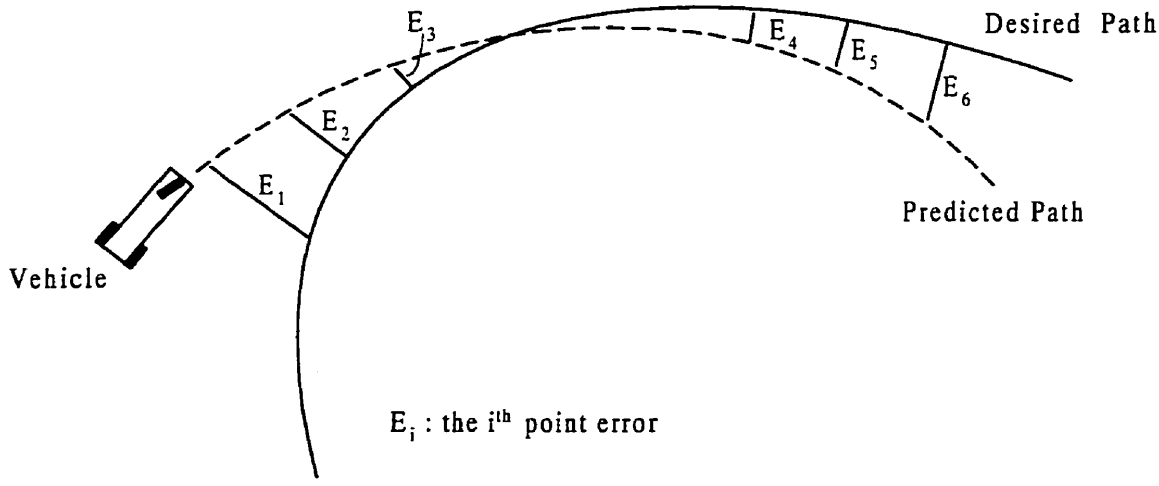

Figure 2.3 Concept of error generation in preview-predictor models.

Peng et al. (Peng et al., 1993) have presented a sophisticated optimal preview solution for the lateral control of vehicles. This optimal preview control algorithm was developed by minimizing a quadratic performance index. The design method is known as the Frequency Shaped Linear Quadratic (FSLQ) optimal control approach. It removes some limitations from classical preview-predictor models, such as stability guaranty. A qualitative review over many Preview and Optimal Preview tracking models, with different cost functions, has been done by Guo (Guo et al., 1993).

The preview-predictor tracking models can also be a good solution for modeling both guidance and control compensatory reactions of a driver. Although the notion of guidance is not explicitly considered here, the common point with the previous class is that somehow they both tried to compensate vehicle dynamic and human delays. One advantage of this class is that there is only one model for generating the control command so that contradictory behavior between the two submodel commands is eliminated. However, they still have following limitations:

- they are generally constructed for the lateral control of linear systems thus little knowledge about their behavior with non linear dynamic systems is accessible,
- the integral of performance index in the optimal-preview models are difficult to solve for any arbitrary weighting function,
- the desired trajectory must be completely known before executing any driving task therefore modifying the trajectory during execution is impossible and,

- in the case of rapid changes in the desired trajectory (severe maneuvers), preview-predictor models fail to follow the desired trajectory.

1.2.4 Models with Nonlinear Feedback

In recent decades, the theory of nonlinear control has been developed and successfully applied to many dynamic systems (Slotin, 1991). Researchers in robotics added adaptive and robust control techniques on the nonlinear control of robot manipulators and obtained satisfactory agreements with predicted simulation results (Spong, 1989). For mobile systems, such as cars in the IVHS, dealing with nonlinear equations of motion is inevitable. The extension of nonlinear control toward mobile systems has firstly been made for omnidirectional mobile robots with two independently actuated wheels (Jagannathan et al., 1994), (Lu et al., 1994), (Munoz et al., 1994), (Saha et al., 1989), (Shim et al., 1995). Among different sorts of mobile robots, these have the best mobility and they are usually used in the FMS. Recently, the necessity of highway automation brought attention to another type of mobile robots, i.e. car-like mobile robots with front steerable wheels (D'Andrea-Novel et al., 1995), (DeSantis, 1994 and 1995) (Micaelli et al., 1994), (Ollero et al., 1995). Since our research can be categorized in this class, the literature surveys of appendices A, B, and C, give more details on previous efforts on kinematics, dynamics and control problems of car-like mobile robots.

Chapter 2

Synthesis of Results

The problem of modeling a human driver behavior in the concept of the IVHS and the design of the control level have previously been introduced. This chapter is devoted to the steps made toward the design of this level seeking the highest possible degree of compatibility with the supervision level in order to facilitates the integration of driver intelligent activities in the supervision level model.

2.1 Controller for Car-like Mobile Robots

A car-like mobile robot is a rigid body dynamic system with several d.o.f.'s and restricted mobility due to the holonomic and nonholonomic constraints. Kinematics of a car-like mobile robot is similar to ones of actual cars by their front steerable wheels and options of being driven by front, rear or all wheels. To construct an efficient controller that responds to high speed manoeuver, a vehicle dynamic model is required, on which the controller would be implemented. As it has been discussed in the literature survey, existing models falls either in the category of complete dynamic models or of the kinematic models.

The complete models are developed to emulate almost all characteristics of a real car, including tire pneumatic, suspension effects and many d.o.f.'s which are essential for vehicle

handling analyses but do not play an important role in the vehicle planar movements. The vehicle kinematic models or linearized dynamic models are not complete enough to be used in the design of an efficient controller. In the concept of IVHS, vehicles are driving with high speed and large variation of steering angle what cannot be reproduced by kinematic models. Besides, the kinematic or linearized models fail to reproduce the dynamic forces resulting from coupling effect of steering and traction dynamics.

The compromise is however made on a dynamic model of a planar car-like mobile robot which includes the dynamic terms of a real car which is required for the vehicle lateral and speed control. This nonlinear dynamic model includes both steering and traction dynamics to simulate the planar movements of a car-like mobile robot (figure 3.1). This model is used as the base of the further control law developments its computer development is given in appendix D.

Although deformations of tires (caused by tire slippage) results in the changes of the vehicle configuration, tire dynamics are not modeled in the proposed vehicle dynamics. Because in the Cartesian frame, N, and in the time interval Δt between two feedback signals of the vehicle states, this changes are smaller by order of magnitude in comparison with the configuration changes in the same direction resulting from the steering and traction commands during this time-interval. In other word, it is assumed that the lateral deviation of the vehicle caused by the tire deformation has a very small effect on the vehicle lateral error and it can be compensated by the feedback control system. This is valid while the

vehicle manoeuver imposes the lateral acceleration inferior from 0.3g on each of the tires. After 0.3g slippage starts and the tire cannot reproduce reaction forces. It should be mentioned here that the criterion is the acceleration and the vehicle can have high speed and still be far from the limit. It is also implicitly assumed that, from a vibration standpoint, the tire dynamics are damped enough so that they will not destabilize either of the proposed path-tracking schemes.

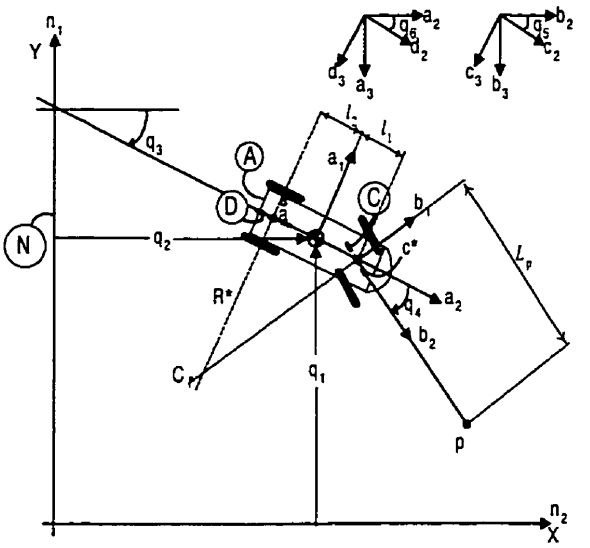

Figure 3.1 Planar car-like mobile robot with steerable control-point P.

The classical Input/Output Feedback Linearization (I/OFL) method has been chosen to compensate for the given system nonlinearities (figure 3.2), i.e. the effect of inertial, Coriolis and centrifugal dynamic forces acting on the vehicle. "The most important property of the I/OFL method is not necessarily that the nonlinearities can be canceled by the nonlinear feedback. Once an appropriate coordinate system is found in which the system can be

linearized, the nonlinearities are in the range space of the inputs", (Spong, 1989). In addition, the simple structure of this method can facilitate the application of other techniques such as robust or adaptive control.

The control problem of omnidirectional mobile robots had been well studied before in the context of the FMS. These robots have a high degree of mobility because of their independently actuated wheels. Considering previous researches, the kinematics of car-like mobile robots have been compared to the ones of omnidirectional robots in appendix A. The major kinematic difference between these two robot families is that the restricted kinematics of a car-like mobile robot results in a singular and configuration dependent Jacobian matrix (a column of zeros). This matrix relates the Cartesian velocities of the vehicle main body (body A in figure 3.1) to the angular speeds of the joints, here, the steering and traction or propulsion rotational speeds.

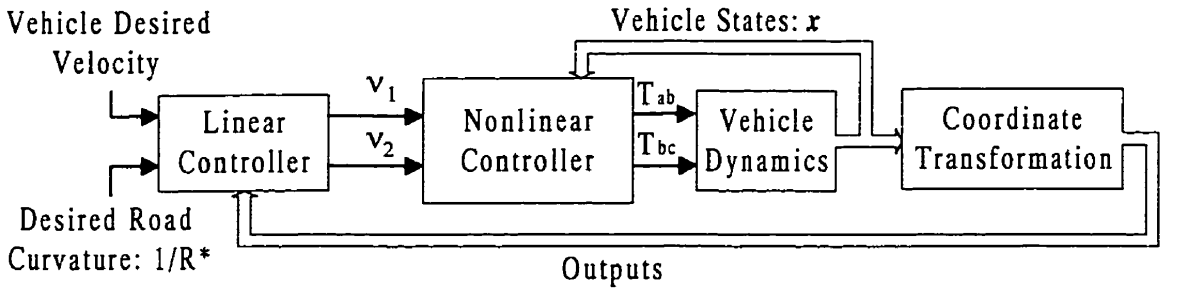

Figure 3.2 Architecture of an I/OFL using desired trajectories

Remembering from introduction that the vehicle speed control has been defined as controlling the vehicle speed independently from the vehicle position, i.e. from the vehicle

lateral control, the first step toward the development of a control law has been made to control the vehicle speed and the instantaneous curvature ($1/R^*$) of the vehicle, respectively as the longitudinal and the lateral control outputs. These choices grant a full-rank decoupling matrix and makes the I/OFL feasible for any vehicle arbitrary configuration. Since the controlled system is under nonholonomic constraints, the method can only ensure the stability of the so called external dynamics by its nature, but a part of the system dynamics, i.e. the so called internal dynamics, stays unobservable by the method and its stability must be verified separately. This stability is ensured by completing the diffeomorphism which shows that the unobservable speeds stays bounded, if the external dynamics are stable.

The first paper contributions are:

- bringing in evidence the kinematic difference between two mobile robot families mainly the inevitable singular Jacobian matrix.

- the development of a vehicle dynamic model which includes the steering dynamics and which has a relatively simple and compact mathematical form.

- the realization of the independent speed control based on the developed dynamic model using the combination of an I/OFL and a time-invariant proportional

derivative linear controller, this while ensuring the stability of the internal dynamics.

This controller can well realize the speed control objective but still has limitations in vehicle lateral control. Although, controlling the vehicle instantaneous curvature is somehow equivalent to the control of the vehicle instantaneous orientation in the Newtonian reference frame, the control problem of the vehicle position still stays unsolved. In fact, the inevitable singular Jacobian matrix does not intervene in this process because the vehicle Cartesian coordinates have not been controlled.

2.2 Control Problem of Vehicle Cartesian Coordinates

The control of vehicle Cartesian coordinates, in a Newtonian reference frame N, is known as the path tracking problem of mobile robots. Many researchers proposed algorithms to control the Cartesian coordinates of a fixed point on the vehicle such as the center of gravity (c.g.). For an omnidirectional mobile robot, such a control-point is an appropriate choice, because the angular velocity of each actuated wheel affects both of the Cartesian velocities of the control-point and it results in a configuration independent and non singular Jacobian matrix. But, the kinematics of a car-like mobile robot is quite different and choosing any fixed control-point on the vehicle results in a singular Jacobian matrix (appendix B). This singularity is the major obstacle in solving the path tracking problem of a car-like mobile robot, especially in the I/OFL procedure.

In the second paper, the proposed looking ahead path-tracker scheme has its control-point attached to the steering wheel instead of being on the vehicle main body (point P in figure 3.1). Therefore, the associated Jacobian matrix is no longer singular since both traction and steering velocities, i.e. joint speeds, affect the movements of this control-point. The idea behind this choice is similar to the action of a child pulling his cart after him. The kinematics of a child-cart with steerable front wheels is very similar to car-like mobile robots. If the child attaches his pulling rope to any fixed point on the cart, ex. the *c.g.*, he can hardly control its lateral movements, meanwhile, if he attaches his pulling rope on the handle in front of the steering wheel, he can run through any desired path and the cart will follow him.

Although, the above explanation justifies the consideration of a steerable control-point in front of the vehicle, more certitude is required to figure out how the control of a virtual point in front of the vehicle would be related to the control of a fixed point on the vehicle. To this end, an off-line path planning process is presented in the second paper. This process consists of finding the desired path of the steerable point P from the desired path of a fixed-point, for instance the midpoint between the rear tires named d^* (appendix B). By this process, the path tracking problem of the control-point P is converted to the one of point d^* and studying the control problem of the vehicle Cartesian coordinates is completed.

The proposed scheme controls implicitly the vehicle orientation, i.e. when the control-point follows the desired path, vehicle's orientation will achieve the path orientation due to one of the nonholonomic constraints which relates the vehicle Cartesian speed and orientation.

This deduction is confirmed through the simulations. Hence, a relatively complete solution for the problem of the vehicle configuration, i.e. position and orientation, in the Cartesian space has been presented. A detailed discussion on the choice of the control-point, the control law development, the stability of the internal dynamics, and the offline path planning toward defining the desired path of point P from the desired path of point d^* is presented in appendix B.

In the second paper, the principal contributions are:

- the realization of a complete vehicle lateral control which ensures the stability of the system for both observable (linearized) and unobservable (internal) dynamics. Using the specific steerable control-point for I/OFL, the system stability cannot be affected by the kinematic fact of the car-like robots, i.e. the singularity of the Jacobian matrix.

- the offline path planning process which relates the desired path of the steerable point P and a complete simulation analysis for different path forms. It is shown that, for paths composed of straight lines and circular arc segments, the vehicle speed can also be controlled with the limit of having constant value in the arc segments.

The proposed looking ahead path-tracking scheme is a solution to the control problem of the vehicle configuration, known as the vehicle lateral control. This scheme partly solves the vehicle speed control for paths composed of straight lines and circular arc segments. But still, there is an undesired dependency between the lateral and the longitudinal (speed) control aspects especially in the concept of the IVHS where it is essential to have an independent control on the vehicle speed, because changes in the vehicle speed might be requested, any time, independent from the vehicle position on the path. The independent speed control is also the necessary condition for the integration of driver intelligent activities in the proposed driver model. This undesired dependence is created from the definition of the conventional inputs of the control scheme, i.e. the time-dependent desired trajectories for the vehicle Cartesian coordinates of a control-point. Actually, we hypothesize that a human driver never defines any desired trajectory in the conventional form to cancel the vehicle lateral offset. In other word, as it has already discussed before, he does not associate a specific time to the instantaneous position of his vehicle and he bases the lateral control of his vehicle on a more realistic factor which is the geometric lateral-offset of his vehicle from the desired path.

2.3 Independent Speed Control with Geometric Lateral-offset Tracking

It is defined in the IVHS concept that by overseeing the vehicle control system, a supervisor coordinates the traffic activities and generates the desired path and speed for the vehicle controller. The task of the supervisor would be easier if these desired terms are the direct inputs of the control system on the vehicle instead of the time-dependent trajectories. If not,

to generate the desired trajectories, the speed profile should be known for the whole path, and any changes in this profile requires the inevitable regeneration of the desired trajectories. The vehicle speed profile cannot be fixed for the whole desired path of the vehicle specially in the presence of other vehicles in the IVHS concept, where the speed profile might be under frequent changes because of many factors such as road and environmental conditions, traffic situation, critical lateral acceleration, etc. Hence, the desired trajectories, as inputs of the control level in the proposed driver model, creates an incompatibility between the control and the supervision level. A major step toward increasing this compatibility is to render the vehicle speed control independent from its lateral control and the key point is by-passing the generation of the desired trajectories.

Let us redefine the objective of the vehicle speed control as: "achieving a desired speed", and one of the vehicle lateral control as: "measuring the vehicle lateral-offset from a given desired path and canceling this offset in a smooth stable manner". Following these definitions, the vehicle speed control must be independent from its lateral control. In other words, when the vehicle is on the path, with the zero lateral-offset, the vehicle speed can possibly be changed without affecting vehicle lateral control.

The trajectory tracking strategy is based on generating commands to track a previously generated desired trajectory which is a function of time i.e., at instant t, the Cartesian coordinates of the control-point have to be at a predefined position given by the associated desired trajectories which is commonly used in the control of robot manipulators. The idea

behind this strategy can be visualized considering an imaginary virtual-car on the path with a predefined speed profile. A control level, based on this strategy must ensure the instantaneous match between the configuration of the mobile robot and the virtual-car. Let us suppose, for instance, that the mobile robot is on the path and it has already achieved the desired speed, but the perfect match is not yet made between the mobile robot and the virtual-car, i.e. there is no geometric lateral-offset but it is slightly behind the virtual-car.

In the trajectory tracking strategy the distance between the vehicle and the virtual-car is recognized as an error in the vehicle position. The error recognition takes place because the robot position offset has been computed from a moving virtual-car and not from the path that the vehicle should follow. The cancellation of this error requires an acceleration command and causes changes in the already settled vehicle speed, i.e. increase of the vehicle speed error. This visualization is to figure out how the dependence between the vehicle lateral and speed control, caused by the generation of desired trajectories, results in a contradiction between vehicle lateral and speed control.

The problem exists also in reverse: if the control level is designed based on this strategy, any time the supervision level asks for speed modifications, the regeneration of all desired trajectories is inevitable. The reverse effect can be visualized as substituting the previous virtual-car by a newly defined one based on the new desired speed profile.

The geometric lateral-offset tracking scheme, is a new manner for the development of a control law without generating any desired trajectories. The architecture of this scheme is shown in figure 3.3. This scheme removes the dependence between the vehicle lateral control and its speed control, and consequently, the explained contradiction will no longer reproduce.

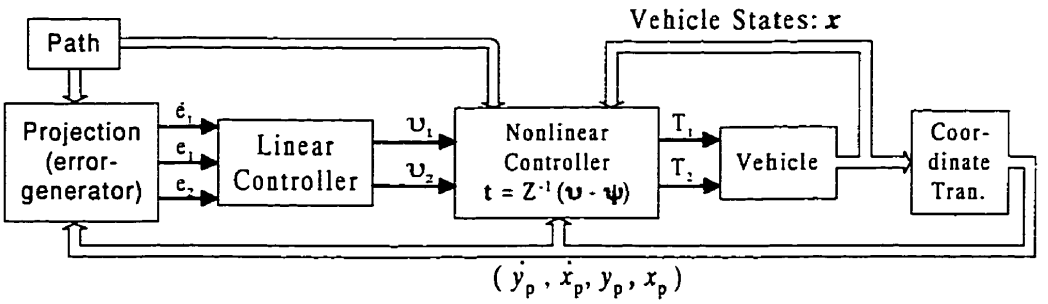

Figure 3.3 Geometric lateral-offset tracking and speed control diagram.

System inputs in this scheme are: i) the geometric characteristics of the road and ii) the constant desired speed. , which can be modified at any time by the supervision level. Even though, further modifications are necessary to increase the performance and robustness of the proposed geometric lateral-offset tracking scheme, its architecture models very closely the compensatory reactions of a human driver for realizing a driving task.

The definition of the geometric lateral-offset is the distance between the instantaneous position of the vehicle control-point and the nearest point on the desired path (figure 3.4) and the speed error is the difference between the vehicle actual and desired speed. No virtual-car is defined in this scheme and while the vehicle is physically on the path, no lateral error

will be recognized. Here, the lateral-offset is defined by the on-line (instantaneous) projection of the control-point position on the desired path and not by the error between the robot and the virtual-car. Further explanations to reveal the advantages of the geometric lateral-offset tracking scheme on the conventional time dependent trajectory tracking methods are shown in appendix C. The proposed scheme is only verified for the desired paths composed of straight lines and circular arc segments. The following explanations are to clarify the reasons behind this development.

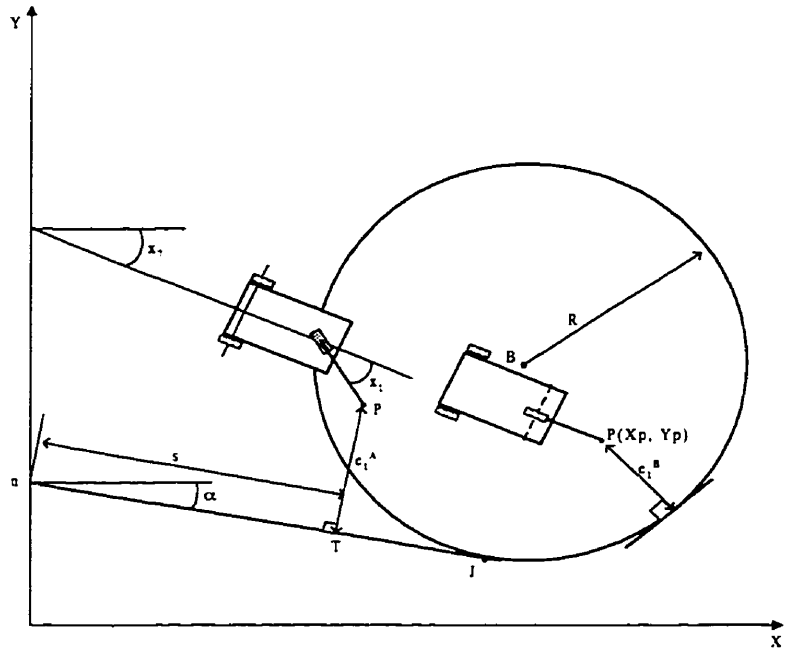

Figure 3.4 Lateral-offset definition of linear and circular arc segments.

Consider that the desired path is a general function in the Cartesian plane. Either in the conventional form of $y = f(x)$ or in parametric form of $[x = f_1(s),\ y = f_2(s)]$. As shown in

figure 3.4, the nearest point T is the perpendicular projection of the control-point P on the desired path and the lateral-offset is defined to be:

$$e_1 = \sqrt{(x_P - x_T)^2 - (y_P - y_T)^2} \tag{30}$$

where (x_T, y_T) is either the solution of the following differential equation;

$$\begin{gathered} \frac{df(x_T)}{dx}[f(x_T) - y_P] - (x_T - x_P) = 0 \\ y_T = f(x_T) \end{gathered} \tag{31}$$

for $y = f(x)$ presentation of the desired path or the solution of;

$$\begin{gathered} \frac{df_2(s_T)}{ds}[f_2(s_T) - y_P] - \frac{df_1(s_T)}{ds}[f_1(s_T) - x_P] = 0 \\ x_T = f_1(s_T) \\ y_T = f_2(s_T) \end{gathered} \tag{32}$$

As it is seen, for a general desired path in the Cartesian frame, finding the instantaneous lateral-offset is not straight forward. For instance, paths of frequent maneuvers such as U-turn and 270 degree turns on the existing roads and highways cannot be presented in the form of one smooth function and they should be presented by several functions. Even if we present the desired path by several functions, instead of one continuous one, the analytical solution of equations (31, 32) does not exist for a majority of continuous functions.

The numerical solution as an alternative results in finding more than one solution for x_T (or s_T) in most cases. Although, the nearest point on the path from the vehicle is the hint to filter the right answer between the found solutions, having numerical algorithms, in the analytical process of a control law development because not only it adds a variable delay in the process but also the stability of the control system becomes dependent to the stability of the numerical algorithm.

It must be noted that: 1) breaking the desired path into different segments is inevitable, 2) the robot pathway through the already constructed roads and highways can be well approximated by straight lines and circular arc segments and 3) a car-like mobile robot can follow such paths more easily than any arbitrary paths because the path following results in constant steering angle due to the kinematics of car-like robots. In addition, Desaulniers et al. (Desaulniers et al., 1995) showed that, for car like robots, the shortest path between two positions is achieved by a combination of line segments and circular arcs of minimal turning radius. This combination is also proven to be the optimal path between each of two arbitrary configurations (Souères et al., 1996). Hence, paths composed of straight lines and circular arc segments, with their special characteristic of having constant curvature (constant steering angle), appears as the ideal way of planning a car-like robot desired path.

The main contributions of this paper are:

- the development of a geometric path tracker for a car-like mobile robot in which the exponential convergence of the vehicle lateral-offset and the vehicle speed error to zero are ensured for both FWD and RWD robots.

- the vehicle configuration is controlled commanding only one geometric output while the stability of the unobservable dynamics is ensured by completing the diffeomorphism after the I/OFL is applied.

- the speed control is realized independently from the lateral-offset tracking and the system performance is verified by injecting desired speeds with discontinuous changes.

Conclusion

In the vehicle/driver/road system, the driver decision making procedure has been described by a model with three levels: a control level to model driver compensatory reactions, a supervision level to realize the driver intelligent activities and a definition level to define the road itinerary, speed limit, etc. The control level plays the most important role as an intermediary between the vehicle and the supervision level. The vehicle is a dynamic system in which variables change continuously and receives the commands from the control level. Meanwhile, the supervision level, in which driver intelligent activities are modeled, modifies the desired values of the control level in a discontinuous manner, for example, sudden change of the vehicle desired speed. Thus the control level must be compatible with both continuous variation of vehicle variables as well as with the discontinuous variation of its desired inputs, for example the desired speed. In this thesis, the objective has been to integrate driver compensatory reactions, which consist of constructing a control level considering the mentioned compatibility. To this end, the independent vehicle speed control and the cancellation of the vehicle lateral-offset from the desired path are defined as the concrete objectives to be realized employing the existing theory of nonlinear control and robotics.

In the first step, a complete kinematic analyses of such mobile robots is done and a dynamic model is developed for the class of car-like mobile robots which can model the essential

planar movements of a ground vehicle which play an important role for vehicle speed and lateral control. In this model the generally neglected steering dynamics are considered in order to obtain the nonlinear coupling effect of steering and traction dynamics on each other. Based on the developed dynamic model, the independent control of the vehicle speed plus the instantaneous curvature are realized using the I/OFL technique. The exponential convergence of the errors and the stability of the system internal dynamics have been verified theoretically and by simulation. A comparison between the kinematics of two vastly used families of mobile robots, i.e. the omnidirectional and car-like robots, revealed the fact that a car-like mobile robot has a singular Jacobian matrix for any fixed point on the vehicle main body (body A). This is the major obstacle for the vehicle lateral control, i.e. controlling the Cartesian coordinates of a fixed-point such as the c.g.

In the second step, the vehicle lateral control was completed by controlling the Cartesian coordinates of a steerable point (point P) attached to the front tire, instead of a fixed-point. The same dynamic model and the same nonlinear control technique has been used for this realization. It is proven mathematically that the desired path of this steerable point can be derived from the desired path of any fixed point on the vehicle, for instance the center of rear tires (point d^*). In other word, the path tracking problem for any fixed-point on the vehicle can be trans formed to the path tracking problem of the steerable point. This solution protects the nonlinear control law development from being affected by the singularity of the Jacobian matrix. In fact, the kinematic nature of the mobile robot is respected and the control law is

developed by detouring the singularity problem without losing any generality or feasibility. Also, this scheme solves partly the vehicle speed control for paths composed of straight lines and circular arc segments. However, it is essential that the vehicle speed control be realized independently from the vehicle lateral-offset tracking and all at the same control level and the conventional control approach, in which inputs are the desired trajectories, fails to fulfil this independence.

In the third step, the geometric lateral-offset tracking scheme has been introduced to realize the independent speed and lateral control by one control law. In this scheme, the system inputs are the geometric characteristics of the desired paths in Cartesian space and the desired speed. This approach allows the independent control of the vehicle speed and facilitates the integration of the driver intelligent activities at the supervision level. Speed modification, which is the result of most driver intelligent activities to avoid dangerous situations, is then possible without affecting the vehicle lateral control and this is granted from removing the desired trajectory generation from the supervision level structure. Based on this scheme, a control law was developed for the vehicle speed control as well as for tracking purposes of the vehicle lateral-offset from the paths composed of straight lines and circular arc segments. However, the scheme is applicable to any form of paths solving the explained mathematical complexities. The same dynamic model and nonlinear control technique have been employed and the performance and reliability of the designed system have been verified through simulation.

The design of the supervision level, which incorporates the driver intelligent activities, and its interaction with the control and definition levels, also, solving the mathematical complexities of the geometric lateral-offset tracking scheme for the paths with another form than straight lines and circular arc segments could be the starting point for further researches. Finally, the performance of the scheme should be verified on complete vehicle models which includes tire pneumatic, differential drive, suspension and several d.o.f's.

References

ALLEN R.W., SZOSTAK H.T., ROSENTHAL T.J., JOHNSTON D.E., (August 1986). Test Methods and Computer Modeling for the Analysis of Ground Vehicle Handling, Paper 86115 in SAE Special publication, SAE, pp. 1-19.

ALLEN R.W., SZOSTAK H.T., ROSENTHAL T.J., (1987). Steady State and Transient Analysis of Ground Vehicle Handling, Paper 870495 in SAE Special publication, SAE, Warrendale, Pa., pp. 49-78.

ASTOLFI A., (1995). Exponential Stabilization of a Car-like Vehicle, IEEE International Conference on Robotics and Automation, 0-7803-1965-6/95, pp.1391-1396.

BAKKER E. et al., (Feb. 1984). Tyre modeling for vehicle Dynamic Studies, SAE 840561.

BAUMGARTNER E.T., SKAAR S.B., (1994). An Autonomous Vision-Based Mobile Robot, IEEE Transactions on Automatic Control, vol. 39, no. 3, pp. 493-502.

BLOCH A.M., REYHANOGLU M., McCLAMROCH N.H., (1992). Control and Stabilization of Nonholonomic Dynamic Systems, IEEE Transactions on Automatic Control, vol. 37, no.11, pp. 1746-1757.

BILLING A.M. (Dec. 1977). Modeling Driver Steering in Normal and Sever Maneuvers, special Report, univ. Of Toronto. An Over view of Simulation in high way Transportation, part II, pp. 151-165.

BISHOP J.R., (Feb. 1993). Intelligent Travel: The Automated Highway System, Proceeding of the Intelligent Autonomous System Conference, Pittsburgh, PA, pp. 120-125.

CAMPION G., BASTIN G., D'ANDREA-NOVEL, B., (Feb. 1996). Structural Properties and Classification of Kinematic and Dynamic Models of Wheeled Mobile Robots, IEEE Transactions on Robotics and Automation, vol. 12, no.1, pp. 47-62.

CANUDAS de WIT C., SORDALEN O.J., (1992). Examples of Piecewise Smooth Stabilization of Driftless NL Systems with less Inputs than States, IFAC Nonlinear Control Systems Design, Bordeaux, France, pp. 57-61.

CHEN CHI. T, (1984). Linear System Theory and Design, Holt, Rinehart and Winston, Inc.

CLARK S.K., (Aug. 1981). Mechanics of Pneumatic Tires, NHTSA DOT HS 805-952, Book-Code: TL270 M487.

CORNELL L., (Dec. 1968). Vehicle Dynamics in Single Vehicle Accidents-Validation and Extensions of a Computer Simulation, Cornell Astronautic Laboratory, CAL Report. VJ-2251-V-3.

CORON J.M., D'ANDREA-NOVEL B., (1992). Smooth Stabilization Time-Varying Control Laws for a Class of Nonlinear Systems, Application to Mobile Robots, IFAC Nonlinear Control Systems Design, Bordeaux, France, pp. 413-418.

GRAIG J.J., (1989). Introduction to Robotics, Adisson-Wesley Publishing Company, ISBN 0-201-09528-9.

CROLLA D.A., SCHWANGHART H., (1992). Vehicle Dynamics-Steering I, Journal of Terra- mechanics, vol. 29, no. 1, pp. 7-17.

D'ANDREA-NOVEL B., CAMPION G., BASTIN G., (1995). Control of Nonholonomic Wheeled Mobile Robots by State Feedback Linearization, The International Journal of Robotic Research, vol. 14, no. 6, pp. 543-559.

DENG Z., BRADY M., (1993). Dynamic Tracking of a Wheeled Mobile Robot, International Conference on Intelligent Robots and Systems. Part 2, pp. 1295-1298.

DeSANTIS R.M., (1994). Path-tracking for a Tractor-Trailer-like Robot, International Journal of Robotic Research, Vol. 13, No. 6, pp. 533-544.

DeSANTIS R.M., (Dec. 1995). Modeling and Path-tracking Control of a Mobile-Wheeled Robot with a Differential Drive, Robotica, Vol. 13, pp. 401-410.

DeSANTIS, R.M., (1995) Path-tracking for car-like robots with single and double steering, IEEE Transactions on Vehicular Technology vol. 44 no. 2, pp. 366-377.

DESAULNIERS G., SOUMIS, F., (Dec.1995). An Efficient algorithm to find a shortest path for a car-like robot, IEEE Transactions on Robotics and Automation vol. 11 no. 6, pp. 819-828.

DONGES E., (1978). A Two Level Model of Driver steering Behavior, Human Factors, pp. 691-707.

ELLIS J.R., (1969). Vehicle Dynamics, London Business Book Limited, SBN 220 99202 9, chapters 1, 2 and 9.

EHSANI S.M., TÉTREAULT, (Aug. 1995). Supervision Task in a Driver Model, AIAA Guidance Navigation and Control Conference Proceeding.

EHSANI S. M., TÉTREAULT M., GOU M., (1996). Kinematics, Dynamics and Control of a Car-like Mobile Robot, submitted to The International Journal of Vehicle Mechanics and Mobility, Vehicle System Dynamics.

EHSANI S.M., TÉTREAULT M., GOU M., BIGRAS P., (1996). Looking Ahead Path tracking of a Car-like Mobile Robot , submitted to IEEE/ASME Journal of Mechatronics., nov. 1996.

EHSANI S.M., TÉTREAULT M., GOU M., DeLAFONTAINE J., (1997). Lateral-offset Tracking and Speed Control of a Car-like Mobile Robot, submitted to IEEE Transactions on Robotics and Automation, July 1997.

FENTON R.E., MELOCIK G.C., OLSON K.W., (1976). On the Steering of Automated Vehicles: Theory and Experiments, IEEE Transactions on Automatic Control, vol. AC-21, no.3, pp.306-315.

FENTON R.E., MAYHAN R.J., (Feb. 1991). Automated Highway Studies at the Ohio State University, An Overview, IEEE Transactions on Vehicular Technology vol. 40 no.1 pp.100-113.

FENTON R.E., BENDER J.G., RULE R.G., (Sep. 1974). Synchronous Longitudinal Control of Individual Vehicles, International Symposium on Traffic Control and Transportation Systems, 2nd, Monte Carlo, Monaco, 16-21.

GARROTT R.W., WILSON D.L., SCOTT R.A., (1982). Closed Loop Automobile Maneuvers Using Preview- Predictor Models, SAE Report no. 820305.

GORINEVSKY D., KAPITANOVSKY A., GOLDENBER G.A., (1993). An Architecture for Control of Car Motion and Application to Parking, ASME DSC-vol. 52, Advanced Automotive Technologies.

GUO K., GUAN H., (1993). Modeling of Driver/Vehicle Directional Control System, Journal of Vehicle System Dynamics, vol. 22, pp. 141-184.

HAUKSDOTTIR A.S., FENTON R.E., (Nov.1985). On the Design of a vehicle Longitudinal Controller, IEEE Transactions on Vehicular Technology, vol. 34, no. 4, pp.182-187.

HAYES-ROTH B., (1993). Intelligent Control, Artificial Intelligence Journal 59, pp. 213-220.

HAYES-ROTH B., (1985). A blackboard Architecture for Control, Artificial Intelligence Journal 26, pp. 251-321.

HEMAMI A., MEHRABI M.G., CHENG R.M.H., (1992). A Synthesis of an Optimal Control Law for Path Tracking in Mobile Robots, Automatica, vol.8, no.2, pp. 383-387.

HESS R.A., (1987), Handbook of human factors, Edited by G. Slavendy, Wiley, New York, pp. 1212-1242.

HESSBURG T., PENG H., TOMIZUKA M., (June 1991). An Experimental Study on Lateral Control of a Vehicle, Proceeding of the 1991 American Control Conference, vol. 3, pp. 3084-3089.

HULBERT S., (1979). Human Factors in Transportation, Accident Factors edition, National Safety Council, Chicago.

JAGANNATHAN S., ZHU S.Q., LEWIS F.L., (1994). Path planning and control of a mobile base with nonholonomic constraints, Robotica, vol. 12, pp. 529-539.

JUBERTS M., RAVIV D., BISHOP R.J., (1993). Autonomous Road Following, a vision based approach, Robot System Division, National Institute of Standards and Technology.

JURIE F., RIVES P., GALLICE J., BRAME J.L., (1994). High Speed Vehicle Guidance Based on Vision, Control Engineering Practice, Vol.2, No.2, pp. 289-297.

KANE T.R., LEVINSON D.A., (1985). Dynamics Theory and Applications, McGraw-Hill Series in Mechanical Engineering, New York, ISBN 0-07-037846-0.

KONZ S., McDOUGAL D., (1968). The Effect of Background Music on the Control Activity of an Automobile Driver, Human Factors, , 10 (vol.3), pp. 233-244.

KROLL C.V., (1970). A Preview Predictor Model of Driver Behavior in Emergency Situations, Federal Highway Administration Rep. Cont. no. CPR-11-3988.

KUSIAK A., (1985). Material Handeling in Flexible Manufacturing Systems, Material Flow, vol. 2, pp. 79-95.

LANGER D., ROSENBLATT J.K., HEBERT M., (1994). A Behavior-Based System for Off-Road Navigation, IEEE Transactions on Robotics and Automation, vol.10, pp.776-783.

LEFEBRE D. R., SARIDIS G. N., (May 1992). A Computer Architecture for Intelligent Machines, IEEE International Conference on Robotics and Automation, pp. 2745-2750.

LU P., LIN K.-C., (1994). Nonlinear Control of an Autonomous Tracked Vehicle, Transactions of the Institute of Measurement and Control, vol. 16, no. 4, pp. 214-220.

MAC ADAM C.C., (Sep. 1980). An Optimal Preview Control for linear Systems, Journal of Dynamic systems Measurement and Control ASME, vol. 102, pp. 188-190.

MAC ADAM C.C., (June 1981). Application of an Optimal Preview Control for Simulation of Close-Loop Automobile Driving, IEEE Transaction on System Man and Cybernetics, vol. SMC 11, no.6, pp. 393-399.

MAEDA T. et al., (1977). Performance of Driver-Vehicle System in Emergency Avoidance, SAE paper 770130.

MASTINU G., FAINELLO M., (1992). Study of Pneumatic Tire behavior on Dry and Rigid Road by Finite Element Method, Vehicle System Dynamics, vol.21, pp. 143-165.

MC RUER D.T., ALLEN R.W., WEIR D.H., KLEIN R.H., (1997), New Results in Driver Steering Control Models, Human Factors, pp. 381-397.

MC RUER D.T. , GRAHAM D., KERNEL E., REISENER W., (July 1965). Human Pilot Dynamics in Compensatory Systems, Report of Wright-Patterson AFB, Ohio.

MC RUER D.T., KRENDEL E., (1974). Mathematical Models of Human Pilot Behavior, N.A.T.O. AGARDograph no. 188, 72 pages.

MC RUER D.T., HENRY R.J., (1968). A Review of the Quasi-Linear Pilot Models, IEEE Transaction on Human Factors in Electronics, HFE-8(3), pp. 231-249.

MICAELLI A., SAMSON C., (1994). Trajectory Tracking for Two-Steering-Wheeled Mobile Robots, IFAC Symposium on Robotic Control, Capri, Italy, pp. 218-224.

MUNOZ V., OLLERO A., PRADO M., SIMON A., (1994). Mobile Robot Trajectory Planning with Dynamic and Kinematic Constraints, IEEE International Conference on Robotics and Automation pt 4, piscataway, NJ, USA, p. 2802-2807.

NARENDRAN V.K., HEDRICK J.K., (1994). Autonomous Lateral Control of Vehicles in an Automated Highway System, Vehicle System Dynamics, vol. 23, pp. 307-324.

NALECZ A.G., (Feb. 1987). Investigation into the Effect of Suspension Design on the Stability of Light vehicles, SAE Paper no. 870497, International Congress of Automotive Crash Avoidance research, Detroit, Michigan.

OELEN W., BERGUIS H., NIMEIJER H., CANUDAS de WIT C., (June 1995), Hybrid stabilizing control on a real mobile robot, IEEE Robotics & Automation Magazine vol. 2 no. 2, pp. 16-23.

OLLERO A., HEREDIA G., (1995). Stability Analysis of Mobile Robot Path Tracking, Proceeding of the IEEE International Conference on Intelligent Robots, vol. 3, pp.461-466.

PENG H., TOMIZUKA M., (Dec. 1993). Preview Control for Vehicle Lateral Guidance in Highway automation, Journal of Dynamic Systems Measurement and Control, vol. 115, pp. 679-686.

SAHA S.K., ANGELES J., (1989). Kinematics and Dynamics of a Three-wheeled 2-DOF AGV, Proceedings of the IEEE Conference on Robotics and Automation, pp. 1572-1577.

SAKAI H., (1991). Theoretical and Experimental Studies on the Dynamic Properties of Tires, Part 1 --Review of theory of rubber friction, International Journal of Vehicle Design, vol.2, no.1, pp.78-110.

SAMSON C., (Feb. 1993). Time-varying feedback stabilization of car-like wheeled mobile robots, International Journal of Robotics Research vol. 12 no. 1, pp. 55-60.

SAMSON C., (1995). Control of Chained Systems Application to Path Following and Time-varying Point-Stabilization of Mobile Robots, IEEE Transactions on Automatic Control vol. 40, no.1, pp. 64-77.

SARIDIS G. N., (1985). Toward the Realization of Intelligent Controls, Proceeding of the IEEE workshop on Intelligent Control PP.78-81.

SARKAR N., YUN X., KUMAR V., (1994). Control of Mechanical Systems with Rolling Constraints: Application to Dynamic Control of Mobile Robots, International Journal of Robotics Research, vol. 13, no. 1, pp. 55-69.

SAYERS M.W., FANCHER S.P., (1985). A Hierarchy of Symbolic Computer-Generated Real-Time Vehicle Dynamic Models, Transport Research Record, pp. 88-97.

SHIM H-S., KIM J-H., KOH K., (1995). Variable Structure Control of Nonholonomic Wheeled Mobile Robot, IEEE International Conference on Robotics and Automation, 0-7803-1965-6/95, pp. 1694-1699.

SLOTIN J.J.,LI W., (1991). Applied Nonlinear Control, Prentice-Hall.

SMILEY A., REID L., FRASER MORRIS, (1980). Change in Driver Steering Control with Learning, Human Factors, no. 22 (vol.4), pp. 401-415.

SMITH D.E., STARKEY J.M., (1991). Overview of Vehicle Models, Dynamics, and Control Applied to Automated Vehicles, ASME Advanced Automotive Technologies, DE-vol. 40, pp.69-87.

SORDALEN O.J., CANUDAS de WIT C., (1992). Path following and Stabilization of a Mobile Robot, IFAC Nonlinear Control Systems Design, Bordeaux, France, pp. 471-476.

SORDALEN O.J., CANUDAS de WIT C., (Dec.1993). Exponential control law for a mobile robot: extension to path following, IEEE Transactions on Robotics and Automation vol. 9, no. 6, pp. 837-842.

SOUÈRES P., LAUMOND J.P., (1996). Shortest Path Synthesis for a Car-like Mobile Robot, IEEE Transaction on Automatic Control, vol. 41, no. 5, pp. 672-689.

SPONG M.W., VIDYASAGAR M., (1989). Robot Dynamics and Control, John Wiley & Sons

SZOSTAK H.T., JOHNSON W.A., ALLEN R.W., ROSENTHAL T.J., (1986). A microcomputer program for analyzing a tire model to be used in vehicle dynamics situations, SCS Multi-conference, SanDiego, CA., Society for Computer Simulation, pp. 205-209.

TAKASAKI G.M., FENTON R.E., (Aug. 1977). On the Identification of Vehicle Longitudinal Dynamics, IEEE Transactions on Automatic Control, vol. AC-22, no. 4, pp.10-615.

TAYEBI A., TADJINE M., RACHID A., (1996). Path Following and Point-Stabilization Control Laws for a Wheeled Mobile Robot, IEEE Proceeding of the 1996 UKACC International Conference on Control, part 2 no. 427/2.

TÉTREAULT M., GOU M. EHSANI S.M., (May 1995). Modéles de Conducteur et Sécurité Routière, IX Canadian Multidisiplinary Road Safety Conference.

THOMPSON S.J., FRASER E.J., HOWARTH C.I., (1985). Driver Behavior in the Presence of Child and Adult Pedestrians, Ergonomics, vol. 28, no. 10, pp. 1469-1474.

TIBURY D., LAUMOND J. P., MURRAY R., SASTRY S., WALSH G., (1992). Steering car-like systems with trailers using sinusoids, IEEE International Conference on Robotics and Automation v. 3. Published by IEEE Service Center, Piscataway, NJ, USA (IEEE cat n 92CH3140-1), pp. 1993-1998.

TIBURY D., SORDALEN J., BUSHNEL L., SASTRY S., (Dec. 1995). A Multi Steering Trailer System: Conversion into Chained form Using Dynamic Feedback, IEEE Transactions on Robotics and Automation vol. 11, no. 6, pp. 807-818.

TOUNSI, M., LEBERT, G., GAUTIER M., (1995). Dynamic identification and control of a nonholonomic mobile robot, IEEE Conference on Control Applications Piscataway, NJ, USA,95CH35764, pp. 520-525.

TRIGGS T.J., (1980). The Influence of Oncoming Vehicles on Automobile Lateral Position, Human Factors, 22, vol. 4, pp. 427-433.

TSUGAWA S., (1994). Vision-Based Vehicles in Japan: Machine Vision and Driving Control Systems, IEEE Transactions on Industrial Electronics, vol.41, no.4, pp.398-405.

WALSH G., TIBURY D., SASTRY S., MURRAY R., LAUMOND J.P., (Jan. 1994). Stabilization of Trajectories for Systems with Nonholonomic Constraints, IEEE Transactions on Automatic Control vol. 39, no. 1, pp. 216-222.

WING M.A., (1992). A novel Intelligent Supervisory Controller for Automated Guided Vehicles, Artificial Intelligence in Engineering, 7, pp. 1-12.

WONG J.Y., (1978). Theory of Ground Vehicles, Wiley-Interscience, Wiley New York.

YUN X., YAMAMOTO Y. (1993). Internal Dynamics of a Wheeled Mobile Robots, IEEE International Conference on Intelligent Robots, Yokohama, Japan, p. 1288-1294.

YOSHIMOTO K., (1981). A Self-Paced Preview Tracking Control Model of An Automobile Driver, Proceeding of IFAC 8th Triennial World Congress, vol. 15.

ZWAHLEN H.T., (1976). The Effect of Alcohol on Driving Skills and Reaction Times, Journal of Occupational Accidents 1, pp. 21-38.

Appendices

Appendix A: Kinematics Dynamics and Control of a Car-like Mobile Robot

Kinematics, Dynamics and Control of a Car-like Mobile Robot

Saéd Ehsani [1], Mario Tétreault [2] and Michel Gou [3]

Abstract

The paper compares the kinematics of two mobile robot families, i.e., the omnidirectional and the car-like mobile robots. The comparison reveals the important kinematic characteristics of each robot family and concludes that different approaches should be used for each control law development. For the purpose of control, a nonlinear vehicle model is essential to simulate major dynamic behavior of a car-like robot such as the coupling effect of between the steering and main body dynamics. The consideration of steering dynamics in the proposed vehicle model results in a compact relation between the vehicle states and inputs, i.e., steering and traction torques. This compact form facilitates the further control law developments. Unlike recent work in control law development in which the steering dynamics and its nonlinear nature have often been neglected due to its light inertia, the proposed model is used here to develop lateral and longitudinal control commands. The Input/Output Feedback Linearisation has been used to decouple the nonlinear dynamics in the inner control loop, and a linear feedback control design specification ensures the stability of the system. The stability of the unobservable (internal) dynamics is also shown by completing the diffeomorphism. Moreover, few researchers have studied the nonlinear control of a car-like robot. Simulations results are presented to show the validity of the approach.

1. INTRODUCTION

Automatic vehicle control has been applied to flexible manufacturing systems for Automatic Guided Vehicles (AGV's), and the idea is now expanding into other research fields such as Autonomous Land Vehicles and Automated Highway Vehicles (Tsugawa 1994). The ultimate goal for Automated Highway Vehicles (AHV's) is to increase highway capacity and to decrease the number of automobile accidents. Complete vehicle automation requires research in many areas including sensors, actuators, vision, image processing, kinematics, dynamics, path planning, navigation and control. While research is ongoing in those areas, control strategy development for vehicles operating at higher speeds and accelerations is particularly interesting.

Vehicle dynamics are very important in the design of controllers, particularly for AHV's operating at high speed and acceleration on sharply curved paths. Most of the work currently being done on the development of AGV's control systems is based on linearized dynamic models or kinematic models, which are only valid at low speeds and for small deviations from the linearisation point. Other limitations, such as constant longitudinal speed and constant or small road curvature, are also imposed on the desired trajectory. However, these assumptions are inappropriate and limit the application of the results.

This paper presents a nonlinear dynamic model of a car-like mobile robot which is used for lateral and longitudinal control law development. Our two degrees of freedom (DOF's)

mobile robot under nonholonomic constraints simulates major dynamic behavior of a real vehicle even at high speed and with varied road curvature. Due to its simple mathematical form, our model can be used in the design of controllers without imposing any limitations, such as constant speed or small road curvature, on the desired trajectory. Input/Output feedback linearisation has been used to decouple the nonlinear dynamics as an inner control loop, and a linear feedback control design specification ensures the stability of the system.

Section Two presents a survey of vehicle dynamics and control. The next section introduces the kinematics and dynamics of our planar car-like robot assuming slippage-free condition. Comparisons are made between the kinematics of a car-like robot and those of an omnidirectional mobile robot to reveal some vehicle kinematic characteristics which lead to different control properties related to the two mobile robot families. The fourth section discusses vehicle lateral and longitudinal control in which the control law is derived to ensure system stability. Simulations included in section Five verify control law performance and the last section concludes the paper. Through the paper as well as in the mathematic equations , vectors are presented by bold small-letters and matrices by capital letters.

2. LITERATURE SURVEY

The literature studies both complex and simplified vehicle models depending on the application. Researchers working on complex models (Allen 1987) want to emulate a real vehicle's behavior. However, there is no work reported, which incorporates these complex

vehicle models into vehicle control strategies because they have many algebraic and differential equations and it is not essential to consider all vehicle DOF's in order to develop control laws. Simplified models (Fenton 1976) consider only meaningful DOF's in the control objective. Regarding control of a vehicle under slippage-free condition, the vehicle lateral and longitudinal behavior can be simulated by using a planar vehicle model.

While dynamics and control of omnidirectional mobile robots (Saha 1989), (Jagannathan 1994), (Sarkar 1994), (Lu 1994), (Shim 1995), (DeSantis 1995) have already been thoroughly studied, this paper focuses on car-like mobile robots. A review (Smith 1991) of vehicle models used in control design points out that those most widely used by researchers are "bicycle" models (Ellis 1969) where nonholonomic constraints or speed dependencies between DOF's are not considered. Even recently, researchers have used this bicycle model to develop their control or guidance strategies (Tsugawa 1994), (Baumgartner 1994), (Hemami 1992) and (Jurie 1994). The vehicle models are either kinematic, which are inappropriate for high speeds, or linearized, which are only valid for small deviations from the linearisation point. These vehicle models do not consider a tire model because it is not of primary importance in control design of mobile robots, even though tire dynamics affect the vehicle dynamics at some speeds and vehicle configurations. Also, some authors (Baumgartner 1994), (DeSantis 1994) have employed a control point different from the vehicle center of gravity (c.g.).

Few researchers have developed lateral and longitudinal control strategies based on a nonlinear dynamic model of a car-like mobile robot, because its kinematics are more complex and the equations of motion (e.o.m.) are highly coupled. The controller design is different from that used for an omnidirectional robot because the steering angle and the wheel traction both affect the lateral and longitudinal control. DeSantis (1994) has considered a vehicle model without steering dynamic, so the steering angle, or its derivative, becomes the system input. This assumption may simplify the vehicle dynamic e.o.m. but it complicates the control law development. In fact, assumptions such as constant speed and constant road curvature, which results in a time-invariant P.I.D. controller, impose limitations on the desired trajectories. The PATH research group (Narendran 1994) has developed an auto-tracking control law where the control outputs are the car heading angle and its distance from a lead car which is supposed not to have any error from the desired path. Small heading angle assumption limits the application on the sharply curved paths and their work does not include any longitudinal speed control.

3. KINEMATIC AND DYNAMIC ANALYSIS

The literature survey reveals that the kinematics and dynamics of a car-like mobile robot must be studied in more detail since existing models, used for developing control laws, neglect either vehicle dynamics and its nonlinearities, or the steering dynamics. A vehicle is a complex dynamic system, but it is not necessary to consider its whole complexity in the development of an efficient control law. Only important kinematic and dynamic

characteristics should be considered. A planar vehicle can simulate all basic vehicle configurations, i.e., position and orientation, which play a role in path tracking. Also, it is the simplest vehicle model that can be chosen to develop the control law. Other assumptions are slippage-free motion and negligible pneumatic tire and soil effects. Figure 1 shows the planar car-like robot whose characteristics are explained as follows:

i) The vehicle is a front-wheel drive car-like robot with three tires. The front tire represents a virtual-tire replacing front wheels of a real vehicle. This assumption is not restrictive because the front wheels are linked to each other and represent only one DOF.

ii) The fixed frame N is chosen as the Newtonian reference frame. Each rigid body has a frame attached to its c.g. with unit vectors representing the inertial central principal axes. For example, the main body A has an attached frame with unit vectors $\boldsymbol{a}_i$ (i = 1,2,3), shown in figure 1. Two frames, B and C, have been attributed to the virtual-tire, both at the front center C^*. Frame B is massless and reproduces the steering angle δ with respect to body A while frame C describes front tire tractional rotation and has a simple rotation of q_5 with respect to B. The total mass of the main body, m_A, includes the rear tires while m_C is the mass of the virtual-tire. Their inertial principal axes are $[I_{A1}, I_{A2}, I_{A3}]$ and $[I_{C1}, I_{C2}, I_{C3}]$ respectively.

iii) Lengths between front and rear tires from vehicle c.g. along the main body center line are l_1 and l_2 respectively, so that $l_a = l_1 + l_2$. The virtual tire radius is ρ.

iv) There are five generalized coordinates that define the articulation space. The first three, $[q_1, q_2, q_3]$, define the configuration of body A while the other two, [⌐/ q_5], are used respectively for virtual-tire steering angle and front wheel tractional rotation. The symbol ⌐/ has been used instead of the fourth generalized coordinate q_4 to follow the standard notation of the steering angle.

3.1 Kinematics

In this paper, Kane's method (Kane 1985) is used to develop vehicle kinematics and dynamics. This method has been compared with classical Newton-Euler and Lagrangian methods and is considered better (Crolla 1992), especially for systems with several generalized coordinates under nonholonomic constraints. Following Kane's method, the space of generalized speeds, which is a linear combination of generalized coordinate derivatives, is defined as:

$$\begin{aligned} u_1 &= \dot{\delta} \\ u_2 &= \dot{q}_5 \\ u_3 &= \dot{q}_1 \cos q_3 - \dot{q}_2 \sin q_3 \\ u_4 &= -\dot{q}_1 \sin q_3 - \dot{q}_2 \cos q_3 \\ u_5 &= \dot{q}_3 \end{aligned} \tag{1}$$

In Cartesian space, angular velocity of bodies and their c.g. linear speeds are derived as functions of generalized speeds:

$$
\begin{aligned}
{}^N\omega^A &= u_5 \boldsymbol{a}_3 \\
{}^N\omega^C &= (u_1 - u_5)\boldsymbol{a}_3 - u_2 \boldsymbol{b}_1 \\
&= u_2 \cos\delta \boldsymbol{a}_2 - u_2 \sin\delta \boldsymbol{a}_2 - (u_1 - u_5)\boldsymbol{a}_3 \\
{}^N\boldsymbol{v}^{A^*} &= u_3 \boldsymbol{a}_1 - u_4 \boldsymbol{a}_2 \\
{}^N\boldsymbol{v}^{C^*} &= (-l_1 u_5 - u_3)\boldsymbol{a}_1 - u_4 \boldsymbol{a}_2
\end{aligned}
\tag{2}
$$

where, for example, ${}^N\omega^A$ is the angular velocity of body A with respect to the Newtonian reference frame N. The symbol "*" refers to the c.g.

3.1.1 *Nonholonomic Constraints*

Slippage-free motion is a nonholonomic constraint which imposes dependencies between the generalized speeds. To obtain the constraint equations, velocities of two constrained points[4] are derived as:

$$
\begin{aligned}
{}^N\boldsymbol{v}^{\hat{a}} &= (l_2 u_5 - u_3)\boldsymbol{a}_1 - u_4 \boldsymbol{a}_2 \\
{}^N\boldsymbol{v}^{\hat{c}} &= (-l_1 u_5 - \rho u_2 \sin\delta - u_3)\boldsymbol{a}_1 - (u_4 - \rho u_2 \cos\delta)\boldsymbol{a}_2
\end{aligned}
\tag{3}
$$

where $\hat{a}$ is the center point between the rear tires and $\hat{c}$ is the point of contact between the virtual-tire and the road.

The constraint equations can be derived given that ${}^N\boldsymbol{v}^{\hat{a}} \cdot \boldsymbol{a}_1 = 0$ and ${}^N\boldsymbol{v}^{\hat{c}} = 0$:

$$
u_3 = \rho\left(\frac{l_1}{l_a} - 1\right) u_2 \sin\delta \quad , \quad u_4 = \rho u_2 \cos\delta \quad , \quad u_5 = \frac{\rho}{l_a} u_2 \sin\delta \tag{4}
$$

Because of the dependency caused by the constraints, only two DOF's remain independent: steering speed u_1 and traction speed u_2. By substituting u_3, u_4 and u_5 in eq. (2) of the car-like robot, the main body velocities, i.e. linear and angular velocities of body A, become functions of the system configuration and the virtual-tire rotational speed u_2. Let us define $\dot{\boldsymbol{q}} = [u_1 \;\; u_2]^T$ as the vector of articulation speeds and $\dot{\boldsymbol{P}} = [\,{}^N v^{A^*} \;\; {}^N \omega^A]$ as the column vector of Cartesian velocities defined in reference frame N. Substituting eq. (4) into $\dot{\boldsymbol{P}}$ results in matrix form: $\dot{\boldsymbol{P}} = J_{32}\dot{\boldsymbol{q}}$. The configuration dependent Jacobean matrix J_{32} is:

$$J_{32} = \begin{bmatrix} 0 & \rho(\frac{l_1}{l_a} - 1)\sin\delta \\ 0 & \rho\cos\delta \\ 0 & \frac{\rho}{l_a}\sin\delta \end{bmatrix} \tag{5}$$

3.1.2 *Kinematic Comparison with Omnidirectional Robots*

It is of interest to point out some kinematic differences between a car-like robot and an omnidirectional mobile robot since they influence the design of the controller. The Jacobean matrix given by eq. (5) has a column of zero because the linear and angular velocities of a car-like robot are dependent variables due to the application of nonholonomic constraints.

Therefore, there is no inverse kinematic solution for any system configuration if these variables are chosen as control outputs.

To compare with an omnidirectional robot, the virtual tire of the vehicle, shown in figure 1, is replaced by a caster wheel and the two rear wheels are independently actuated. Superscript "o" is used for the omnidirectional robot to define $\dot{\boldsymbol{P}}^{o} = [\,{}^{N}\boldsymbol{v}^{A^*} \;\; {}^{N}\boldsymbol{\omega}^{A}]$ and $\dot{\boldsymbol{q}}^{o} = [u_1^{o} \;\; u_2^{o}]^T$ with u_1^{o} and u_2^{o} being the linear velocities of the actuated wheels along the unit vector $\boldsymbol{a}_2$.

Writing the relation $\dot{\boldsymbol{P}} = J_{32}^{o}\,\dot{\boldsymbol{q}}$, the Jacobean matrix can thus be found as:

$$J_{32}^{o} = 1/2\begin{bmatrix} l_1 & -l_1 \\ 1 & 1 \\ 1 & -1 \end{bmatrix}$$

This Jacobean matrix is a constant full-rank matrix and is not configuration dependent. The non-singular Jacobean J_{32}^{o} permits the control of vehicle position and orientation (Saha 1989). For a car-like robot, the dependency between Cartesian velocities, both of which are only functions of the second articulated speed u_2, results in a different control design. Intuitively, this confirms that the state linearisation of a car-like robot under nonholonomic constraints is impossible (Bloch 1992).

Furthermore, the kinematic differences between a car-like robot and an omnidirectional robot can also be explained by the pivot point displacement, ie the displacement of the point around which the vehicle turns. For a car-like robot, this point lies at the intersection of the virtual-tire axis and the rear tire rotational axis (C_r in figure 1) which is not a stationary point with respect to frame A. Two factors, a geometrical and a velocity parameter, influence the linear and angular velocities of a car-like robot: i) the pivot point location which depends on the steering angle δ, not on its derivative u_1, and ii) the virtual-tire traction speed u_2. Thus, it seems that the two controlled outputs should be chosen from two spaces: one from geometrical space and the other from velocity space.

For an omnidirectional mobile robot, the pivot point is stationary and permits its angular and linear velocities to be graphically decomposed into two vectors (figure 2): angular velocity with a magnitude of $(u_1^o - u_2^o)/2$ and linear velocity with a magnitude of $(u_1^o + u_2^o)/2$.

Because these two vectors are explicit functions of both articulated speeds, they can be controlled separately.

3.2 Vehicle Dynamics

3.2.1 *Equations of Motion*

The vehicle e.o.m.'s have been derived following Kane's method. Let T_{ab} be the steering torque applied from body A to B with the same signs as u_1, and T_{bc} be the traction torques applied from B to C with the same signs as u_2. Thus, the car-like e.o.m.'s are written as:

$$\begin{aligned} I_{C3}\dot{u}_1 - K_4\sin\delta\dot{u}_2 - K_4\cos\delta u_1u_2 &= T_{ab} \\ K_4\sin\delta\dot{u}_1 - [(K_5 - K_6)\sin^2\delta - K_7]\dot{u}_2 - K_8\sin\delta\cos\delta u_1u_2 &= T_{bc} \end{aligned} \tag{7}$$

where the steering speed u_1 and the traction speed u_2 are the only two independent generalized speeds in the set of equation (1), and I_{C3} is the virtual-tire inertia around unit vector c_3. The constants K_i are given in the appendix. Due to the constraint equations (4), the vehicle has only two DOF's which are represented by the two independent generalized speeds u_1 and u_2, thus, vehicle velocities and accelerations in Cartesian space become functions of these two independent speeds.

Defining $\boldsymbol{t} = [T_{ab} \;\; T_{bc}]^T$ as the vector of input torques, the e.o.m. can be shown in a more compact form as:

$$M\ddot{\boldsymbol{q}} + \boldsymbol{c}^* = \boldsymbol{t} \tag{8}$$

where $M(\delta)$ is the mass matrix and $\boldsymbol{c}^*(\delta, u_1, u_2)$ is the vector of centrifugal and coriolis forces while slippage-free condition is respected. Since the determinant of the mass matrix $M(\delta)$ is never zero in eq. (8) for any δ, the system e.o.m. can be written as:

$$\ddot{\boldsymbol{q}} = M^{-1}[\boldsymbol{t} - \boldsymbol{c}^*] \tag{9}$$

It is more convenient to study a nonlinear control system using the state space equations. Defining the state variables $x_1 = \delta$, $x_2 = \dot{\delta}$, $x_3 = q_5$, $x_4 = \dot{q}_5$, the system e.o.m. can be rewritten as follows:

$$\begin{aligned}
\dot{x}_1 &= x_2 \\
\dot{x}_2 &= f_1(x_1)x_2x_4 - g_1(x_1)T_{ab} - g_2(x_1)T_{bc} \\
\dot{x}_3 &= x_4 \\
\dot{x}_4 &= f_2(x_1)x_2x_4 - g_2(x_1)T_{ab} - g_3(x_1)T_{bc}
\end{aligned} \tag{10}$$

where f_1, f_2, g_1, g_2 and g_3 are nonlinear functions of x_1 and are given in the appendix. The nonholonomic constraint equations are defined in state space as:

$$\begin{aligned}
\dot{x}_5 &= x_4(K_1K_{15}\sin x_1\cos x_7 - \rho\cos x_1\sin x_7) \\
\dot{x}_6 &= x_4(K_1K_{15}\sin x_1\sin x_7 - \rho\cos x_1\cos x_7) \\
\dot{x}_7 &= K_1x_4\sin x_1
\end{aligned} \tag{11}$$

3.2.2 *Comparison with Previous Models*

Our dynamic model of a car-like robot has two major advantages over other models. First, it does not neglect the effect of the main body dynamics on the steering and second, one of the system inputs is the steering torque instead of the steering angle. Although steering dynamics may not require a great amount of torque to achieve the desired steering angle, neglecting it removes one system DOF. Also, in other models, the type of steering input was changed from a torque to a geometrical or kinematic parameter. Using the steering angle as one of the inputs complicates the manipulation of e.o.m.'s and the development of the input-output relationship when the dynamic model is used to develop the control law. The consideration of the steering dynamics in our model adds the previously ignored DOF to the system and results in more homogeneous e.o.m.'s. The simple compact form of eq. (8) can be achieved because the input vector t is a vector of torques. Later in this paper we will see how this consideration simplifies the control law development.

4. CONTROL

4.1 Design of the controller

To control the car-like mobile robot given by eq. (10), the well known input-output feedback linearisation method for nonlinear control has been chosen (Slotine 1991). This approach constructs a nonlinear control law as an inner control loop which transforms the original system model to an equivalent linear model. Thus, an outer control loop is used for the new equivalent model to satisfy the traditional linear control design specification.

Figure 3 shows the basic architecture of our lateral/longitudinal controller. The inner control loop returns the system states to a nonlinear controller to compensate for the vehicle nonlinearities by adding the inverse dynamics and it produces a new linear system with new manipulated variables $v = [v_1 \; v_2]^T$. The state space eq. (10) has to be modified by the coordinate transformation to generate a new space which corresponds to the chosen output control variables $y = [y_1 \; y_2]^T$.

The choice of the new transformed coordinates strongly affects the design of the nonlinear controller since the objective is I/O linearisation. To achieve the lateral and longitudinal control of the mobile robot, the control system manipulates two torque inputs. Therefore, one output variable must be associated with the lateral control while the other one is related to the longitudinal control. Like previous work, the new outputs are: 1. the instantaneous

vehicle radius of curvature, that is, the distance between C_r and $\hat{a}$ measured from the vehicle rear center point, i.e., $y_1 = 1/R^*$, and 2. the vehicle velocity, i.e., $y_2 = {}^N\boldsymbol{v}^{\hat{a}} \cdot \boldsymbol{a}_2$, which have been chosen respectively as the lateral and the longitudinal control variables. Their desired values are expressed as the system input vector $\boldsymbol{y}^d = [y_1^d \; y_2^d]^T$.

The choice of the control point $\hat{a}$ instead of the c.g. presents two benefits. First, when the vehicle instantaneous curvature y_1 tracks its desired value, the error on vehicle orientation (heading angle) is also nullified because the perpendicular line to $\overline{C_r\hat{a}}$ is the vehicle orientation. Secondly, the velocity of the c.g. is the summation of both normal (lateral) and tangential (longitudinal) speeds of the vehicle but it is preferable to control a pure longitudinal speed. Under slippage-free condition, the normal speed at the rear center is zero, i.e. ${}^N\boldsymbol{v}^{\hat{a}} \cdot \boldsymbol{a}_1 = 0$. Thus, by choosing the control point $\hat{a}$, the second output becomes a pure longitudinal velocity.

Let us now apply the feedback linearisation method. The elements of the output vector $\boldsymbol{y}$ are related to the system states as follows:

$$y_1 = \frac{1}{l_a}\tan x_1 \quad \text{and} \quad y_2 = \rho x_4 \cos x_1 \tag{12}$$

To obtain I/O linearization, the vehicle dynamic inputs T_{ab} and T_{bc} must appear explicitly. Thus, the outputs must be differentiated (once for y_2 and twice for y_1) to obtain the following relationship:

$$z = \boldsymbol{h}(x) - D(x_1)t \tag{13}$$

with:

$$D = \begin{bmatrix} d_{11} = K_{17}(1 - \tan^2 x_1) g_1(x_1) & d_{12} = K_{17}(1 - \tan^2 x_1) g_2(x_1) \\ d_{21} = \rho \cos x_1 g_2(x_1) & d_{22} = \rho \cos x_1 g_3(x_1) \end{bmatrix}$$

where $\boldsymbol{h} = [h_1 \;\; h_2]^T$ is the vector of nonlinear functions of the system states given in appendix.

The vector $z = [\ddot{y}_1 \;\; \dot{y}_2]^T$ defines the outputs in the new transformed space of $\{y_1, \dot{y}_1, y_2\}$. Our system is "linearisable" because the inverse of the matrix $D(x_1)$ exists for any value of the steering angle between the physical limits $-\pi/2 < x_1 < \pi/2$. Thus, the nonlinear control output is chosen as:

$$t = D^{-1}(\nu - \boldsymbol{h}) \tag{15}$$

where ν is the new manipulated vector to be determined. By replacing eq. (15) in (13), the nonlinearities are canceled, and a simpler relationship between the output and the new manipulated vector ν, i.e., $z = \nu$, is obtained.

The design of the tracking controller is produced using linear control techniques. For instance, defining $e = y^d - y$ as the tracking error and choosing the new control inputs as:

$$\begin{aligned} v_1 &= \ddot{y}_1^d + \eta_1 e_1 + \eta_2 \dot{e}_1 \\ v_2 &= \dot{y}_2^d + \eta_3 e_2 \end{aligned} \tag{16}$$

with η_1, η_2, η_3 being positive constants, the tracking error of the closed loop system for both lateral and longitudinal control parameters presents exponentially stable error dynamics. Therefore, if the initial lateral and longitudinal errors are zero, then for all t greater than zero perfect tracking is achieved; otherwise, $e(t) = [e_1(t)\ e_2(t)]$ converges exponentially to zero.

4.2 Internal dynamics

The order of our dynamic system given by Eqs. (10) and (11) is seven while the vector relative degree of the designed controller is [2,1]. Therefore, a part of the system dynamics with an order of four, called the internal dynamics, has been rendered unobservable in the I/O linearization. If the internal dynamics is stable, our control design problem has been solved with the control law developed in the previous section. Otherwise, the controller is practically meaningless, because the instability of the internal dynamics would imply undesirable phenomena such as violent vibration of the mechanical unit. For a general discussion of internal dynamics, see (Slotine 1991).

To complete the coordinate transformation to become a diffeomorphism, the vector $\zeta = [y_1 \;\; L_f y_1 \;\; y_2 \;\; x_5 \;\; x_6 \;\; x_7 \;\; x_3]^T$ is chosen as the complete associated transformation, whose Jacobean matrix $\partial\zeta/\partial \boldsymbol{x}$ is :

$$\frac{\partial \zeta(\boldsymbol{x})}{\partial \boldsymbol{x}} = \begin{bmatrix} A & 0 & 0 & 0 & 0 & 0 & 0 \\ B & A & 0 & 0 & 0 & 0 & 0 \\ C & 0 & 0 & \rho c_1 & 0 & 0 & 0 \\ 0 & 0 & 1 & 0 & 0 & 0 & 0 \\ 0 & 0 & 0 & 0 & 1 & 0 & 0 \\ 0 & 0 & 0 & 0 & 0 & 1 & 0 \\ 0 & 0 & 0 & 0 & 0 & 0 & 1 \end{bmatrix} \tag{17}$$

where A, B, C are given in the appendix. Because the determinant of the Jacobean matrix, ie $|\partial\zeta(\boldsymbol{x})/\partial \boldsymbol{x}| = \rho/\cos(x_1)$, is never zero for $-\pi/2 < x_1 < \pi/2$, then $\zeta(\boldsymbol{x})$ becomes a valid state transformation.

The stability of the designed controller depends on the behaviors of the proposed internal dynamics $\dot{\zeta}_{int}$. With the vector ζ defined as $\zeta(\boldsymbol{x}) = [\zeta_1 \;\; \zeta_2 \;\; \zeta_3 \;\; \zeta_4 \;\; \zeta_5 \;\; \zeta_6 \;\; \zeta_7]$, the derivative of the internal dynamics $\dot{\zeta}_{int} = [\dot{\zeta}_4 \;\; \dot{\zeta}_5 \;\; \dot{\zeta}_6 \;\; \dot{\zeta}_7]$ is related to the controlled outputs as follows:

$$\dot{\zeta}_{int} = 1/\rho \begin{bmatrix} K_1 K_{15} t_1 c_7 - \rho s_7 \\ K_1 K_{15} t_1 s_7 - \rho c_7 \\ K_1 t_1 c_{17} \\ 1/c_1 \end{bmatrix} \zeta_3 \tag{18}$$

where

$$c_i = \cos(x_i) \qquad s_i = \sin(x_i)$$
$$t_i = \tan(x_i) \qquad c_{ij} = \sin(x_i - x_j)$$

Putting system outputs equal to zero, the zero dynamics is yield to $\dot{\zeta}_{zero} = 0$. It is easily seen from eq. (18) that even if internal dynamics is not necessarily bounded, $\dot{\zeta}_{int} = [\dot{\zeta}_4 \ \dot{\zeta}_5 \ \dot{\zeta}_6 \ \dot{\zeta}_7]^T$ will stay bounded for bounded values of ζ_3. Hence, the system stability will not perturbed since it is only affected by the derivatives of the internal dynamic.

In a real system, the inner control loop used to linearize the system approximately because the linearisation relies on the system model, both for the controller design and for the computation of the new transformed states ζ. If there is any uncertainty, it will cause error in the computation of both of the new transformed states ζ and of the control input vector v. However, the most important property of the I/O feedback linearisation method is not necessarily that the nonlinearities can be exactly canceled by nonlinear feedback. Once an appropriate coordinate system is found in which the system can be linearized, the

nonlinearities are in the range space of the input (Spong 1989). This fact eases the application of other techniques such as *robust* or *adaptive* control design.

5. SIMULATION

Simulations have been performed using Matlab (Simulink) to verify the behavior of the vehicle dynamic model and the effectiveness of the proposed control law. The vehicle parameters given in the appendix have been selected to closely resemble most of today's middle class front wheel vehicles, such as the Honda Accord. The gains for the linear outer loop control have been chosen to obtain a critically damped system for the decoupled nonlinear subsystem. The system performance has been studied under three circumstances and simulations have been carried out for: 1) the effect of initial conditions, 2) piecewise continuous trajectories, and 3) the effect of modeling uncertainties. The first two simulations validate our control law when applied to the car-like mobile robot given by eq. (10). The last simulation verifies the performances of our control system when the vehicle under control is different from the one used to develop the control laws.

5.1 Effect of Initial Conditions

Nonlinear systems frequently have more than one equilibrium point, and their stability may depend on initial conditions. The nonlinear control law (inner control loop) developed in the previous section transforms the original nonlinear system model to an equivalent linear

system. Therefore, our system should behave like a linear system in which the equilibrium point is unique and its stability is independent of initial conditions. To verify the effect of initial conditions on the performance of our control law, mobile robot behavior is simulated under sharp changes from vehicle initial state to different initial desired values.

The initial state of the vehicle is an equilibrium at $[y_1 \;\; y_2] = [0 \;\; 0]$: zero steering angle, which is equivalent to a zero road curvature, and zero velocity. The desired trajectory is a constant road curvature with constant speed: $[y_1^d \;\; y_2^d] = [1/R_i \;\; V_i]$. In spite of different initial values for lateral and longitudinal controlled outputs, both system errors converge exponentially to zero and remain there (figure 4).

5.2 Piecewise Continuous Trajectories

The following simulation verifies the tracking capabilities of our controller when both desired inputs change. To make the first two derivatives continuous, the desired trajectories have been constructed using a combination of third order polynomials and constant step offsets (figure 5). These time-variable input functions vary independently, and the vehicle can accelerate or decelerate while the desired road curvature is being tracked. To respect the slippage-free condition, the desired trajectory is defined in such a way that the lateral acceleration stays below the critical acceleration, which is around 0.6g in normal road condition.

Figures 6 and 7 show the simulation results. In figure 6, the errors on path curvature and vehicle speed remain very small during the trajectory tracking. The maximum error on path curvature is 1.2×10^{-5} m^{-1} while the maximum error on velocity is 3.2×10^{-7} m/s. Maximum errors occur at the junction of the third order polynomial with the constant steps because there is no continuity imposed on the angular and linear accelerations of the vehicle. Fifth order polynomial transitions would reduce the magnitude of the errors. The commands generated by our control system produce a smooth variation of the steering angles, reasonable traction torque and acceptable tractional power (figure 7).

5.3 Effect of Modeling Uncertainties

As discussed in Section 4, the nonlinear control law (inner control loop) exactly transforms the system to a linear one if the vehicle under control corresponds to the simplified model. In practice, the vehicle dynamics is more complicated than our two DOF dynamic model, and there are always uncertainties on some parameters, e.g. the mass associated with the passengers. Thus, the inner control loop does an approximate linearisation of the real system. Because our simplified model reproduces major vehicle dynamics behaviors, the control law should remain valid. Therefore, the purpose of the next simulation is to verify the efficiency of our controller when the vehicle under control is different from our simplified vehicle model.

To this end, system performance is verified in the presence of parameter uncertainties. The vehicle mass and inertia are increased by 50% and the vehicle size by 20% while the controller parameters and the desired trajectories are kept the same. Figure 8 shows the resulting errors in both output variables, but even in the presence of very poor model estimation, it can be seen that the resulting output errors are still very small. Although a theoretical robustness analysis was not performed, it appears from extensive simulations that the scheme is quite robust.

6. CONCLUSION

A method for controlling a car-like mobile robot under nonholonomic constraints has been developed. Differences between the nature of a car-like robot and a wheeled mobile robot have been highlighted and a nonlinear feedback loop, which guarantees the I/O stability of the system, has been designed. In spite of the kinematic complexities of the car-like mobile robot compared to the omnidirectional one, our vehicle model has a compact mathematical form. Unlike other nonlinear controller designs based on kinematic vehicle models, our control scheme is based on a nonlinear vehicle dynamic model. Lateral and longitudinal outputs are controlled independently and no limitations, such as low speed or smooth curvature, are imposed on the desired trajectories from the controller. The internal dynamics and its stability is discussed in details and it has been shown that it stays stable while the controller is tracking its objectives. Therefore, this work can be used for development of control strategies in highway vehicle automation.

REFERENCES

Allen R.W., Rosenthal T.J. and Szostack H.T., 1987, *Steady State and Transient Analysis of Ground Vehicle Handling*, SAE Paper, No. 870495, pp. 49-78.

Bloch A.M., Reyhanoglu M., and McClamroch N.H., 1992, *Control and Stabilization of Nonholonomic Dynamic Systems,* IEEE Transactions on Automatic Control, Vol. 37, No.11, pp. 1746-1757.

Baumgartner E.T. and Skaar S.B., 1994, *An Autonomous Vision-Based Mobile Robot*, IEEE Transactions on Automatic Control, Vol. 39, No. 3, pp. 493-502.

Crolla D.A. and Schwanghart H., 1992, *Vehicle Dynamics-Steering I*, Journal of Terramechanics, Vol. 29, No. 1, pp. 7-17.

DeSantis R.M., 1994, *Path-tracking for a Tractor-Trailer-like Robot*, International Journal of Robotic Research, Vol. 13, No. 6, pp. 533-544.

DeSantis R.M., 1995, *Modeling and Path-tracking Control of a Mobile-Wheeled Robot with a Differential Drive*, Robotica, Vol. 13, pp. 401-410.

Ellis J.R., 1969, *Vehicle Dynamics*, Business Books Limited, London, 240 p.

Fenton R.E., Melocik G.C. and Olson K.W., 1976, *On the Steering of Automated Vehicles: Theory and Experiments*, IEEE Transactions on Automatic Control, Vol. AC-21, No.3, pp.306-315.

Hemami A., Mehrabi M.G., and Cheng R.M.H., 1992, *A Synthesis of an Optimal Control Law for Path Tracking in Mobile Robots*, Automatica, Vol.8, No.2, pp. 383-387.

Jagannathan S., Zhu S.Q. and Lewis F.L., 1994, *Path Planning and Control of a Mobile Base with Nonholonomic Constraints*, Robotica, Vol. 12, pp. 529-539.

Jurie F., Rives P., Gallice J. and Brame J.L., 1994, *High Speed Vehicle Guidance Based on Vision*, Control Engineering Practice, Vol.2, No.2, pp. 289-297.

Kane T.R. and Levinson D.A., 1985, *Dynamics Theory and Applications,* McGraw-Hill Series in Mechanical Engineering, New York, 379 p.

Langer D., Rosenblatt J.K. and Hebert M., 1994, *A Behavior-Based System for Off-Road Navigation*, IEEE Transactions on Robotics and Automation, Vol.10, No.6, pp.776-783.

Lu P. and Lin K.-C., 1994, *Nonlinear Control of an Autonomous Tracked Vehicle*, Transactions of the Institute of Measurement and Control, Vol. 16, No. 4, pp. 214-220.

Narendran V.K. and Hedrick J.K., 1994, *Autonomous Lateral Control of Vehicles in an Automated Highway System*, Vehicle System Dynamics, Vol. 23, pp. 307-324.

Saha S.K. and Angeles J., 1989, *Kinematics and Dynamics of a Three-wheeled 2-DOF AGV*, Proceedings of the IEEE Conference on Robotics and Automation, pp. 1572-1577.

Sarkar N., Yun X. and Kumar V., 1994, *Control of Mechanical Systems with Rolling Constraints: Application to Dynamic Control of Mobile Robots*, International Journal of Robotics Research, Vol. 13, No. 1, pp. 55-69.

Shim H.-S., Kim J.-H. and Koh K., 1995, *Variable Structure Control of Nonholonomic Wheeled Mobile Robots*, Proceedings of the 1995 IEEE International Conference on Robotics and Automation, Nagoya, Japan, part 2/3, pp. 1694-1699.

Slotine J.J and Li W., 1991, *Applied Nonlinear Control*, Prentice-Hall, 207 p.

Smith D.E. and Starkey J.M., 1991, *Overview of Vehicle Models, Dynamics, and Control Applied to Automated Vehicles*, ASME, Advanced Automotive Technologies, DE-Vol. 40, pp.69-87.

Spong M.W. and Vidyasagar M., 1989, *Robot Dynamics and Control*, John Wiley & Sons, 336 p.

Tsugawa S., 1994, *Vision-Based Vehicles in Japan: Machine Vision Systems and Driving Control Systems*, IEEE Transactions on Industrial Electronics, Vol.41, No.4, pp.398-405.

ACKNOWLEDGMENTS

The authors wish to thank PhD students P. Bigras, J. Sévigny, and D.A. Rey for their valuable comments, suggestions and discussions. We would also like to acknowledge our appreciation of the NSERC for their financial support under grant OGP0138153.

Appendix

The mobile robot parameters and the constants used in dynamic e.o.m.'s, eq. (7) are defined as:

$\rho = 0.33\ m$ $\quad l_1 = 1.41\ m$ $\quad l_a = 2.82\ m$

$I_{C3} = 0.1455\ kg.m^2$ $\quad I_{C1} = 0.1\ kg.m^2$ $\quad I_{A3} = 2232\ kg.m^2$

$m_A = 1416\ kg$ $\quad m_C = 5\ kg$

$K_1 = \rho / l_a$ $\quad K_2 = l_1^2 - 2 l_a l_1$ $\quad K_3 = K_1^2 K_2$

$K_4 = K_1 I_{C3}$ $\quad K_5 = K_3 m_A$ $\quad K_6 = K_1^2 (I_{C3} + I_{A3})$

$K_7 = I_{C1} + \rho^2 (m_A + m_C)$ $\quad K_8 = K_1^2 m_A l_1 (l_1 - 2 l_a) + K_6$ $\quad K_9 = K_5 + K_6$

$K_{10} = -K_4^2 - K_9 I_{C3}$ $\quad K_{11} = I_{C3} K_7$ $\quad K_{12} = K_4 (K_8 - K_9)$

$K_{13} = -K_4 K_7$ $\quad K_{14} = K_4^2 - K_8 I_{C3}$ $\quad K_{15} = l_1 - la$

$K_{16} = l_1 / la$ $\quad K_{17} = 1 / la$

The derived functions in the state space, eq. (10), and the nonlinear control functions of section 4 are derived as:

$$f_1(x_1) = M^* (K_{12} \sin^2 x_1 - K_{13}) \cos x_1$$

$$f_2(x_1) = M^* K_{14} \sin x_1 \cos x_1$$

$$h_1(\boldsymbol{x}) = K_{17} (1 + \tan^2 x_1)[2 x_2^2 \tan x_1 + f_1(x_1) x_2 x_4]$$

$$h_2(\boldsymbol{x}) = \rho x_4 x_2 [f_2(x_1) \cos x_1 - \sin x_1]$$

$$g_1(x_1) = M^* (K_9 \sin^2 x_1 - K_7)$$

$$g_2(x_1) = -M^* K_4 \sin x_1$$

$$g_3(x_1) = M^* I_{C3}$$

where $M^* = 1/(K_{10}\sin^2 x_1 - K_{11})$ is the inversion of the mass matrix determinant.

List of figures

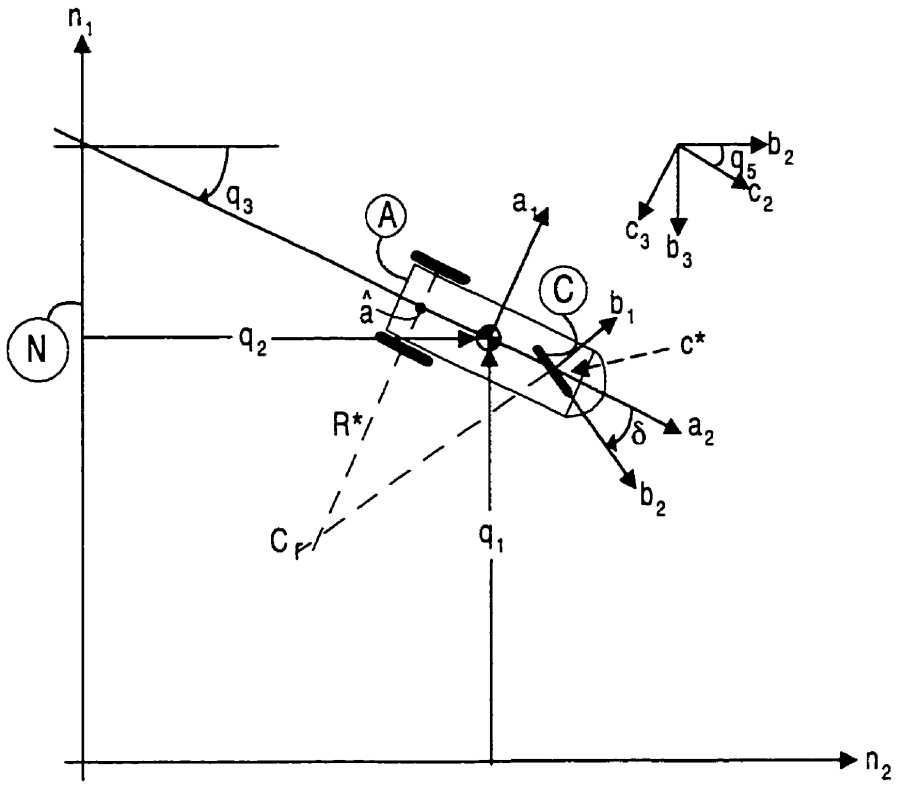

Figure 1 - A car-like planar vehicle with front wheel traction and steering.

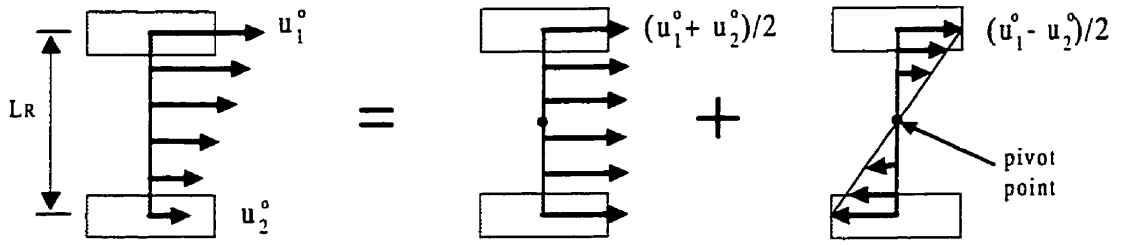

Figure 2 - Superposition of angular and linear velocities of an omnidirectional mobile robot.

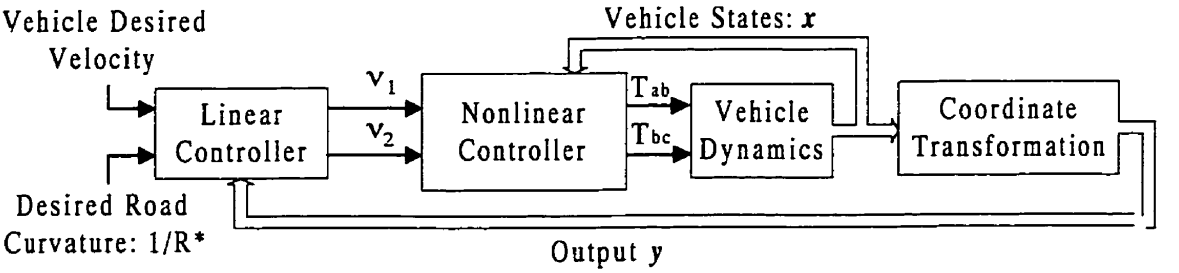

Figure 3- Architecture of our lateral/longitudinal controller.

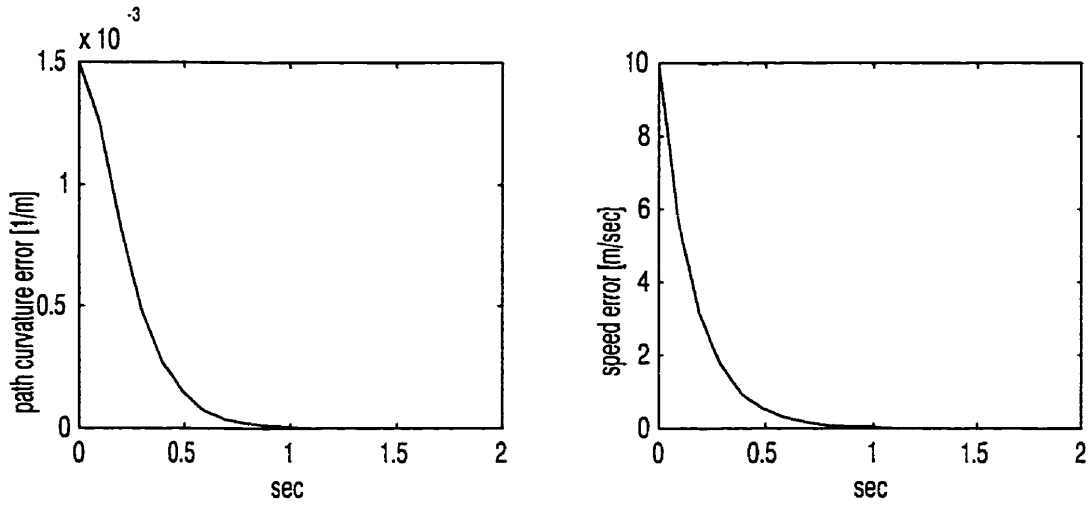

Figure 4 - Simulation result for the initial condition effect having the outer loop designed for critical damping and response time of 0.5 sec.

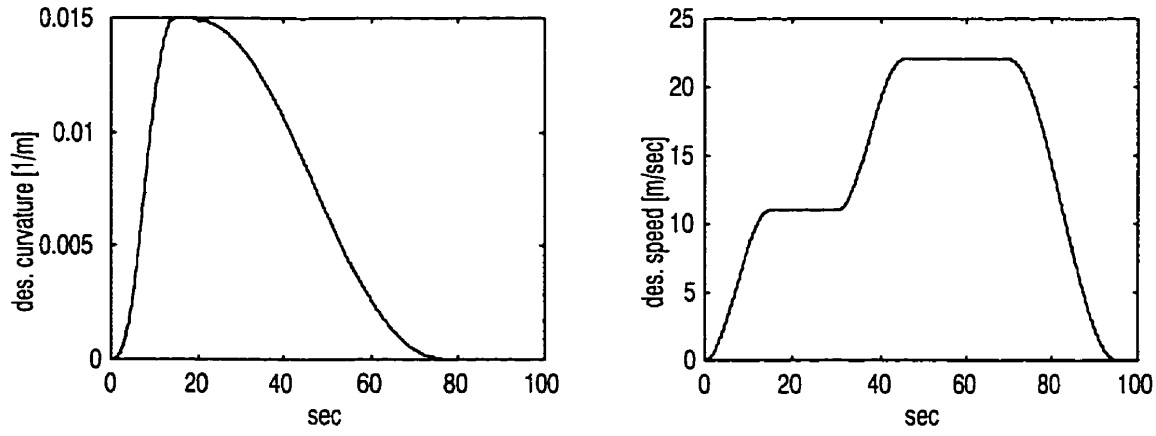

Figure 5 - Desired lateral (path curvature) and longitudinal (speed) control inputs.

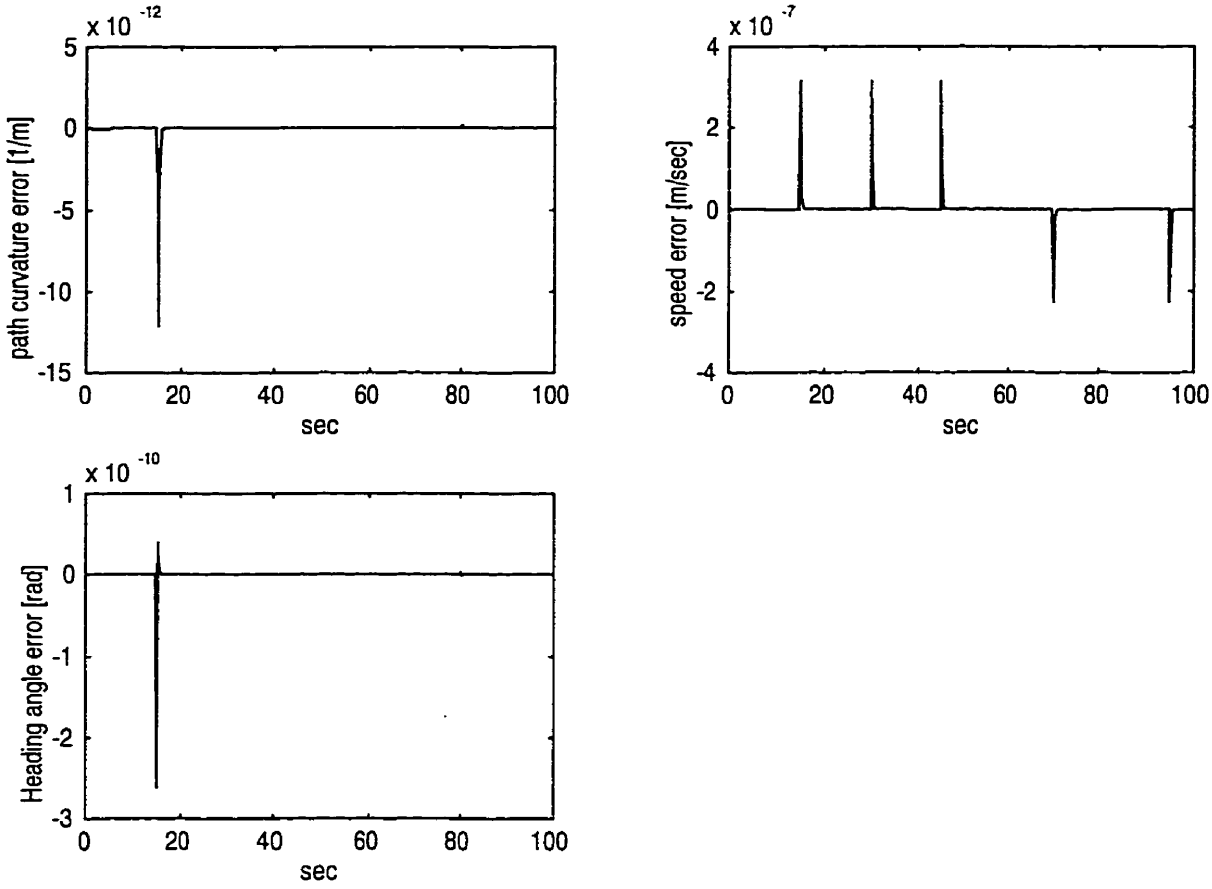

Figure 6 - Tracking results of the simulation with the input trajectories of figure 5.

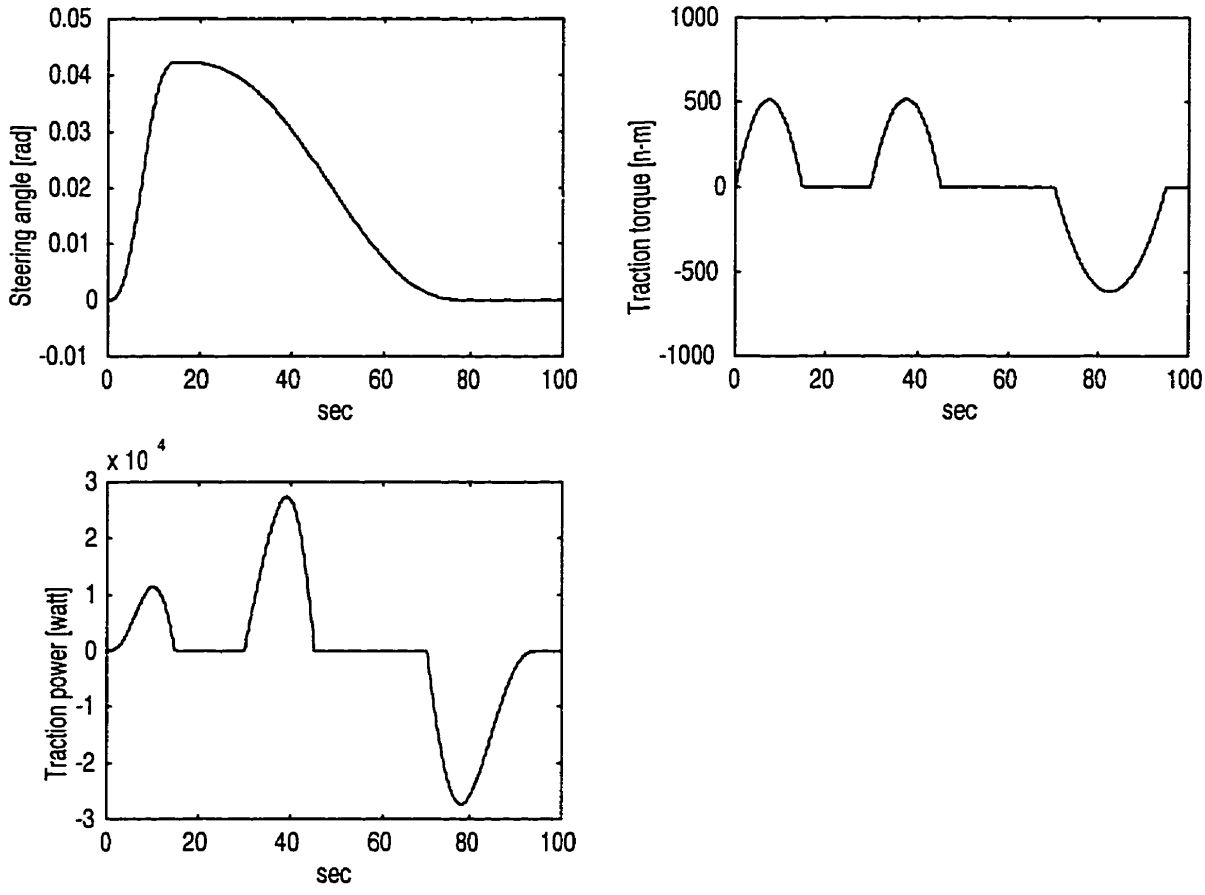

Figure 7 - Variations of some system characteristics during the trajectory tracking of figure 5.

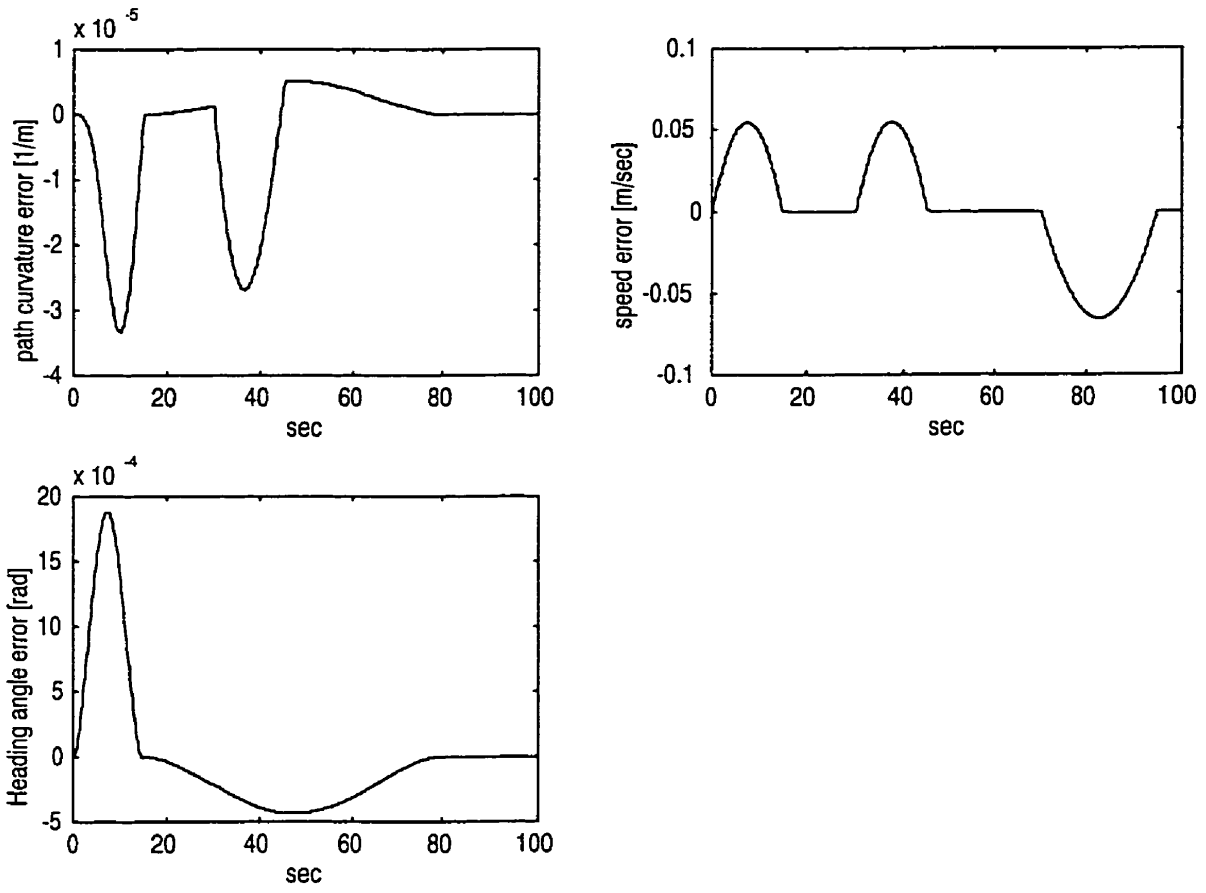

Figure 8 - Tracking results of the lateral and longitudinal control outputs with parameter uncertainties.

List of footnotes:

1. **Saéd M. Ehsani** is a Ph.D. student at the Mechanical Engineering Department (design section), of École Polytechnique de Montréal. P.O. Box 6079 "Station Centre-Ville", Montréal, Québec, Canada, H3C 3A7. E-Mail: saed@gpa.etsmtl.ca, Fax. (514) 340-5867, Tel. (514) 733-7233

2. **Mario Tetreault** is a professor at the Automated Production Engineering Department of "École de Technologie Supérieure". 4750 Henri-Julien Street, Montréal, Québec, Canada, H2T 2C8

E-Mail: tetreaul@gpa.etsmtl.ca, Fax. (514) 289-9042, Tel. (514) 289-8800 ext. 7602

3. **Michel Gou** is a professor at the Mechanical Engineering Department (design section) of École Polytechnique de Montréal, P.O. Box. 6079 "Station Centre-Ville", Montréal, Québec, Canada, H3C 3A7. E-mail michel.gou@mailsrv.polymtl.ca, Fax. (514) 340-5867, Tel. (514) 340-4669

Appendix B: Looking Ahead Path Tracking of a Car-like Mobile Robot.

Looking Ahead Path-tracking for a Car-like Robot

Ehsani, S.M., Ph.D.
Mechanical Engineering Department,
École Polytechnique de Montréal,
2900 Édouard-Montpetit, Montreal, H3C 3A7, Canada.
Email: saed@gpa.etsmtl.ca, Fax (514) 396-8595

Tétreault, M., Professor,
GPA Department,
École de Technologie Supérieure,
1100 Notre-Dame Ouest, Montréal, H3C 1K1, Canada.
Email: tetreaul@gpa.etsmtl.ca, Fax (514) 396-8595

Bigras, P., Professor,
GPA Department,
École de Technologie Supérieure,
1100 Notre-Dame Ouest, Montréal, H3C 1K1, Canada.
Email: bigras@gpa.etsmtl.ca, Fax (514) 396-8595

Gou, M., Professor,
Mechanical Engineering Department,
École Polytechnique de Montréal,
2900 Édouard-Montpetit, Montreal, H3C 3A7, Canada.
Email: michel.gou@mail.polymtl.ca, Fax (514) 340-5867

Abstract

This paper studies the path tracking of a car-like mobile robot subject to nonholonomic constraints. To develop the control law, a planar vehicle model is chosen to simulate the rigid-body dynamics. Although the smooth state stabilization of such systems is impossible, an Input/Output Feedback Linearisation can be achieved by choosing a steerable *control-point* in front of the robot. Also, the consideration of steering dynamics results in a compact mathematical form of equations of motion and makes the control law development straight forward. The developed control law ensures the exponential convergence of the control-point Cartesian coordinates to the desired values. Completing the diffeomorphism,it is shown that speeds in the system unobservable (internal) dynamics stay bounded for bounded external dynamic outputs. The control of the vehicle speed becomes also possible for paths composed of straight line and circular arc segments. Simulations are carried out to verify the system performance and to show that even without any off-line path planning the point tracking of the steerable point results in a minor change in the vehicle maximum lateral error.

Keywords: Nonholonomic systems, nonlinear control, path tracking, mobile robot, car-like, internal dynamics stability

1. INTRODUCTION

Recently, control of mobile systems with nonholonomic constraints is one of the active research areas which consists of kinematics, dynamics as well as nonlinear control of mobile robots. The consideration of vehicle rigid-body dynamics in the control law development has advantages over the controllers based on kinematic models which restrict the application to low speed and smooth maneuvers in order to ensure the system stability.

Nonlinear systems without drift having less inputs than states have been shown not to be stabilized by pure smooth state feedback [2],[3]. Example of such systems are mobile robots with nonholonomic constraints. Related works can be classified into two different families due to the kinematic behavior of mobile robots: the omnidirectional mobile robots with two independently actuated wheels [9],[11],[14],[17],[18],[24] and car-like mobile robots which is our field of interest [5],[7],[8],[10],[12],[22],[23]. Omnidirectional robots have simpler kinematics and dynamics than car-like mobile robots. More precisely, the Jacobian matrix between Cartesian speeds and speeds of the actuated wheels is independent from the robot configuration with constant terms. This fact results in a simpler inverse kinematics and eases the control law development . The path tracking and stability of omnidirectional robots have been widely studied before, and control laws have been developed based on both kinematic [11], [18] and dynamic [9],[14],[22],[24] models.

Mathematically, the kinematic equations of both robot families can be converted to the so-called canonical chain form equations. Therefore, a new approach, i.e. chain form system,

has been introduced to model the kinematics of a class of nonholonomic mechanical systems [1],[4],[13],[20],[21]. By this approach, the motion planning and kinematic control of car-like mobile robots pulling n passive or steerable trailers linked together with rigid bars can be studied, solving a set of canonical chained form equations [20]. Then, the kinematic control problem of single mobile robots becomes a subgroup of n chained robots [13]. Since these controllers are based on kinematic models, they are limited to low speed applications.

Controllability implies that any configuration should theoretically be reached in finite time from any other configuration by applying an adequate control input. The non-existence of smooth state-feedbacks enhances the chance of designing controllers with time varying feedbacks [2],[5],[12],[23] or variable structures [15], as alternatives. The Input/Output Feedback Linearisation (I/OFL) is also another alternative [8],[9],[14],[24] with the advantage of having a time-invariant structure.

Kinematics of car-like robots are more complex than ones of omnidirectional robots. As a result, few controllers have been developed for this family of robots, especially with the consideration of dynamics. Among the existing work, DeSantis [7] has used the I/OFL method and presented a design procedure for path tracking controllers which is applicable to car-like robots and which relates path tracking assignment parameters, such as vehicle speed and the radius of curvature, to the controller structure and gains. However, this work resulted in a time-variant controller capable of tracking a planned path using linear control technics. Andréa-Novel et al. [6] figured out that for car-like mobile robots a possible choice

of linearisation is the Cartesian coordinates of a point attached to the steering wheel. They concluded that the point tracking problem of such robots is solvable with an appropriate choice of the control-point.

In this paper, a dynamic model of a planar car-like robot which includes the usually neglected steering dynamics is developed. Both inputs of this dynamic model are torques and both are of the same nature with the advantage of having physical interpretation. Based on this model, a control law is developed using the I/OFL for a chosen control-point in front of the vehicle in order to solve the point tracking problem of a car-like robot for any desired paths in the Cartesian space. Reproduction of one of the basic human driver behavior, i.e. looking ahead in front of the vehicle, is the idea behind this choice. The stability of tracking errors is ensured and the diffeomorphism is completed to show that unobservable speeds in the so-called internal dynamics stay bounded.

Although the steerable control-point is not on the vehicle main body, this paper shows that the path tracking problem of any fixed-point can be transferred to the point tracking of the steerable control-point adding an off-line path planning process. Anyhow, simulations based on a real car size reveal that the point tracking of the steerable control point without path planning only results in a minor increase in the maximum lateral offset of the vehicle. For desired paths composed of straight lines and circular arc segments, the vehicle speed can also be controlled with different constant speed at each segment.

The paper consists of four additional sections. Section 2 presents the dynamic model of the planar car-like robot. The choice of the control-point, the design of the controller and the stability of internal dynamics are discussed in section 3. The simulations are in section 4, and section 5 concludes the paper.

2. Vehicle Dynamics

A real car is a complex dynamic system, but when the goal is the development of an efficient control law, it is not necessary to model the whole complexities such as tire and suspension. A planar car-like mobile robot can simulate the basic vehicle *configurations* changes, i.e. changes of Cartesian position and orientation of the vehicle.

This section summarizes the kinematics and dynamics of a car-like mobile robot. The planar robot of figure 1 is a front-wheel drive vehicle where the steering effect of both front wheels is represented by one virtual-tire (body C). This consideration is not restrictive because the front wheels are linked to each other and represent only one d.o.f. Since body C has two perpendicular rotations with respect to the vehicle main body (body A), the frame of body B is introduced to have one simple rotation between the consecutive attached frames, ie "q_4" between A and B and "q_5" between B and C. Total of five generalized coordinates defines the vehicle joint space. The first three, $[q_1, q_2, q_3]$, are the robot main body configuration in Cartesian space, and the two others, $[q_4, q_5]$, are for virtual-tire steering, and front wheel rotation, respectively.

Defining $u_1 = \dot{q}_4$, $u_2 = \dot{q}_5$, $u_3 = \dot{q}_1 \cos q_3 - \dot{q}_2 \sin q_3$, $u_4 = -\dot{q}_1 \sin q_3 - \dot{q}_2 \cos q_3$, $u_5 = \dot{q}_3$, the system kinematics equations under the usual slipping-free assumption have been derived. Assumption which results in three kinematic constraint equations and two dynamic equations of motions (e.o.m.):

$$\begin{aligned} u_3 &= K_1 K_{15} u_2 \sin q_4 \\ u_4 &= \rho u_2 \cos q_4 \\ u_5 &= K_1 u_2 \sin q_4 \\ I_{C3} \dot{u}_1 - K_4 \sin q_4 \dot{u}_2 - K_4 \cos q_4 u_1 u_2 &= T_{ab} \\ K_4 \sin q_4 \dot{u}_1 - [K_9 \sin^2 q_4 - K_7] \dot{u}_2 - K_8 \sin q_4 \cos q_4 u_1 u_2 &= T_{bc} \end{aligned} \tag{1}$$

where ρ and I_{C3} are respectively the radius and the principal inertia of the virtual-tire around the unit vector c_3 . K_i's are constants defined in the appendix to simplify the e.o.m.'s representation. T_{ab} and T_{bc} are the steering torque applied from body A to B and the traction torques applied from B to C, respectively. The sign of T_{ab} and T_{bc} are respectively defined by the same reference adopted for u_1 and for u_2. With the vector of input torques $\boldsymbol{t} = [T_{ab} \;\; T_{bc}]^T$, the system e.o.m., i.e. last two equations in eq. (1), becomes:

$$M\ddot{\boldsymbol{q}} - \boldsymbol{c}^* = \boldsymbol{t} \tag{2}$$

where $M(q_4)$ is the inertia matrix and $\boldsymbol{c}^*(q_4, u_1, u_2)$ is the vector of centrifugal and Coriolis forces. The above second order differential eq. (2) can be reformulated as a set of first order differential equations which is more convenient for control design. Defining the state space

variables for the FWD robot as: $x_1 = q_4$, $x_2 = \dot{q}_4$, $x_3 = q_5$, $x_4 = \dot{q}_5$, $x_5 = q_1$, $x_6 = q_2$, $x_7 = q_3$, the state-space representation of the system is then:

$$\dot{x} = f(x) - \Gamma(x)t \tag{3}$$

where f and Γ are:

$$f = \begin{bmatrix} x_2 & f_1 x_2 x_4 & x_4 & f_2 x_2 x_4 & x_4(K_1 K_{15} s_1 c_7 - \rho c_1 s_7) & x_4(K_1 K_{15} s_1 s_7 - \rho c_1 c_7) & K_1 x_4 s_1 \end{bmatrix}^T$$

$$\Gamma = \begin{bmatrix} 0 & g_1 & 0 & g_2 & 0 & 0 & 0 \\ 0 & g_2 & 0 & g_3 & 0 & 0 & 0 \end{bmatrix}^T \tag{4}$$

where f_1, f_2, g_1, g_2, g_3 are nonlinear functions, and c_i, s_i, t_i $(i = 1,7)$ are respectively the cosine and the sine of the state space variable x_i.

3. Looking Ahead Path Tracking

To control the car-like mobile robot given by eq. (3), the I/OFL method [16] has been chosen. Although the stabilization via smooth feedback of such a system is not possible, a static input/output linearization, if exist, can ensure the stability of the external dynamics given by the above e.o.m, and the exponential convergence of the tracking error from the desired values. However, the stability of the unobservable (internal) dynamics caused by the constraint equations must also be verified. Figure 2 shows the basic architecture of the I/OFL based controller. The inner control loop returns the system states to the nonlinear controller to compensate the steering and traction dynamic nonlinearities. The result is a new linear system with new manipulated variables $\nu = [\nu_1 \ \nu_2]^T$. Then the state space eq. (3) is brought

to the space of output variables. In this paper, the output variables are the Cartesian coordinates of a steerable point P in front of the vehicle (figure 1).

3.1 **Choice of Control-Point**

For a control law development based on I/OFL method, the important step is to choose the appropriate outputs which results in a non-singular decoupling matrix. As it is seen in literature, a control-point attached to the vehicle main body, such as the center of gravity (c.g.), seems to be the best choice. In fact, it can be an appropriate choice for the family of omnidirectional mobile robots because the angular velocity of each actuated wheel affects both Cartesian velocities of such mobile robots. Kinematics of a car-like mobile robot are quite different from an omnidirectional one since its Jacobian matrix is singular for any control-point attached to the robot main body. In other word, when the angular velocity of the front wheel (around b_1 in figure 1) is zero, the steering commands will not affect motions of such control-points. In the Newtonian reference frame *N*, the position vector of an arbitrary control-points P^* attached to the body *A* in figure 1 is:

$$\boldsymbol{p}^* = \begin{bmatrix} x_{p^*} \\ y_{p^*} \end{bmatrix} = \begin{bmatrix} x_6 \\ x_5 \end{bmatrix} - \begin{bmatrix} \cos x_7 & -\sin x_7 \\ \sin x_7 & \cos x_7 \end{bmatrix} \begin{bmatrix} X_a \\ Y_a \end{bmatrix} \tag{5}$$

and its derivative is :

$$\begin{bmatrix} \dot{x}_{p^*} \\ \dot{y}_{p^*} \end{bmatrix} = \begin{bmatrix} \dot{x}_6 \\ \dot{x}_5 \end{bmatrix} + \dot{x}_7 \begin{bmatrix} -\sin x_7 & -\cos x_7 \\ \cos x_7 & -\sin x_7 \end{bmatrix} \begin{bmatrix} X_a \\ Y_a \end{bmatrix} \tag{6}$$

where X_a and Y_a are any real constant values. Substituting from eq. (3) into eq. (6), the steering speed x_2 does not appear in the right side and the Jacobian matrix stays singular for any P^*.

Let us propose the output variables to be the Cartesian coordinates of the steerable control-point P with the vector of position $\boldsymbol{p} = [x_p \; y_p]^T$. The idea behind this proposition can be explained by observing a kid pulling a child-cart. The kinematics of a child-cart with its steerable front wheels are very similar to a car-like mobile robot. If the child attaches a rope to any point on the main body (ex. the center of front tire axis c^*), he will not be able to guide his cart, but when he attaches his pulling rope on the steering handle (point P), he can run through any desired path and the cart will follow the path.

The Cartesian coordinates of point P are derived from vehicle states as:

$$\begin{aligned} x_p &= x_6 - l_1 \cos x_7 - L_p c_{17} \\ y_p &= x_5 - l_1 \sin x_7 - L_p s_{17} \end{aligned} \tag{7}$$

Kinematically, since the point P is attached to the front wheels, instantaneous motions are allowed in both Cartesian directions. In fact,

$$\dot{\boldsymbol{p}} = \rho \begin{bmatrix} c_{17} \\ -s_{17} \end{bmatrix} x_4 - L_p \begin{bmatrix} -s_{17} \\ c_{17} \end{bmatrix} (x_2 - K_1 x_4 \sin\delta) \tag{8}$$

Hence every instantaneous motion can be selected choosing the steering rate x_2 and linear velocity ρx_4. It is then clear that point P can track any desired path and the Jacobian matrix J_p becomes:

$$\dot{\boldsymbol{p}} = J_p \begin{bmatrix} x_2 \\ x_4 \end{bmatrix} = \begin{bmatrix} N_1 & M_1 \\ N_2 & M_2 \end{bmatrix} \begin{bmatrix} x_2 \\ x_4 \end{bmatrix} \tag{9}$$

where N_1, M_1, N_2 and M_2 are given in the appendix. Although this Jacobian matrix J_p is still configuration dependent, its determinant is constant, $|J_p| = \rho L_p$ and its inverse exists for any $L_p = 0$.

Simulation results will show that for L_p greater than 0.1 meter, the system is far enough from the singularity. For a real size car, the point c^* is placed at least 0.5 meter far from the vehicle sides. Thus, the control-point P can be assumed as a moving point on the vehicle main body pivoting around c^*. Theoretically, the residual error of point c^* for the zero-error point tracking of point P is $L_p \sin x_1$. Even in sever maneuvers where the steering angle reach its largest value (around 25 degree) this residual error is still small for in comparison with the size of a car. Further discussion is given by analyzing simulation results.

3.2 Controller Design

To develop the control law, the system inputs $\boldsymbol{t} = [T_{ab} \;\; T_{bc}]$ must appear explicitly. Thus, eq. (9) is differentiated once more:

$$\ddot{\boldsymbol{p}} = \dot{J}_p \begin{bmatrix} x_2 \\ x_4 \end{bmatrix} + J_p \begin{bmatrix} \dot{x}_2 \\ \dot{x}_4 \end{bmatrix} \tag{10}$$

By substituting eq. (3) into eq. (10):

$$\ddot{\boldsymbol{p}} = \boldsymbol{h} + D\boldsymbol{t} \tag{11}$$

where the vector $\boldsymbol{h} = [h_1 \ h_2]^T$ and matrix D are given in the appendix. Since the determinant of $D(\boldsymbol{x})$ is: $|D| = |J_p||G|$ (Where $G = M^{-1}(x_1)$) and it is never zero for any $\boldsymbol{x}$, the matrix is invertible and the nonlinear control law can be chosen as:

$$\boldsymbol{t} = D^{-1}(\nu - \boldsymbol{h}) \tag{12}$$

with ν as the new manipulated vector to be determined.

Substituting above equation into eq. (11), the considered rigid body nonlinearities are compensated and the relationship between the output vector and the new manipulated vector ν becomes linear i.e. $\ddot{\boldsymbol{p}} = \nu$. Defining the tracking error as: $\boldsymbol{e} = [e_x \ e_y]^T = \boldsymbol{p}^d - \boldsymbol{p}$ the new control inputs are chosen as:

$$\begin{aligned} \nu_1 &= \ddot{x}_p^{\,d} + \eta_1 e_x + \eta_2 \dot{e}_x \\ \nu_2 &= \ddot{y}_p^{\,d} + \eta_3 e_y + \eta_4 \dot{e}_y \end{aligned} \tag{13}$$

where the positive constants gains $\eta_1, \eta_2, \eta_3, \eta_4$ ensure the desired characteristics such as settle time and damping ratio, having the nature of a linear time-invariant P.D. controller. If

the initial position error is zero, then for all t greater than zero perfect tracking is achieved; otherwise, the vector $e(t) = [e_x(t)\ e_y(t)]$ converges exponentially to zero. The zero-error tracking is then ensured for a point which is not fixed on the vehicle, but it pivots very close and around the vehicle center of front tires. An implicit assumption is that nonlinearities caused by the tire deformation cannot destabilize the designed controller and they can be compensated by a robust linear controller. However, studying the mutual effect of tire and rigid body dynamics on the system stability is an interesting research subject which is beyond this paper objectives.

3.3 Internal Dynamics

The proposed dynamics have three nonholonomic constraints which render a part of the system dynamics unobservable after applying the I/OFL method. A general discussion of internal dynamics is given in [16]. If this internal dynamics is stable, our tracking control design is complete with the control law given by eq. (12) and (13). To complete the stability analyses, a diffeomorphic transformation is sought.

Since the relative degree of each output is two, the first four components of this transformation are chosen from the outputs and their Lie derivatives, i.e. x_p, $L_f x_p$, y_p, and $L_f y_p$. To complete the transformation, the steering angle x_1, the rotational angle of the virtual-tire x_3 and the vehicle orientation x_7, are added to form the following vectors:

$$z = T(x)$$

where z and T are $z = [z_1, ..., z_7]^T$ and $T(x) = [x_p, L_f x_p, y_p, L_f y_p, x_1, x_3, x_7]^T$, respectively.

To verify that $T(x)$ is indeed a diffeomorphism, its Jacobian should be invertible. Thus $T(x)$ is a valid state transformation if the determinant of the Jacobian exist everywhere:

$$\frac{\partial T(x)}{\partial x} = \begin{bmatrix} A_1 & 0 & 0 & 0 & 0 & 1 & B_1 \\ C_1 & N_1 & 0 & M_1 & 0 & 0 & D_1 \\ A_2 & 0 & 0 & 0 & 1 & 0 & B_2 \\ C_2 & N_2 & 0 & M_2 & 0 & 0 & D_2 \\ 1 & 0 & 0 & 0 & 0 & 0 & 0 \\ 0 & 0 & 1 & 0 & 0 & 0 & 0 \\ 0 & 0 & 0 & 0 & 0 & 0 & 1 \end{bmatrix}$$

where $A_i, B_i, C_i, D_i, M_i, N_i$ are functions given in the appendix. This matrix determinant is simply $|\partial T(x)/\partial x| = \rho L_p$ and it is never zero for any $L_p = 0$. Hence, the local diffeomorphism is achieved for any x, and the Jacobian is invertible for all x. The stability of the nonlinear controller can be verified observing the speed variation in the internal dynamics. These speeds are given in the normal form as:

$$\dot{z}_{int} = 1/\rho \begin{bmatrix} \cos(z_5 + z_7) & -\sin(z_5 + z_7) \\ K_{18}\sin(z_5 + z_7) - K_1 \sin z_5 \cos(z_5 + z_7) & K_{18}\cos(z_5 + z_7) + K_1 \cos z_5 \cos(z_5 - z_7) \\ K_1 \sin z_5 \cos(z_5 + z_7) & -K_1 \sin z_5 \sin(z_5 + z_7) \end{bmatrix} \begin{bmatrix} z_2 \\ z_4 \end{bmatrix} \quad (15)$$

Putting the vector $[z_2\ z_4]^T$ equal to zero, the zero dynamics becomes $\dot{z}_{zero} = 0$, which does not necessarily means that the system is unstable. Although the vector of internal dynamic states $z_{int} = [z_5\ z_6\ z_7]$, which represents the vehicle planar displacements, is not bounded, the vector of unobservable speeds $\dot{z}_{int} = [\dot{z}_5\ \dot{z}_6\ \dot{z}_7]^T$ stays bounded for bounded $[z_2\ z_4]^T$ and the internal dynamics stay stable. Note that in eq. (15), elements of relating matrix are bounded triangular functions, thus, the speeds of the internal dynamics are bounded.

3.4 **Path planning for point P**

As mentioned before, the control-point P is not fixed on the vehicle main body. Nevertheless, the path tracking problem of any fixed-point can be transformed to the point tracking of the steerable control-point P using an off-line path planing process. In this process the desired path of P is derived from the desired path of any fixed-point on the vehicle, for instance the robot rear center (point d^*) as shown in figure 1.

Based on eq. (7), if the desired path of d^* is $y = f(x)$, the kinematic relation between point d^* and point P is :

$$\begin{aligned} x_p &= x_{d^*} + L_a c_7 + L_p c_{17} \\ y_p &= f(x_{d^*}) - L_a s_7 - L_p s_{17} \end{aligned} \tag{16}$$

o keep d^* on the desired path, the instantaneous curvature of the robot and the desired path must be equal, i.e. $R_d = [1 + (df/dx)^2]^{3/2}/|d^2f/dx^2|$ must be equal to $R = L_a/\tan q_4$. Thus, the desired steering angle is derived as: $\hat{q}_4 = \tan^{-1}([L_a|d^2f/dx^2|/[1 + (df/dx)^2]^{3/2})$.

Suppose that desired trajectories of point d^*, for its Cartesian coordinates are, $x_{d^*}^d(t) = \hat{x}$, and $y_{d^*}^d = f(\hat{x})$ then the desired trajectories of point P will be:

$$\begin{aligned} x_p^d &= \hat{x} + L_a\cos\hat{q}_3 + L_p\cos(\hat{q}_3 + \hat{q}_4) \\ y_p^d &= f(\hat{x}) + L_a\sin\hat{q}_3 + L_p\sin(\hat{q}_3 + \hat{q}_4) \end{aligned} \tag{17}$$

where $\hat{q}_3 = \tan^{-1}(df/dx)$ is the robot instantaneous desired orientation.

With the proposed off-line path tracking, the path tracking problem of a fixed point on the vehicle can be converted as the point tracking scheme of the steerable point P and the error of a fixed-point on the vehicle from its associated desired path can be nullified. However, a real car is not a point and its size is not negligible comparing to the width of the roads. Thus, the vehicle lateral-offset should be measured for more than one point, even if the designed controller ensures only the zero-tracking of one control-point. From control point of view, the theoretical objective is the point tracking of a fixed- point on the vehicle and the fact that, with $L_P \geq 0.1$, the steerable point P can be very close to point c^* (In comparison

with the vehicle size) enhance the chance of considering the desired path directly for point P without using the above off-line path planning. To verify this possibility, simulations are carried out using the same desired paths point d^* and point P and errors of different vehicle points are compared.

4. SIMULATION RESULT ANALYSES

Simulations have been performed using Matlab (Simulink) to verify the effectiveness of the proposed control law under different input trajectories. The vehicle parameters given in the appendix have been selected to closely resemble a today's middle class front wheel drive vehicle. The gains for the linear outer P.D. controller have been chosen to obtain a critically damped system by which in 2.5 seconds the controlled error achieves 5% of its initial value. To study the system performance, simulations are carried out in five steps.

In the first two steps, the variation of the lateral error is verified for three different vehicle points (d^*, *c.g.* and c^*) for $L_P = 1\,[m]$ and $L_P = 0.1\,[m]$ under a severe left and right turn.

In steps 3,4 and 5 the desired path is composed of a straight line followed by a circular arc segment with a turning radius of 75 meter and with $L_P = 1\,[m]$.

4.1 **Lateral error verification under severe left and right turns**

The sine function $y = 25\sin(\pi x/50)$ is chosen to simulate a severe left and right turn. This function is set as the desired path of point P in step 1 and as the desired path of point d^* in step 2, from which the desired path of P is derived using the off-line path planning. The desired trajectories: $X_P^d(t), Y_P^d(t), \dot{X}_P^d(t), \dot{Y}_P^d(t)$ and $\ddot{X}_P^d(t), \ddot{Y}_P^d(t)$ are derived from such path assuming $x = 5t$.

The displacement of the vehicle points d^*, *c.g.* and c^* in the Cartesian plane are shown for $L_P = 1$ in figure 3 and for $L_P = 0.1$ in figure 4. For better visualization, only part of the simulation is shown in these figures, however, the errors are computed for one complete period of 20 seconds.

Variation of these offsets are shown in figures 5 and 6 for different Lp's which shows the exponential convergence of point P from its initial offset to zero. To compute the lateral-offset of the vehicle points, we used the perpendicular projection of each point on the desired path in the Cartesian plane to find the instantaneous geometric offset of each point from the desired path. Figure 7 shows the errors of the vehicle orientation and its curvature comparing to the orientation and the curvature of the desired path.

In the second step, the desired path of $f(x) = 25\sin(\pi x/50)$ is used, this time for the point d^* instead of point P. The choice of point d^* is partly justified by the objective of looking for

zero orientation error. Since the controller is designed for point tracking of P, the desired path of point P is derived using the previously explained path planning process. The variation of different vehicle point offsets are shown in figures 8 and 9 , respectively, for Lp=1 and Lp=0.1 and the variation of the vehicle orientation and curvature error are shown in figure 10.

In both steps, the point tracking of point P results in the exponential convergence of the error of point P from its initial values to zero, besides, the zero lateral offset of point d^* and the zero error on vehicle orientation have been realized in step 2.

In step 1, decreasing the length of L_P from 1 [m] to 0.1 [m] results in decreasing all errors. Meanwhile, in step 2, the errors are almost insensitive to the variation of L_P, evidently, because this length is taken into account into the off-line path planning process. Another observation comes from comparing the two steps for $L_P = 1$ [m]. In spite of using the path planning process, the maximum lateral offset decrease less than 5% (from 0.41 for d^* in step 1 to 0.39 for c^* in step 2). In fact, the lateral offset exists, but for different vehicle points. However, if the lateral-offset is the only criterion, the minimum overall offset can be achieved in step 1 for $L_P = 0.1$ [m] where point c^* follows the desired path with almost no lateral offset.

4.2 Path combined of lines and circular arc segments

In the following three steps, simulations are carried out keeping . The advantage of such paths is that a speed profile can be defined, i.e. vehicle speed can be controlled indirectly without considering it as a controlled output and the desired trajectories are derived using the proposed desired speed profile for such paths. Desaulniers [8] has studied the problem of car-like robots in following any arbitrary paths and concluded that, for this type of robots, the shortest path between two positions is achieved by the combination of line segments and circular arcs of minimal turning radius. Besides, most of existing highways and roads can be modeled using parallel straight lines and circular arcs. Although controlling the vehicle speed is not considered in the design of the controller, special characteristics of such paths grant this possibility.

Let us define the desired speed profile as follows: The vehicle follows the straight line segment and accelerates to the desired speed of the line segment, i.e. $V_{dl} = 20$ [m/sec.] at $t = T_v = 4$, then remains at this speed for 2 seconds and decelerates to the desired speed of the circular segment, i.e. $V_{dc} = 15$ [m/sec.] at $t = T_j = 10$, right before starting the circular arc segment. The desired speed remains constant at V_{dc} in this segment:

$$V_d = \begin{cases} \alpha_1 t^3 - \gamma_1 t & 0 \le t \le T_v \\ V_{dl} & T_v \le t \le T_1 \\ \alpha_2 t^3 + \beta_2 t^2 + \gamma_2 t + \delta_2 & T_1 \le t \le T_j \end{cases} \qquad (18)$$

where $\alpha_i, \beta_i, \gamma, \delta$ $(i = 1,2)$ are found to respect the continuity. If θ is the slop of the line segment in the X-Y frame, the desired x component becomes $\dot{x}_d = V_d \cos\theta$. Then its integral and derivative are found and the equation of line and its derivatives are used to find desired trajectory and its derivatives for Y. The desired trajectory of the circular segment is not that straight forward if we wish to respect the constant desired speed.

Supposing the constraint $\dot{x}_d^2 + \dot{y}_d^2 = V_{dc}$ applies on the circle of $x_d^2 + y_d^2 = R_1^2$ then the solution of the differential equation $R_1^2 \dot{x}_d^2 - V_{dc} x_d^2 - V_{dc}^2 R_1^2 = 0$, i.e. $x_d = R_1 \sin(V_{dc}/R_1)\, t$ and $y_d = R_1 \cos(V_{dc}/R_1)\, t$, and their derivatives define the desired trajectory of x component. In the proposed desired path that the circular arc segment is placed after the line segment of slop θ, at the center (X_1, Y_1) and starts at $t = T_j$, the solution becomes: $x_d = R_1 \sin[\frac{V_{dc}}{R_1}(t - T_j) + \theta] + X_1$ and $y_d = R_1 \cos[\frac{V_{dc}}{R_1}(t - T_j) + \theta] + Y_1$.

Using the given speed profile, the desired path has been converted to the time varying desired trajectories for the Cartesian coordinates of point P or d^*. Similar to step 1 and 2, this path is set as the desired path of point P in step 3 and as the one of point d^* in step 4. Such paths are discontinuous in the second derivation at the junction of line and circular arc segment, where the vehicle lateral acceleration should jump from zero to a definite value, here 3

[m/sec.^{2}]. This requires a sudden steering angle jump, here from zero to 2.15 degree which may perturbs the system dynamics. This perturbation is damped by the critical damping ratio and the settle time of 2.5 second on the steering command after linearisation. In step 5, the mass and the inertial of the vehicle model are different than ones of the model on which the path-tracker design is based. The vehicle mass and inertia are increased about 50% and vehicle size about 20% in order to verify the tracking performance of the developed control law under parameter uncertainties.

In steps 3 and 4, there is no lateral error for the line segment but a constant residual offset is seen for the circular segment. Figure 11 shows how different vehicle points displace in the Cartesian plane while point P tracks the desired path in step 3. The residual offset for the three vehicle points, as shown in figure 12, and the speed error are both negligible. In this step, the simulation results in a 3 degree residual orientation error for the circular segment but a zero curvature error which seems as a contradiction. The zero curvature error shows that the vehicle curvature is the same as the curvature of the desired circular arc. In addition, the steering angle is constant and equal to the expected desired steering angle for this segment. Under such condition a zero orientation error is expected using the same logic behind the proposed path planning process. As a result, this orientation error should be due to the dynamic delay between the orientation change of point P and one of the vehicle main body. The residual speed error of 0.05 [m/sec.], in step 3, is due to the fact that the desired speed profile is used for the desired path of virtual point P. this error increases with the increase of steering angle.

In step 4, (figure 13) the residual offsets of point d^* and *c.g.* are both decreased respectively from $61 * 10^{-3}$ to zero and from $46 * 10^{-3}$ to $12 * 10^{-3}$, but ones of point c^* is increased from $7*10^{-3}$ to $48 * 10^{-3}$. In this step, since the point tracking is applied to point d^* the contradiction between the curvature and orientation errors are vanished and they are both zero. In figure 13, the tracking error of point P is from the derived desired path after path planning process but the other offsets of the vehicle different points are the perpendicular distance between their path an the desired path of d^*. This is because the controller is designed for point P but the path that vehicle should follow is set for d^* in this step. Another positive side of path planning process is that the vehicle reaches to the desired speed without any residual error.

In step 5, under parameter uncertainties, the variation of the tracking error of point P and of the lateral offset of different vehicle points are shown in figures 14 and 15, respectively, for tracking of point P with and without path planning. Despite using only a P.D. linear controller, all errors converge to zero for the line segment where the vehicle accelerates and decelerates. To cancel the residual offsets of the circular segment a more robust linear controller should be designed. Although, while the vehicle accelerates or decelerates the speed error increases, the parameter (mass and inertia) uncertainties brings only a delay in the exponential convergence of speed error to zero. This means that the stability region is vast enough.

5. CONCLUSION

A method for controlling a car-like mobile robot under nonholonomic constraints has been developed. By choosing a steerable control-point (point P) in front of the vehicle, the dynamics Input/Output Feedback Linearization becomes feasible without neglecting the vehicle steering dynamics which enhance the chance of integrating the very important "tire dynamics" in the future models. Considering the vehicle size this steerable point can be seen as a vehicle point pivoting on a tiny circle around the midpoint of front tires. However, an offline path tracking process is proposed to derive the desired path of the steerable point P from the desired path of any vehicle material point, for instance, the vehicle midpoint between the rear tires where the vehicle orientation is kinematically tangent to the path. The nonlinear control law guaranties the stable zero-error tracking of the chosen point as well as the stability of the internal dynamics with the advantage of being time-invariant and having a simple structure. No limitation is imposed on the form of the desired path during the control law development. A speed profile can be applied for paths composed of straight lines and circular arc segments. The controller shows relatively robust behavior in the presence of discontinuity in the desired path and parameter uncertainties of the vehicle even though the linear regulator is a simple P.D.

ACKNOWLEDGMENTS

The authors wish to thank J. Sévigny, and D.A. Rey for their valuable help, suggestions and discussions. We would also like to acknowledge our appreciation of the NSERC for their financial support under grant OGP0138153.

REFERENCES

[1] Astolfi A., 1995, *Exponential Stabilization of a Car-like Vehicle*, IEEE International Conference on Robotics and Automation, 0-7803-1965-6/95, p.1391-1396.

[2] Bloch A.M., Reyhanoglu M., and McClamroch N.H., 1992, *Control and Stabilization of Nonholonomic Dynamic Systems*, IEEE Transactions on Automatic Control, v. 37, n.11, p. 1746-1757.

[3] Brockett R. W., 1983, *Asymptotic stability and feedback linearization, Differential Geometric Control Theory*, Brockett R. W., Willman R. S. and Sussmann H. J. editors, Birkhauser, Boston, MA. p. 181-191.

[4] Canudas de Wit C., Sordalen O.J., 1992, *Examples of Piecewise Smooth Stabilization of Drift less NL Systems with less Inputs than States*, IFAC Nonlinear Control Systems Design, Bordeaux, France, p. 57-61.

[5] Coron J.M., d'Andrea-Novel B., 1992, *Smooth Stabilization Time-Varying Control Laws for a Class of Nonlinear Systems. Application to Mobile Robots*, IFAC Nonlinear Control Systems Design, Bordeaux, France, p. 413-418.

[6] D'Andréa-Novel, B., Campion G. And Bastin, G., "Control of Nonholonomic Wheeled Mobile Robots by State Feedback Linearisation", The International Journal of Robotic Research, vol. 14, no. 6, pp. 543-559, 1995.

[7] DeSantis, R.M., 1995, *Path-tracking for car-like robots with single and double steering*, IEEE Transactions on Vehicular Technology v 44 n 2, p 366-377.

[8] Desaulniers G. and Soumis, F., dec.1995, *An Efficient algorithm to find a shortest path for a car-like robot*, IEEE Transactions on Robotics and Automation v. 11 n. 6, p. 819-828.

[9] Jagannathan S., Zhu S.Q. and lewis F.L., 1994, *Path planning and control of a mobile base with nonholonomic constraints*, Robotica, v. 12, p. 529-539.

[10] Munoz V., Ollero A., Prado M., Simon A., 1994, *Mobile Robot Trajectory Planning with Dynamic and Kinematic Constraints*, IEEE International Conference on Robotics and Automation pt 4, piscataway, NJ, USA, p. 2802-2807.

[11] Oelen W., Berghuis H., Nijmeijer H., Canudas de Wit C., Jun.1995, *Hybrid stabilizing control on a real mobile robot*, IEEE Robotics & Automation Magazine v. 2 n. 2, p. 16-23.

[12] Samson C., 1993, *Time-varying feedback stabilization of car-like wheeled mobile robots*, International Journal of Robotics Research v. 12 n. 1 Feb. p. 55-60.

[13] Samson C., 1995, *Control of Chained Systems Application to Path Following and Time-varying Point-Stabilization of Mobile Robots*, IEEE Transactions on Automatic Control v. 40, n.1, p. 64-77.

[14] Sarkar N., Yun X. and Kumar V., 1994, *Control of Mechanical Systems with Rolling Constraints: Application to Dynamic Control of Mobile Robots*, International Journal of Robotics Research, v. 13, n. 1, p. 55-69.

[15] Shim H-S., Kim J-H., Koh K., 1995, " *Variable Structure Control of Nonholonomic Wheeled Mobile Robot"*, IEEE International Conference on Robotics and Automation, 0-7803-1965-6/95, p 1694-1699.

[16] Slotine J.J and Li W., 1991, *Applied Nonlinear Control*, Prentice-Hall.

[17] Sordalen O.J. and Canudas de Wit C., 1992, *Path following and Stabilization of a Mobile Robot*, IFAC Nonlinear Control Systems Design, Bordeaux, France, p. 471-476.

[18] Sordalen O.J., Canudas de Wit C., dec.1993, *Exponential control law for a mobile robot: extension to path following*, IEEE Transactions on Robotics and Automation v. 9, n. 6, p 837-842.

[19] Spong M.W. and Vidyasagar M., 1989, *Robot Dynamics and Control,* John Wiley & Sons.

[20] Tilbury D., Laumond J. -P., Murray R., Sastry S., Walsh G., 1992, *Steering car-like systems with trailers using sinusoids*, IEEE International Conference on Robotics and Automation v. 3. Publ by IEEE, IEEE Service Center, Piscataway, NJ, USA (IEEE cat n 92CH3140-1), p 1993-1998.

[21] Tibury D., Sordalen J., Bushnel L., Sastry S., dec. 1995, *A Multi Steering Trailer System: Conversion into Chained form Using Dynamic Feedback,* IEEE Transactions on Robotics and Automation v. 11, n. 6, 1995, p 807-818.

[22] Tounsi, M., Lebret, G., Gautier M., 1995, *Dynamic identification and control of a nonholonomic mobile robot*, IEEE Conference on Control Applications Piscataway, NJ, USA,95CH35764. p 520-525.

[23] Walsh G., Tibury D., Sastry S., Murray R., Laumond J.P., Jan.1994, "*Stabilization of Trajectories for Systems with Nonholonomic Constraints*", IEEE Trans. on Automatic Control v. 39, n. 1, p 216-222.

[24] Yun X., Yamamoto Y., 1993, *Internal Dynamics of a Wheeled Mobile Robots*, IEEE international Conference on Intelligent Robots and Systems, Yokohama, Japan, p. 1288-1294.

Appendix

The mobile robot parameters and the constants used in dynamic e.o.m.'s, eq. (1) are:

$\rho = 0.33\ m$ $\quad l_1 = 1.41\ m$ $\quad l_a = 2.82\ m$

$I_{C3} = 0.1455\ kg.m^2$ $\quad I_{C1} = 0.1\ kg.m^2$ $\quad I_{A3} = 2232\ kg.m^2$

$m_A = 1416\ kg$ $\quad m_C = 5\ kg$ $\quad L_p = 1\ m$

$K_1 = \rho / l_a$ $\quad K_2 = l_1^2 - 2 l_a l_1$ $\quad K_3 = K_1^2 K_2$

$K_4 = K_1 I_{C3}$ $\quad K_5 = K_3 m_A$ $\quad K_6 = K_1^2 (I_{C3} + I_{A3})$

$K_7 = I_{C1} - \rho^2 (m_A + m_C)$ $\quad K_8 = K_1^2 m_A l_1 (l_1 - 2 l_a) + K_6$ $\quad K_9 = K_5 + K_6$

$K_{10} = -K_4^2 + K_9 I_{C3}$ $\quad K_{11} = I_{C3} K_7$ $\quad K_{12} = K_4 (K_8 - K_9)$

$K_{13} = -K_4 K_7$ $\quad K_{14} = K_4^2 - K_8 I_{C3}$ $\quad K_{15} = l_1 - La$

$K_{16} = l_1 / La$ $\quad K_{17} = 1 / La$ $\quad K_{18} = \rho / L_p$

The elements of the state space presentation, eq. (3), and the nonlinear control functions are:

$$f_1(x_1) = M^* (K_{12} \sin^2 x_1 - K_{13}) \cos x_1 \qquad f_2(x_1) = M^* K_{14} \sin x_1 \cos x_1$$

$$h_1(\boldsymbol{x}) = K_{17} (1 - \tan^2 x_1)[2 x_2^2 \tan x_1 - f_1(x_1) x_2 x_4]$$

$$h_2(\boldsymbol{x}) = \rho x_4 x_2 [f_2(x_1) \cos x_1 - \sin x_1]$$

$$g_1(x_1) = M^* (K_9 \sin^2 x_1 + K_7) \qquad g_2(x_1) = -M^* K_4 \sin x_1$$

$$g_3(x_1) = M^* I_{C3}$$

where $M^* = 1/(K_{10} \sin^2 x_1 + K_{11})$ is the inversion of the mass matrix determinant.

The elements of Jacobian matrix J_p are:

$$
\begin{aligned}
N_1 &= -L_p \sin(x_1 - x_7) \\
N_2 &= -L_p \cos(x_1 - x_7) \\
M_1 &= \rho \cos(x_1 - x_7) - L_p K_1 \sin x_1 \sin(x_1 - x_7) \\
M_2 &= -\rho \sin(x_1 - x_7) - L_p K_1 \sin x_1 \cos(x_1 - x_7)
\end{aligned}
$$

Matrix G and D are:

$$
G = \begin{bmatrix} g_1(x_1) & g_2(x_1) \\ g_2(x_1) & g_3(x_1) \end{bmatrix}, \quad D = \begin{bmatrix} K_{17}(1+\tan^2 x_1) g_1(x_1) & K_{17}(1+\tan^2 x_1) g_2(x_1) \\ \rho \cos x_1 \, g_2(x_1) & \rho \cos x_1 \, g_3(x_1) \end{bmatrix} = \begin{bmatrix} D_1 & D_2 \\ D_3 & D_4 \end{bmatrix}
$$

the terms of diffeomorphism transformation are:

$$
\begin{aligned}
A_1 &= -L_p S_{17} \\
B_1 &= -l_1 S_7 - L_p S_{17} \\
C_1 &= -L_p x_2 C_{17} - (\rho - K_1 L_p) x_4 S_{17}
\end{aligned}
$$

$$
\begin{aligned}
A_2 &= -L_p C_{17} \\
B_2 &= -l_1 C_7 - L_p C_{17} \\
C_2 &= -L_p x_2 S_{17} - (\rho + K_1 L_p) x_4 C_{17}
\end{aligned}
$$

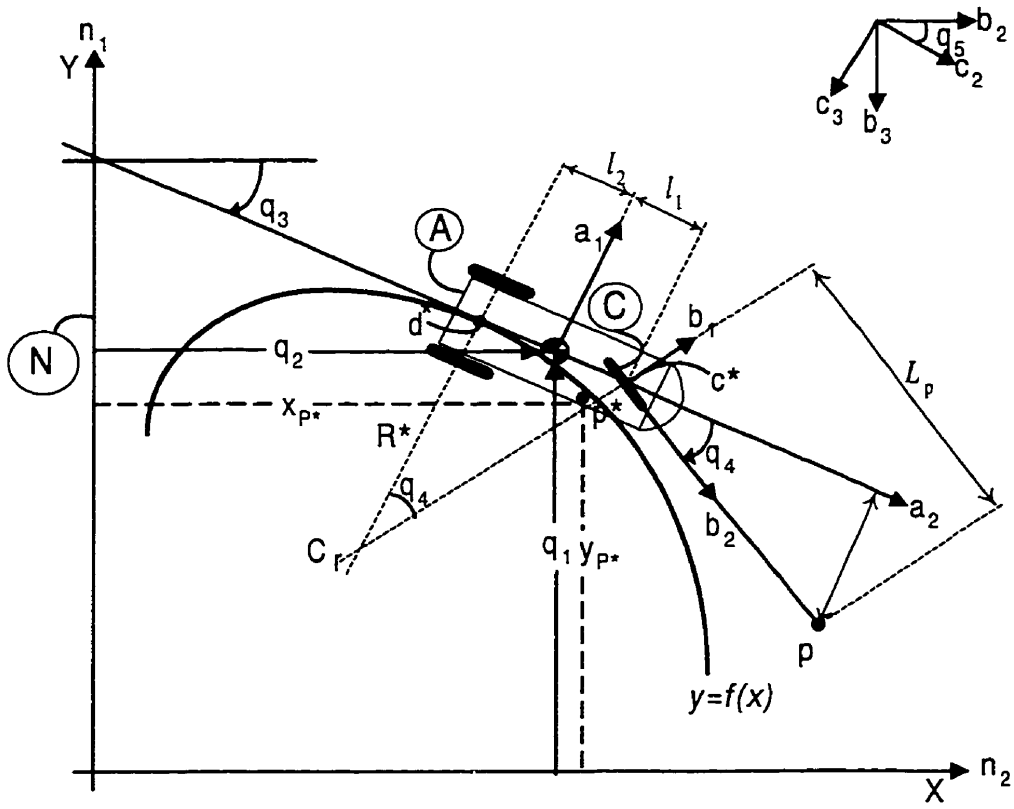

Figure 1 - A car-like planar vehicle with front wheel traction and steerable virtual point P.

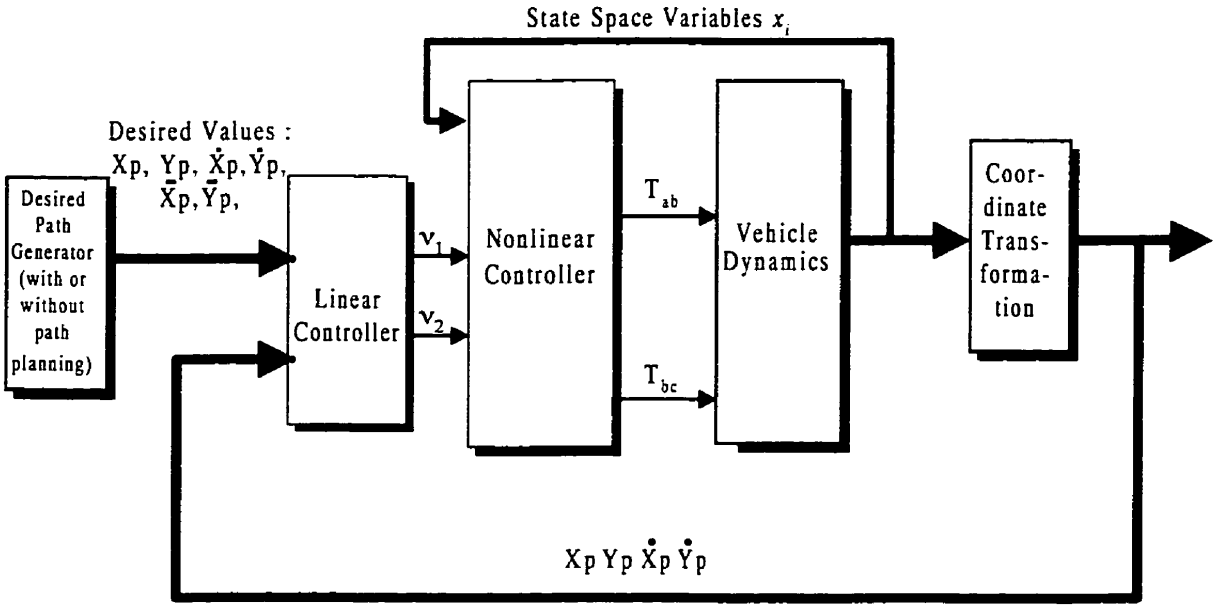

Figure 2 - Architecture of the trajectory tracker

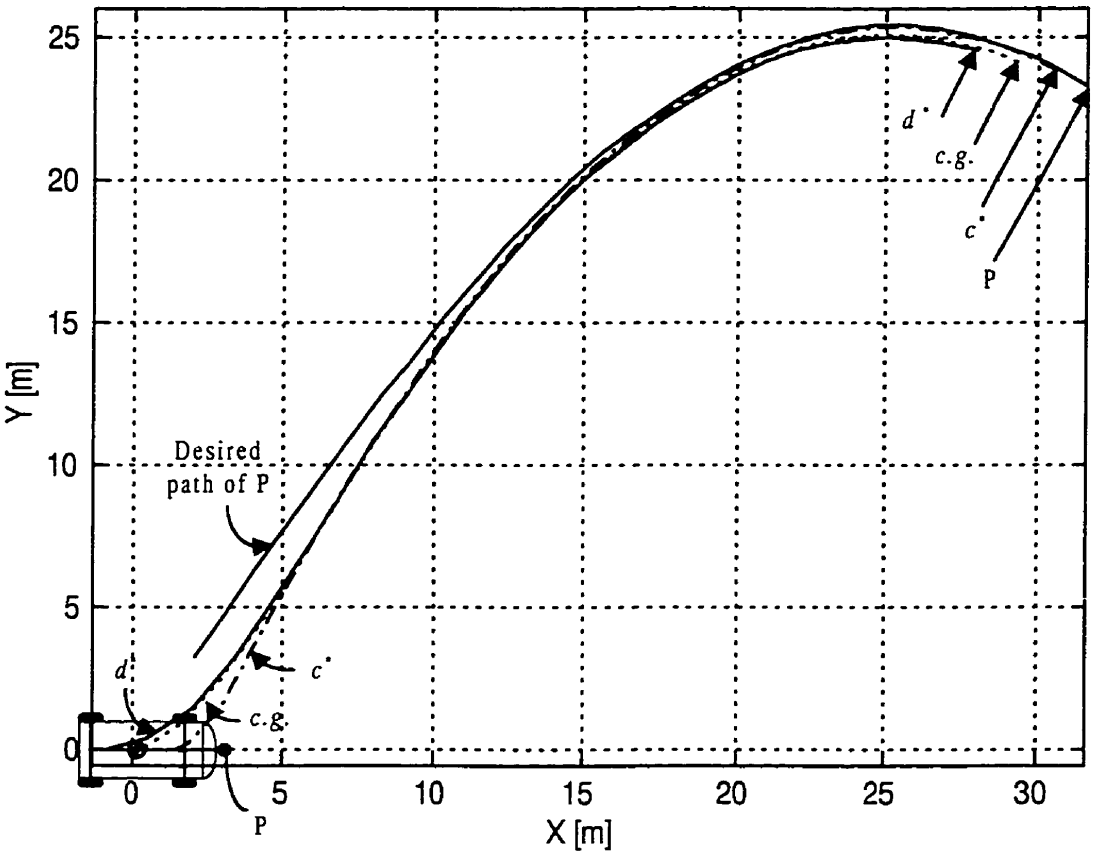

Figure 3 - displacement of the vehicle in X-Y plane with Lp = 1 [m] (step 1).

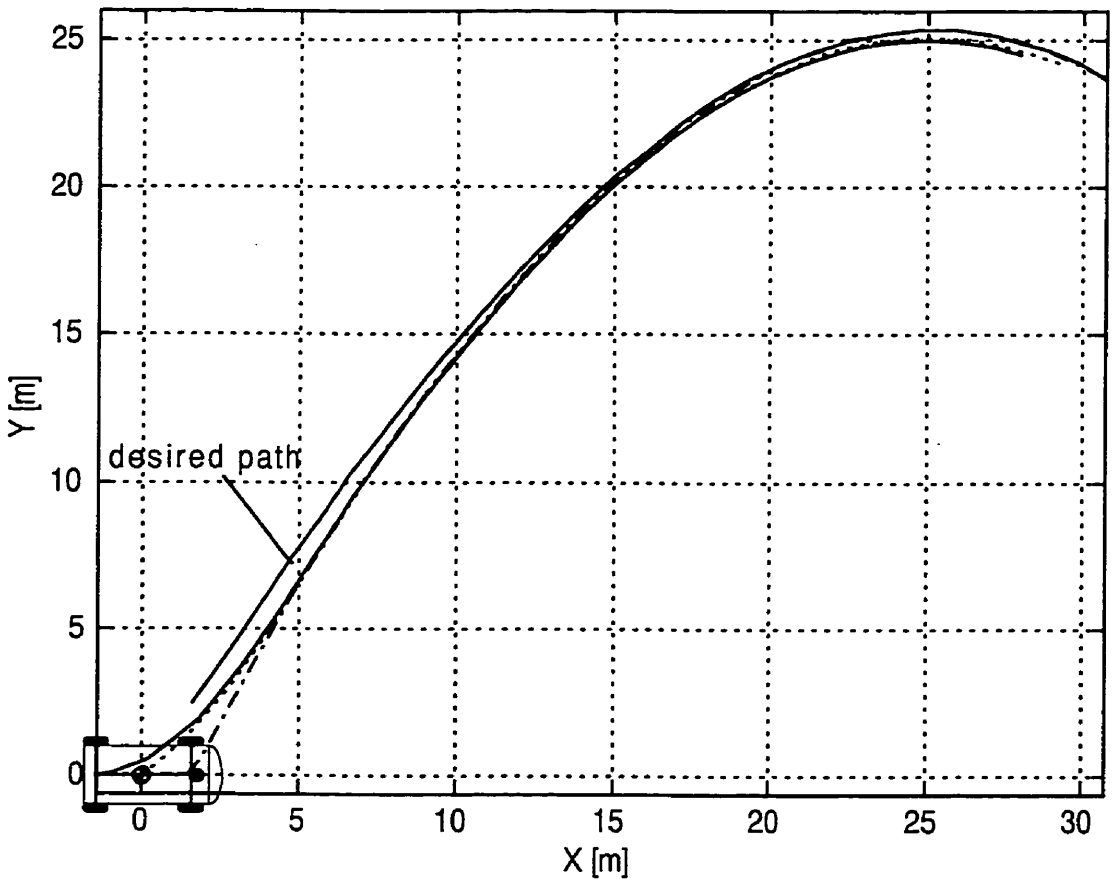

Figure 4 - displacement of the vehicle in X-Y plane Lp= 0.1 [m] (step 1).

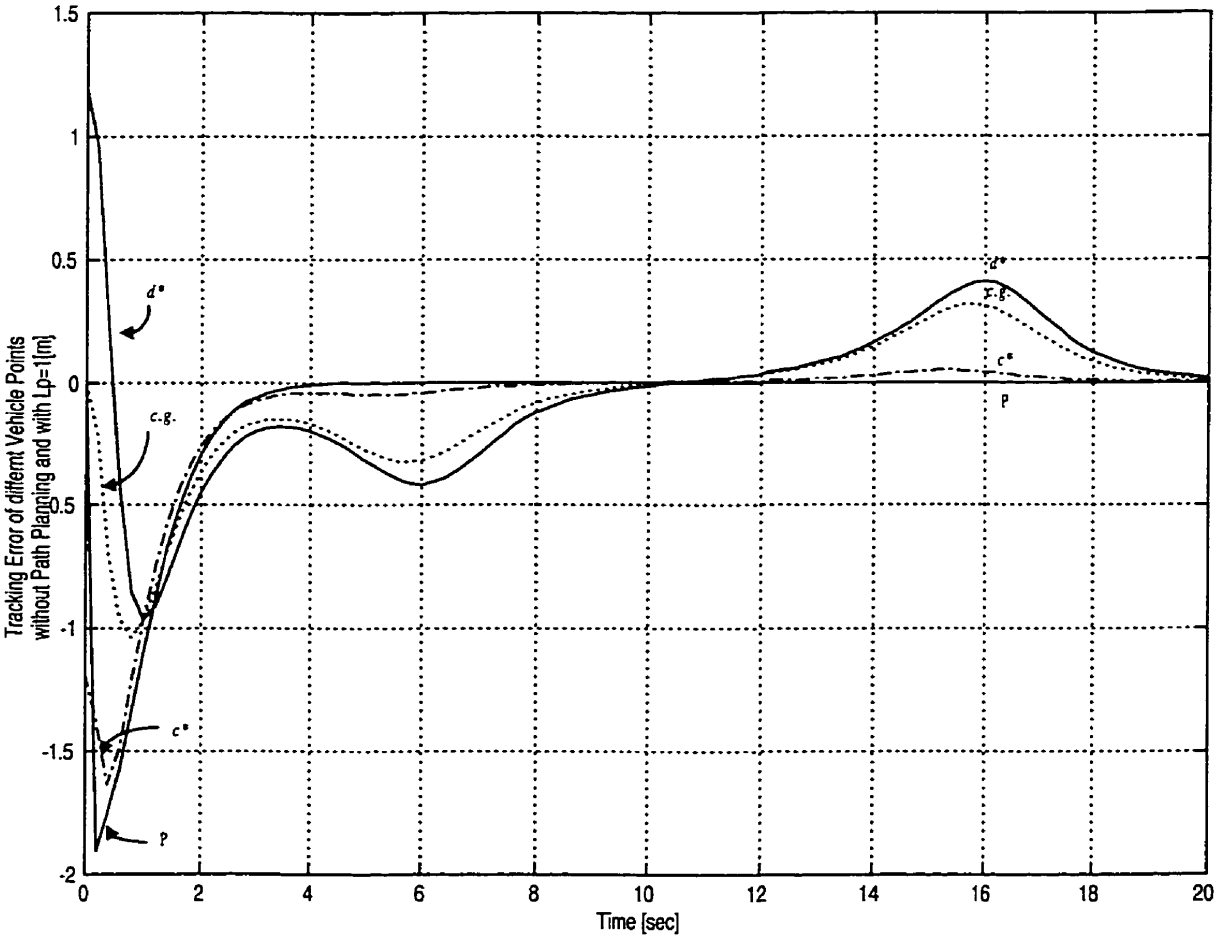

Figure 5 - Time variation of lateral offsets of different vehicle points for Lp=1 (step 1).

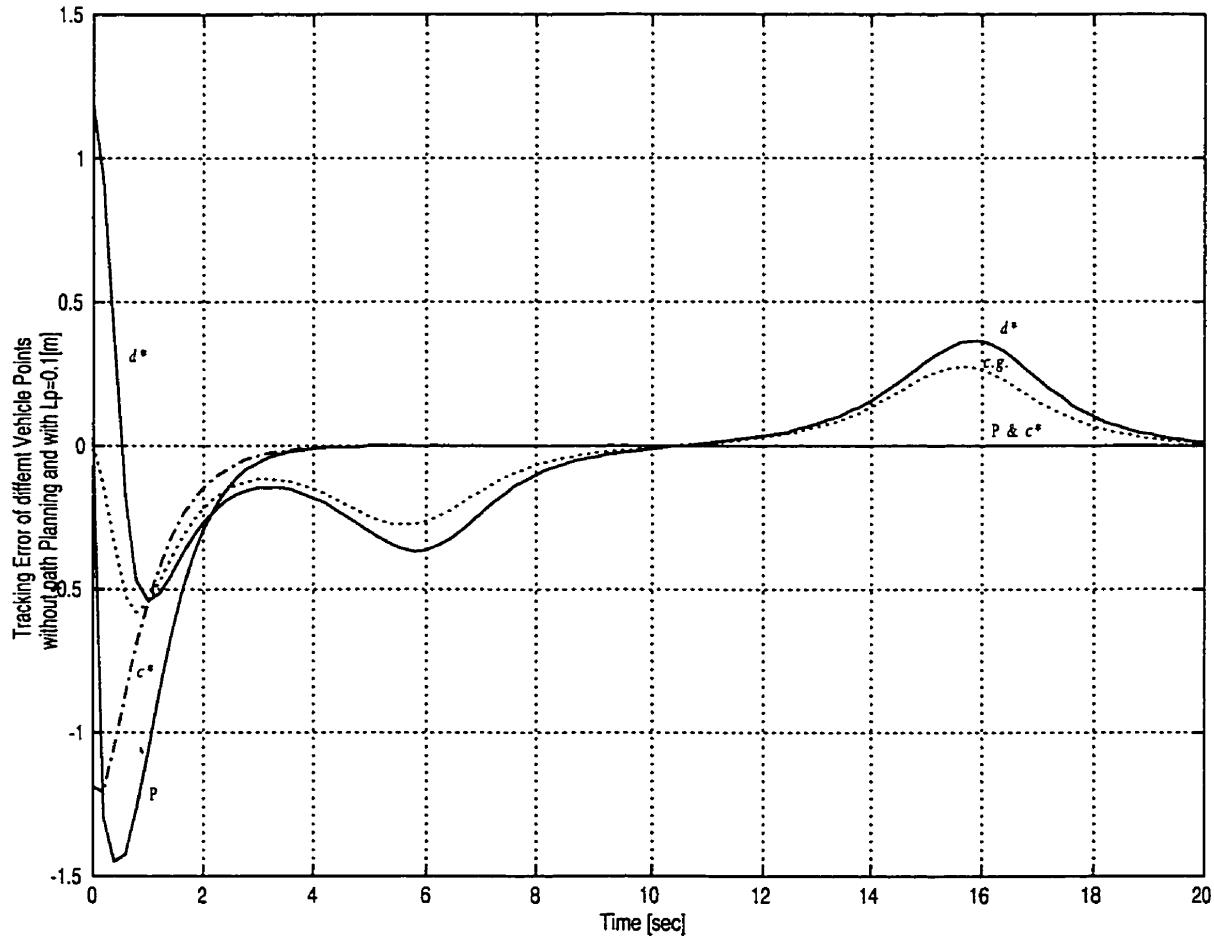

Figure 6 - Time variation of lateral-offsets for different vehicle points for Lp = 0.1 (step 1)

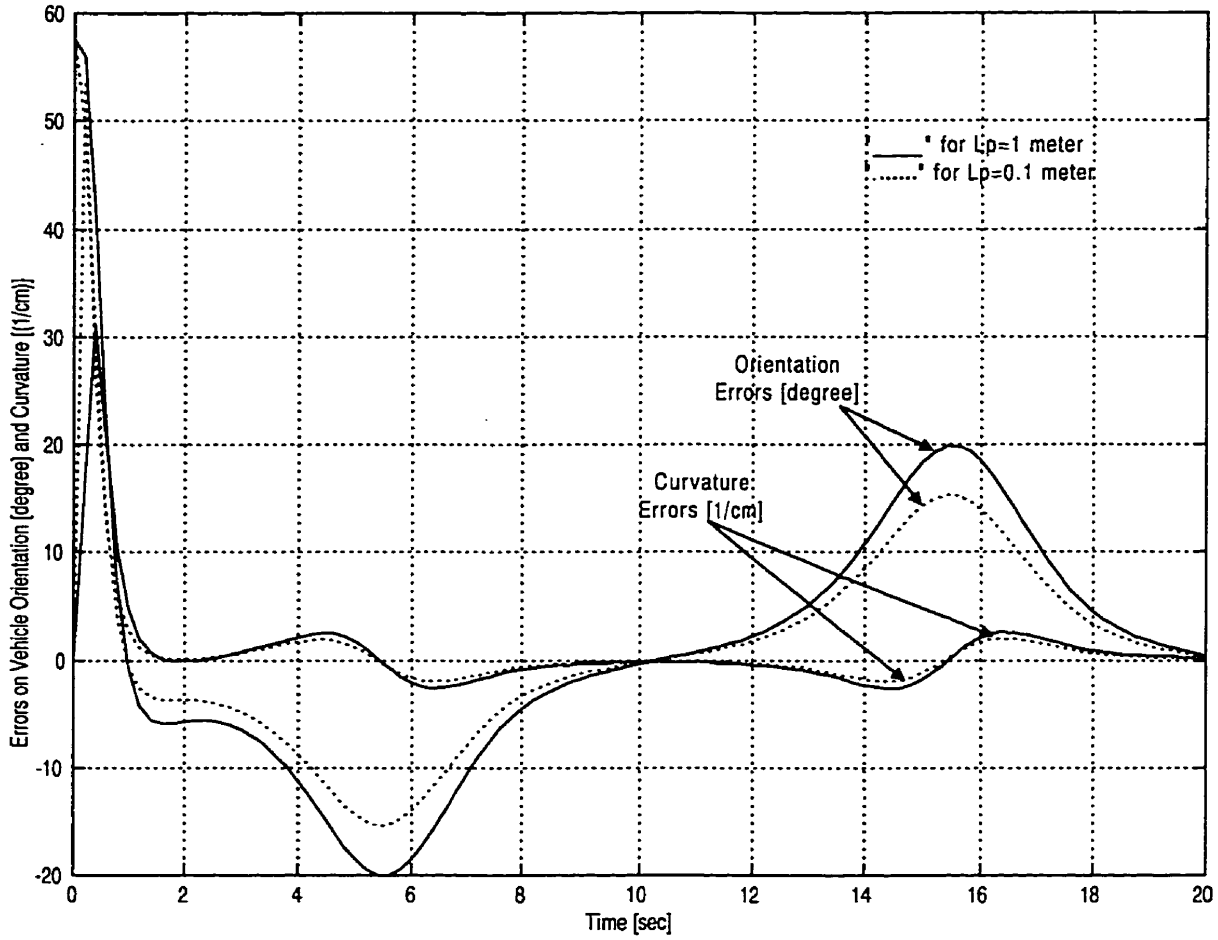

Figure 7 - The orientation and curvature errors without path planning (step 1) .

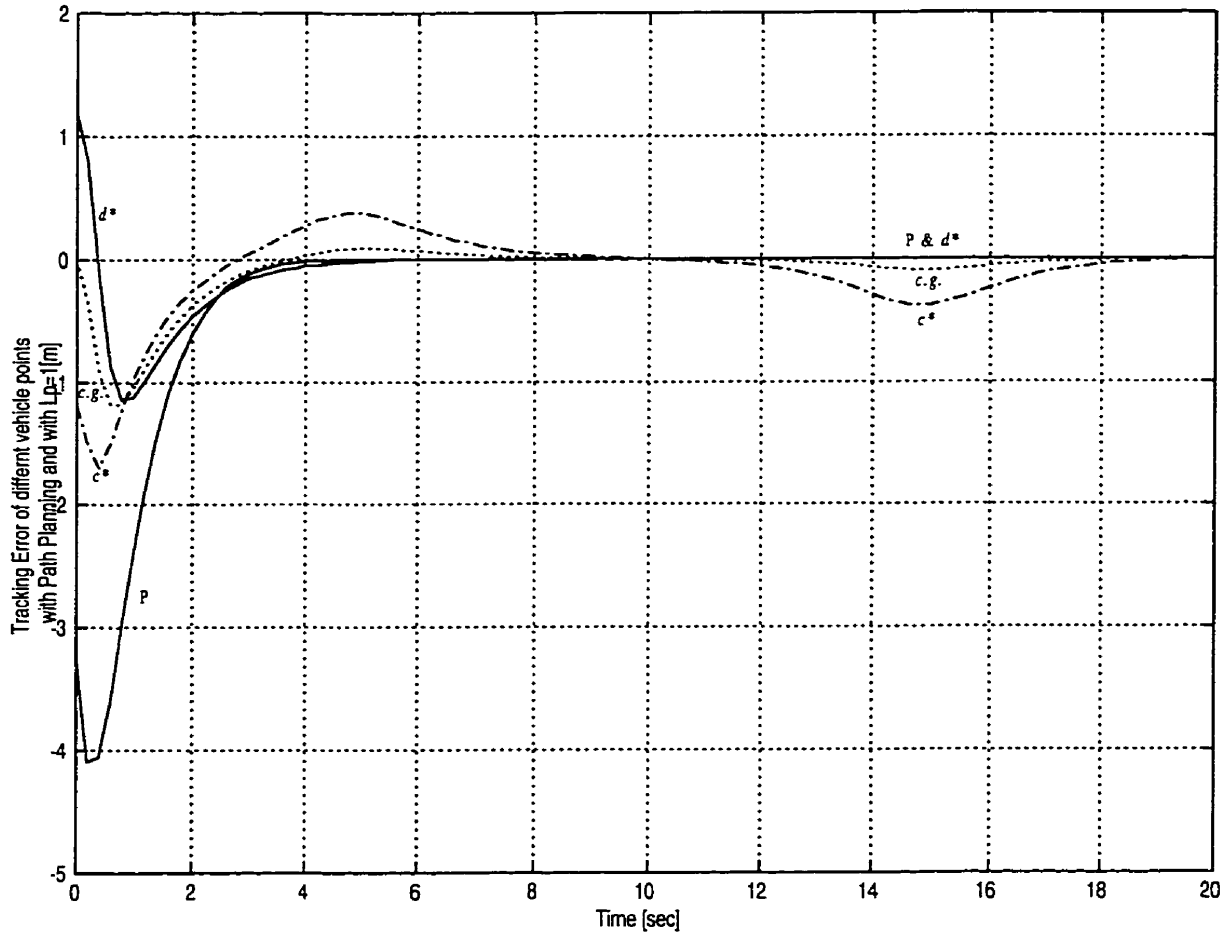

Figure 8 - Time variation for error of point P and lateral-offset of different vehicle points for Lp=1 [m] (step 2)

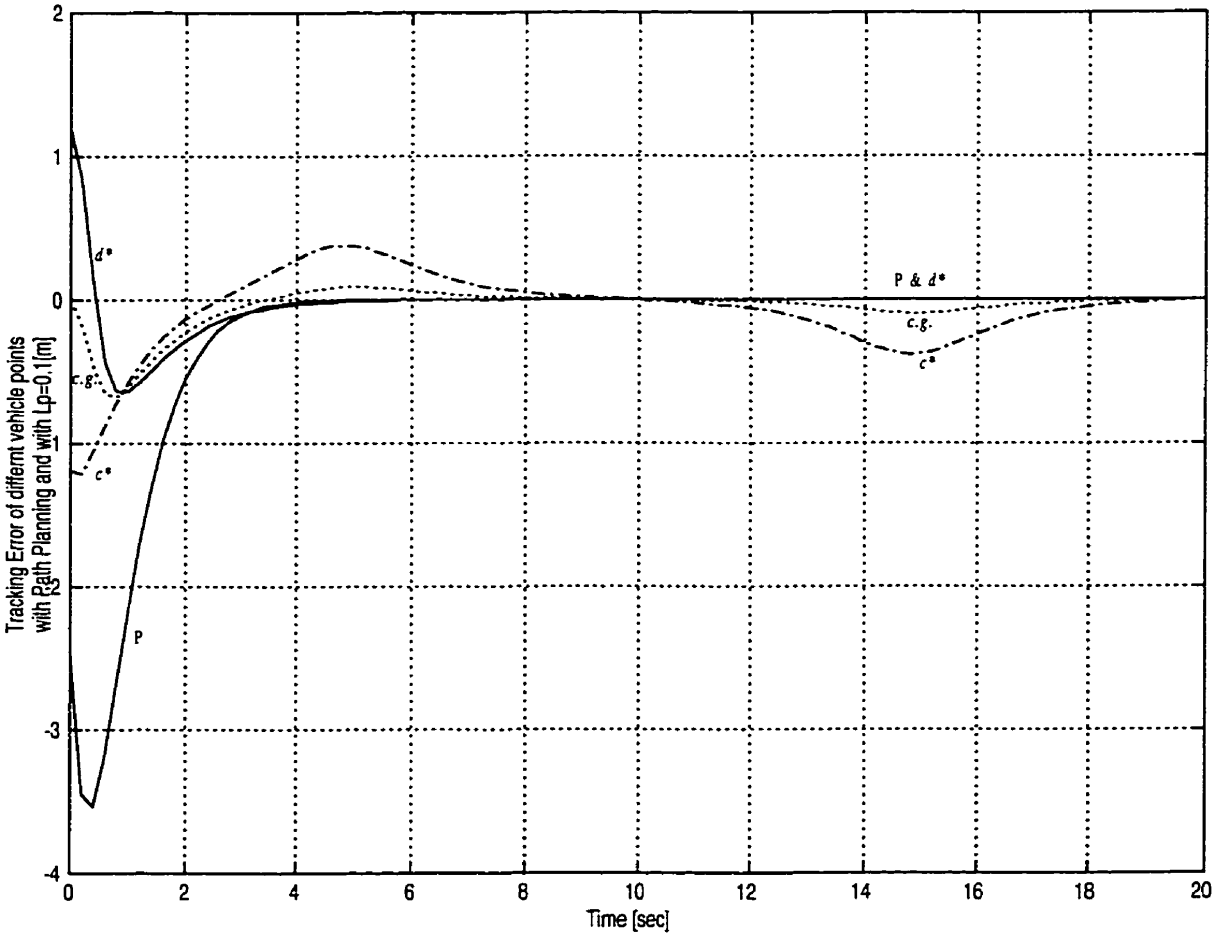

Figure 9 - Time variation for error of point P and lateral-offset of different vehicle points for Lp=0.1 [m] (step 2)

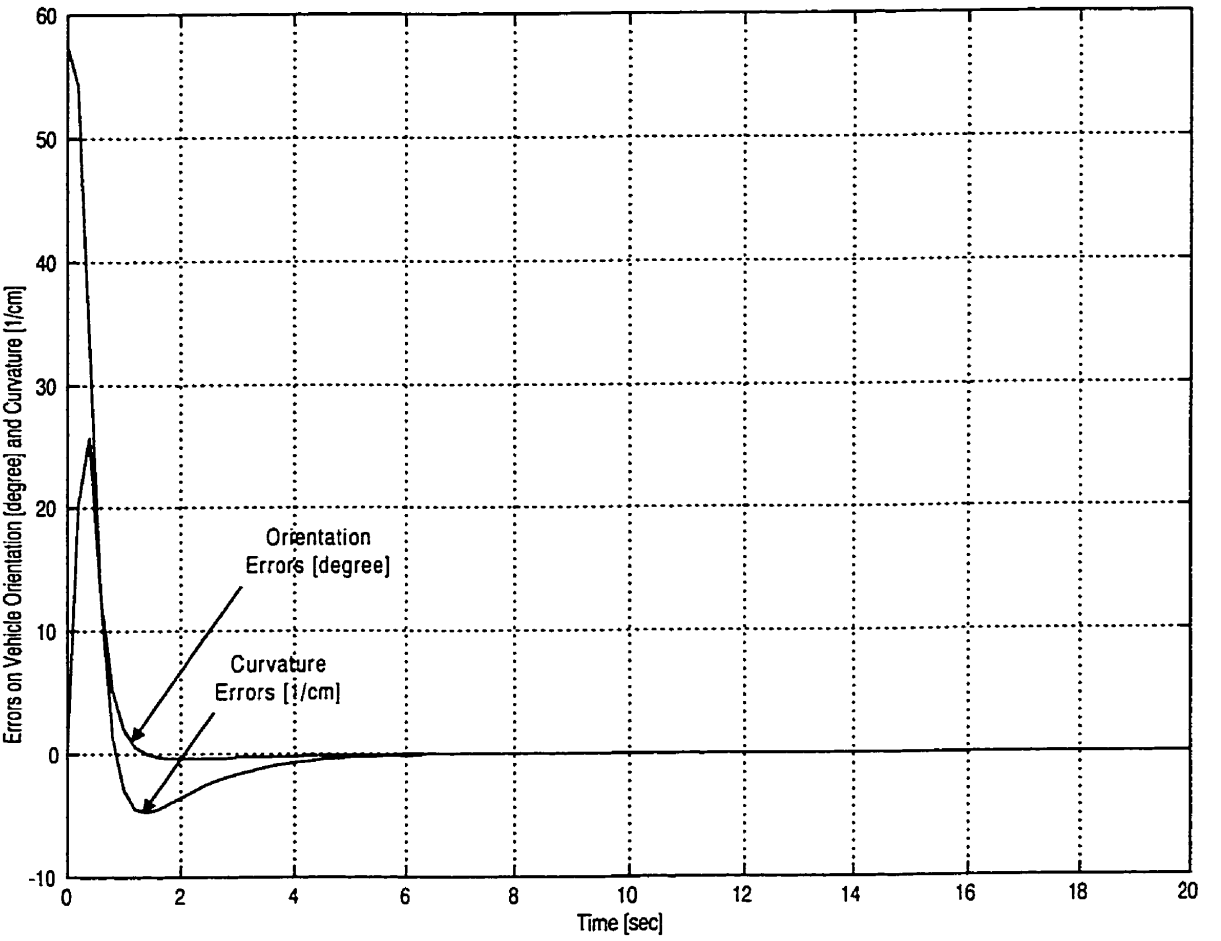

Figure 10 - The orientation and curvature errors with path planning for both Lp=1 and Lp=0.1 (step 2)

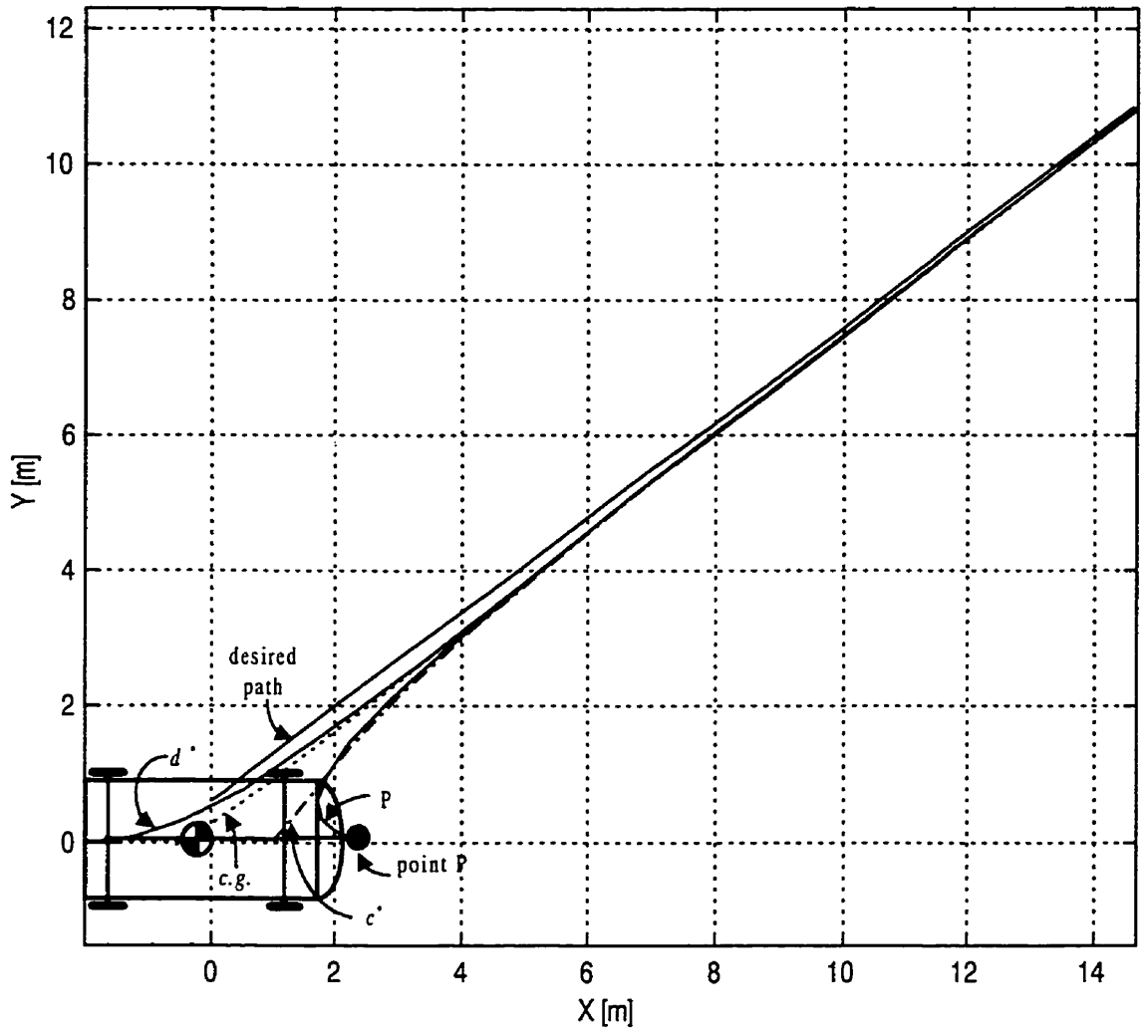

Figure 11 - Trace of different vehicle points when vehicle tracks the desired path in the X-Y plane

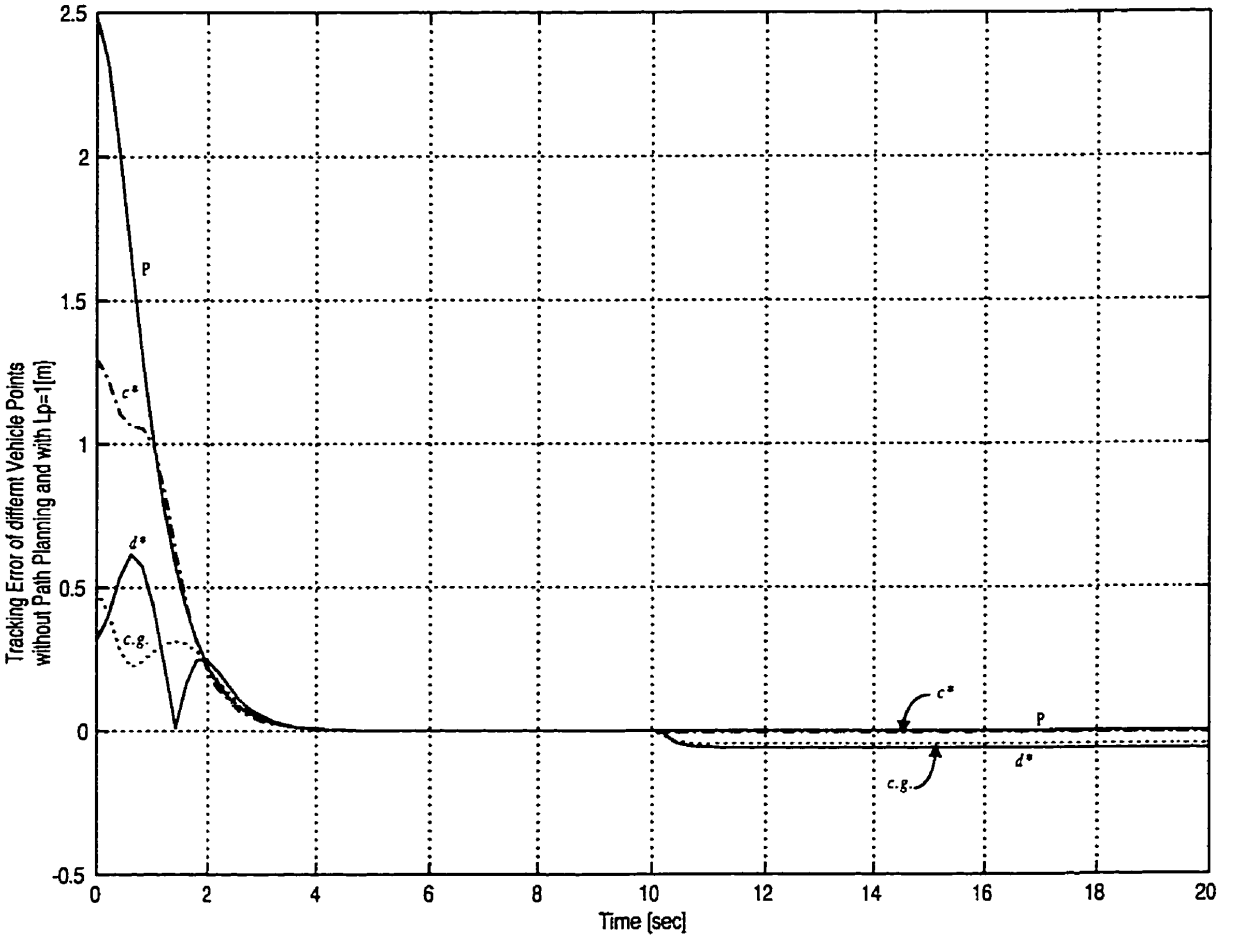

Figure 12 - Time variation of lateral-offsets for a path composed of line and circular arc segments (step 3)

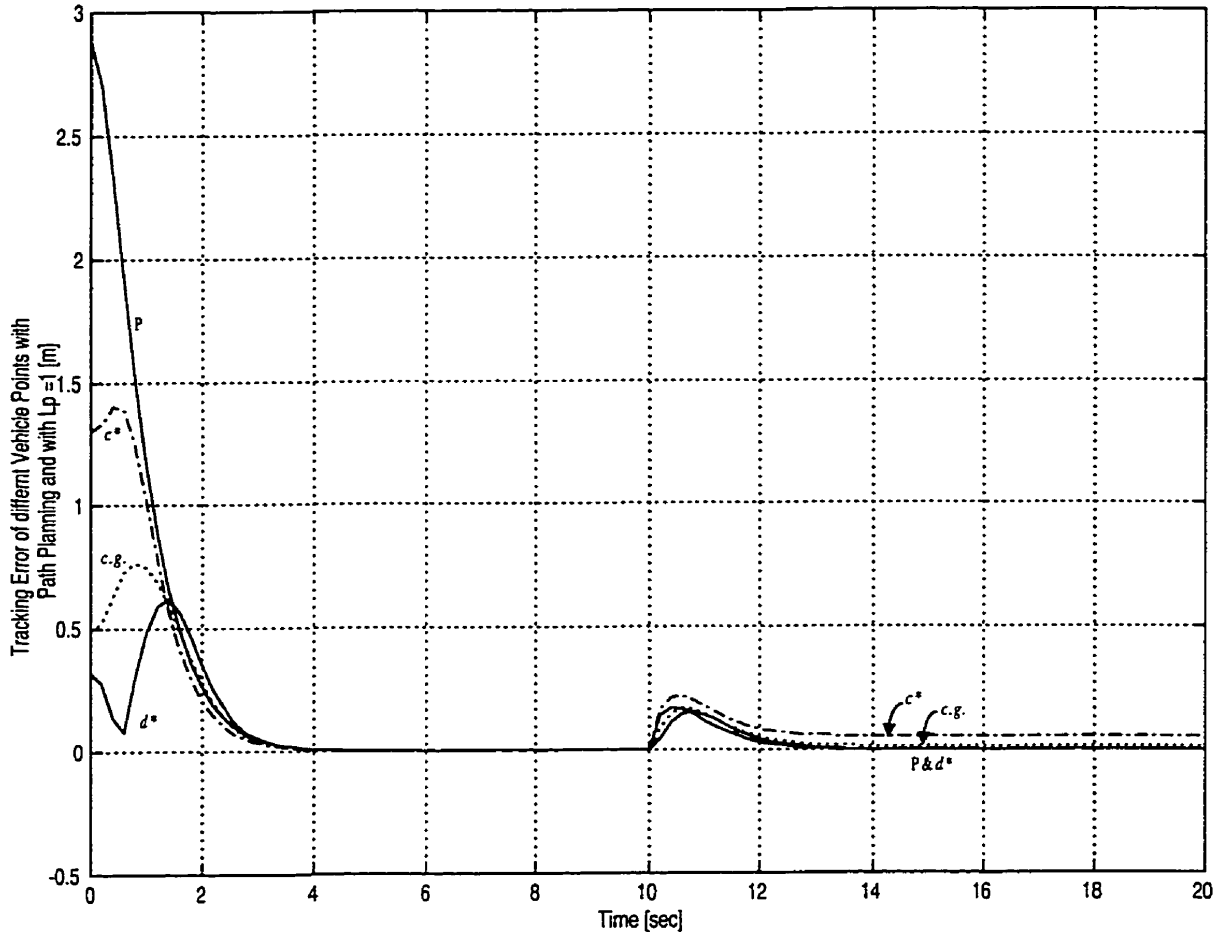

Figure 13 - Time variation of lateral offsets for a desired path composed of line and circular arc segments (step 4).

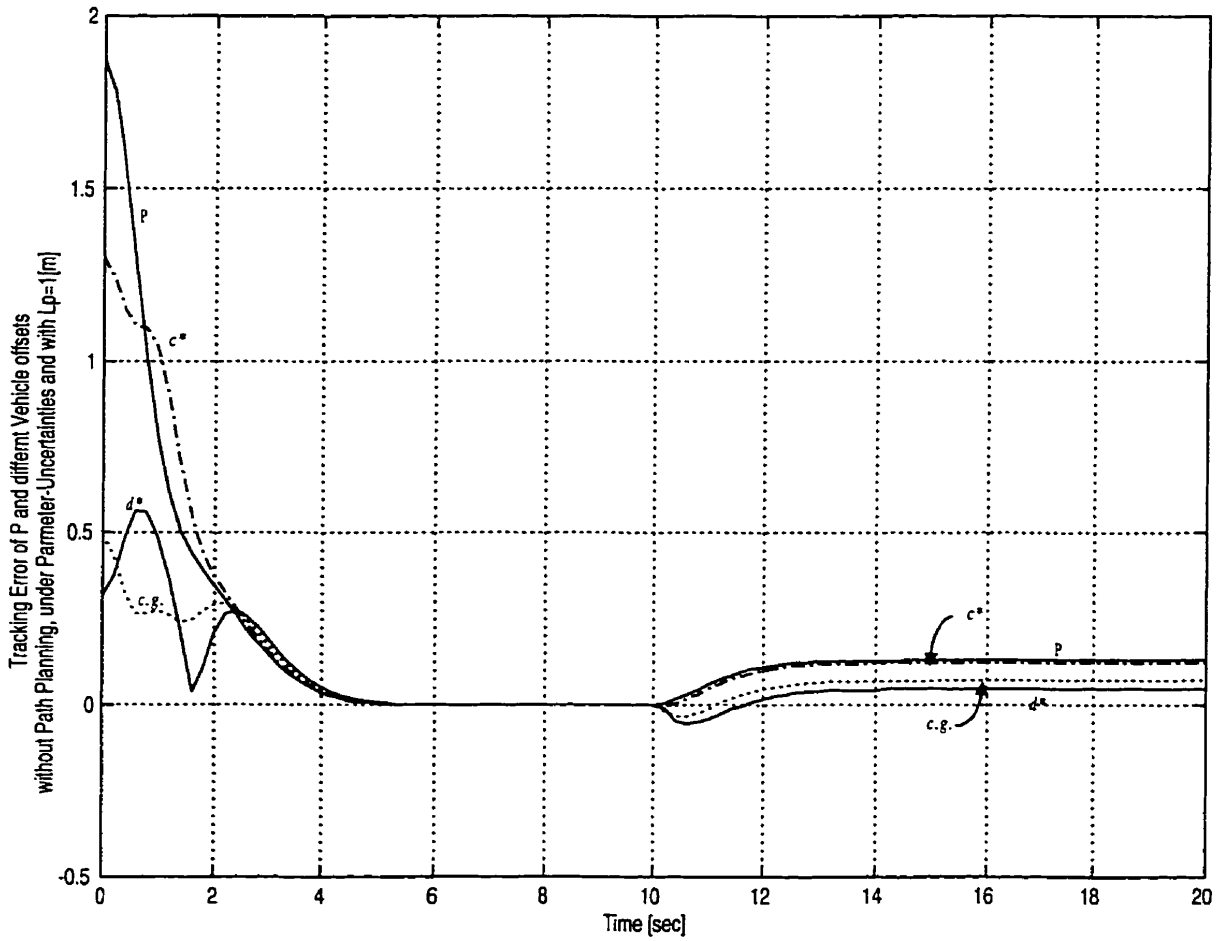

Figure 14 - Tracking error of P and time-variation of different vehicle offsets under parameter uncertainties, without path planning and with Lp = 1 [m] (step 5).

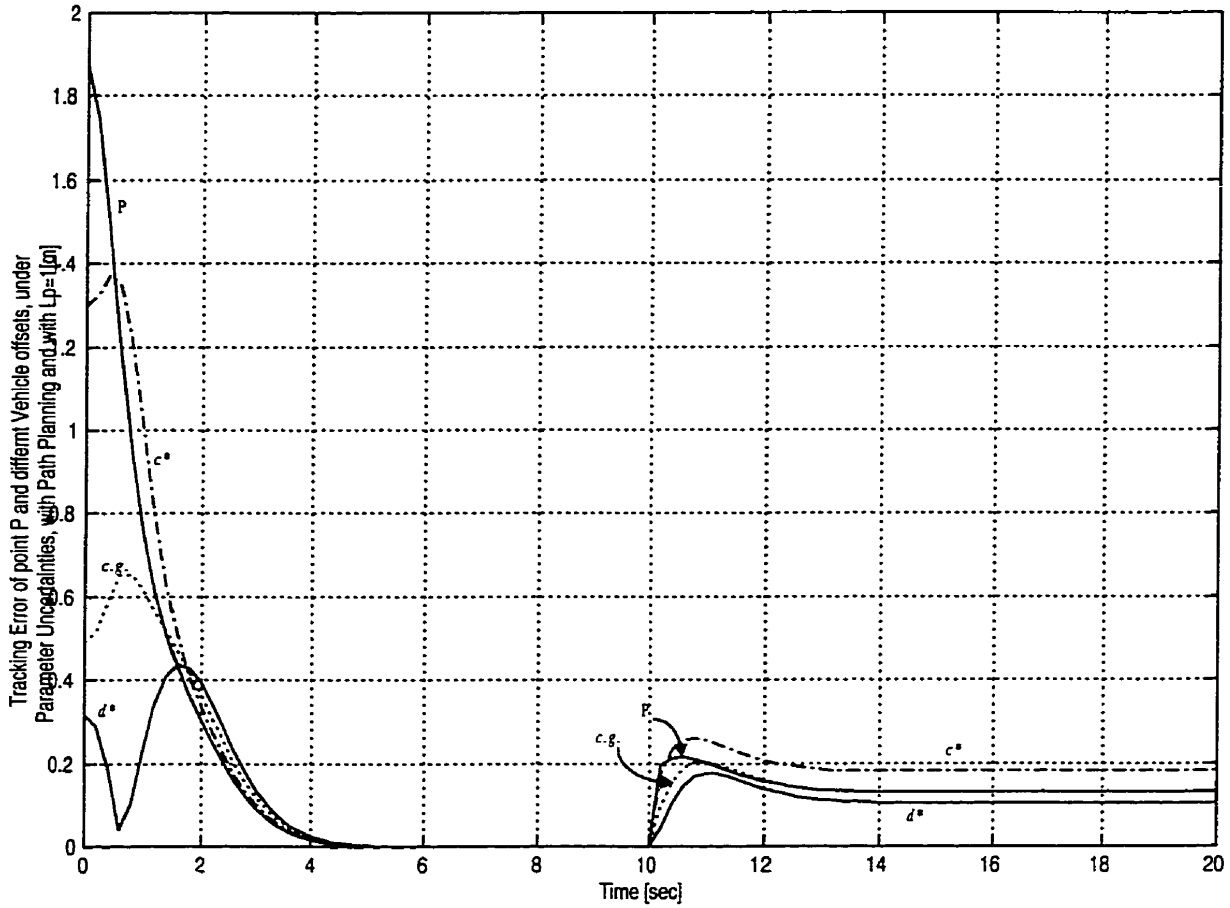

Figure 15 - Tracking error of P and time-variation of different vehicle offsets under parameter uncertainties, with path planning and with Lp = 1 [m] (step 5).

Appendix C: Geometric Lateral-offset Tracking and Speed Control of a Car-like Mobile Robot.

Geometric Lateral-offset Tracking and Speed Control of a Car-like Mobile Robot

Abstract

This paper presents independent lateral-offset tracking and speed control of a car-like mobile robot under nonholonomic (slippage-free) constraints. The state-space representation of the robot dynamic model, which includes the usually ignored steering dynamics, are given for both front and rear wheel drive mobile robots. Although state feedback linearisation of such a system is impossible, a static Input/Output linearisation is feasible for a steerable control-point in front of the vehicle based on the given dynamic model. Unlike previous work on trajectory tracking, the proposed linearisation scheme is based on a purely geometric definition of the lateral-offset. The control law is then developed using an on-line projection of the vehicle position on the geometric desired paths composed of linear and circular arc segments. Since only one output is used for the vehicle lateral control, the vehicle speed is chosen as the second controlled output. The scheme ensures the exponential convergence of both lateral and longitudinal (speed) errors to zero. It is also shown that speeds in the unobservable (internal) dynamics stay bounded while controlled errors are converging toward zero. Simulations are performed to verify the performance of the proposed control law on front and rear wheel drive vehicles.

Keywords: path-tracking, nonlinear control, feedback linearisation, car-like mobile robot.

1. Introduction

Recently, control of mobile robots with nonholonomic constraints has become one of the most active research area, especially in the context of Intelligent Vehicle Highway System (IVHS) toward increasing the existing roads productivity. This research requires the study of kinematics and dynamics as well as nonlinear control of mobile robots. In an IVHS, the control objective is mainly to follow a path at a given speed. Overseeing the vehicle control system, a supervisor coordinates the traffic activities and generates the desired inputs for the vehicle controller. The task of this supervisor would be easier if instead of time dependent trajectories, desired inputs are predefined geometric paths and desired speeds.

Existing mobile robots have been classified [2], [3] into five different families depending on their kinematic behavior. But more attention has been payed to two of these families because of their special characteristics: I) omnidirectional mobile robots, with two independently actuated wheels, which have a high degree of mobility on the plane [2],[3],[4],[7],[11],[12],[13],[16],[17] and II) car-like mobile robots, which are kinematically similar to the actual cars on the road [1],[2],[5],[9],[10]. Because of their higher degree of mobility, omnidirectional mobile robots have simpler kinematics than car-like robots. Omnidirectional robots with their full rank and configuration-independent Jacobian matrix produce a simpler inverse kinematics and ease the control law development. This Jacobian matrix is singular for car-like robots since it has a column of zeros. Car-like robots have a

restricted mobility and the variation of the robot orientation depends on the changes in robot position. This can be explained by the fact that if the omnidirectional robot configuration is derived, applying the nonholonomic constraints, the Jacobian matrix is a full rank matrix with constant terms.

The trajectory trackers based on kinematic models [1],[9],[11],[13],[16] are limited to low-speed applications such as Flexible Manufacturing Systems (FMS). For applications with higher speeds such as IVHS control laws must be developed considering the mobile robot dynamics. Independent from the robot family, the consideration of the vehicle dynamics leads to a nonlinear control problem and, as first trial, the use of classical Input/Output Feedback Linearisation (I/OFL) method [3],[4],[5],[7],[12].

D'andréa-Novel et al. [3] solved the feedback control problem applying the so-called dynamic extension algorithm which is an alternative solution if the system is not linearisable by diffeomorphism. The idea of this algorithm is to *delay* some combination of inputs via the addition of integrators, which may however cause drawbacks in some applications. These integrators enable other inputs to act in the meantime and therefore to obtain an extended decoupled system [3]. DeSantis [5] has introduced a simple, linear and decoupled control structure for paths combined of straight lines and circular arc segments, in which gains are computed using the classical time invariant PID techniques. The major limitations of this work is the occurrence of time-variant gains when either the steering angle or the assigned velocity changes, which happens in most highway automation applications. Also, the

controller becomes time-varying at junction points when the path changes from a straight line to a circular arc and vice-versa.

The common approach in the above literature is the implementation of the I/OFL method for the realization of what is called the trajectory tracking strategy. This strategy is based on generating commands in order to track a previously defined time function desired trajectories. It means that at each instant *t*, the vehicle has to be at a predefined position on the desired trajectory. This strategy can be visualized assuming that the vehicle must track a virtual robot which moves through the desired path. Then, the trajectory tracker ensures the instantaneous match between the configuration (position and orientation) of the real and the virtual robot, canceling the instantaneous error. With this definition, if the real robot is geometrically on the path but behind the moving virtual robot, the trajectory tracker will recognize this situation as an error in the vehicle position. The side effect is the recognition of a "fake" lateral-error that commands the vehicle to accelerate in order to nullify this error even if the vehicle is physically on the path.

In the concept of highway automation, changes in the vehicle speed not only depend on the vehicle position on the path, but also on other factors, such as road and environment conditions, traffic situation, vehicle type, critical lateral acceleration, etc. Hence, a flexible controller is required by which the vehicle speed can be controlled independently from the vehicle lateral-offset path tracking. To this end, Sarkar et al. [12] proposed a *dynamic path-following* scheme for the omnidirectional robot family. Instead of defining desired

trajectories, they have chosen a desired path combined of straight lines and circular arc segments with an arc-length parameter s. Then, the desired speed is set as the derivative of the arc-length $\dot{s}$, and the desired path is a function of the parameter s instead of time t. They concluded that this scheme is more appropriate for vehicle control application than the trajectory tracking strategy. Nevertheless, it seems that the given lateral dynamic path-following still affects the vehicle speed control, because the parameter "s" is a predefined function of time.

This paper presents a purely geometrical scheme for lateral-offset tracking and a speed control of a car-like mobile robot under nonholonomic constraints. The objective of *geometric lateral-offset tracking* is to render the vehicle speed control independent from lateral-offset tracking. This separation removes some limitations and eases its application in realistic situations such as IVHS. In this scheme, lateral-offset error is generated by an on-line projection of the vehicle position on the desired path. Section 2 gives the state space representation of the vehicle rigid body dynamics for both Front Wheel Drive (FWD) and Rear Wheel Drive (RWD) robots. Section 3 shows that the static I/OFL becomes feasible by a steerable control-point in front of the car-like mobile robot considering cross coupling effect between vehicle steering and traction dynamics. This section will also shown that speeds in unobservable dynamics stays bounded while variables of the external dynamics are converging toward their desired values, i.e. errors toward zero. Section 4 presents, comparative simulations in order to verify the performance of the proposed control laws for

both FWD and RWD car-like robots. The last section concludes the paper.

2. Vehicle Dynamics

This section summarizes the kinematics and dynamics of a planar car-like mobile robot driven either by front or rear wheels. In the design of an efficient controller, it is not necessary to model all dynamic complexities of a vehicle. The lateral offset-tracking and speed control of a vehicle can be determined by the planar movements of vehicle in a Cartesian frame. Although tire dynamics has a significant role in vehicle handling analyses, a compromise has been made in this paper on considering the vehicle rigid body dynamics as the base of control law development and of presenting the idea of geometric lateral-offset tracking. While the vehicle follows a path the total cumulative displacement in the Cartesian frame, caused by tire dynamics (wheel slippage), is of small magnitude in comparison with the robot displacements resulting from the steering and traction commands, therefore, it is assumed that the feedback controllers are able to compensate the total error by increasing for example the steering angle or the traction torque.

Figure 1 shows a car-like mobile robot where the steering effect of both front wheels are represented by one virtual-tire (body C). Body C has two perpendicular rotations with respect to (w.r.t) the robot main body A. To have a pure rotation between frames attached to each body, a massless frame B is defined w.r.t frame A by a rotation around a_3 of an angle q_4. The

rotation of front wheel (body C) around b_i is represented by angle q_5. The consideration of one virtual-tire instead of front or rear wheels is not restrictive, because each of the pairs are linked to each other and each represents only one degree of freedom. For a FWD robot the inertial effects of rear wheels are integrated to the body A which results in having one fewer generalized coordinate. As a result, the FWD and the RWD robots have five and six generalized coordinates respectively. In the case of a RWD robot, the sixth generalized coordinates is for the angular rotation of the rigid body D. Like the front wheels, body D is another virtual-tire located at the vehicle rear-center, (point d^* in figure 1), and the rear wheel torque is fed through it.

For both types of robots, the generalized coordinates $[q_1, q_2, q_3]$ define the Cartesian planar coordinates of body A, q_4 represents the steering angle rotation, and q_5 is the front wheel rotation. Although, the driving torque for the RWD robot is fed through the rear virtual-tire, the generalized coordinate q_5 is kept to model the dynamic effect produced due to two perpendicular cross rotations $\dot{q}_4$ and $\dot{q}_5$. For the RWD robot, the generalized coordinate q_6 is added to represent the rear wheel rotation of body D w.r.t body A.

To derive the mobile robots equations of motion (e.o.m.), the method of Kane [8] is used. Let us define $\dot{\boldsymbol{q}} = [\dot{q}_1\ \dot{q}_2\ \dot{q}_3\ \dot{q}_4\ \dot{q}_5]^T$ for the FWD robot and $\dot{\boldsymbol{q}} = [\dot{q}_1\ \dot{q}_2\ \dot{q}_3\ \dot{q}_4\ \dot{q}_5\ \dot{q}_6]^T$ for the RWD robot. Also, $\boldsymbol{u} = [u_1\ u_2]^T$, where $u_1 = \dot{q}_4$ for both robots, and $u_2 = \dot{q}_5$ for FWD robot

and $u_2 = \dot{q}_6$ for a RWD robot.

The non-integrable kinematic constraints, can be represented in a compact form as :

$$\dot{\boldsymbol{q}} = S(\boldsymbol{q})\boldsymbol{u} \tag{1}$$

S is one of the following matrices[1];

$$S = \begin{bmatrix} 0 & K_1 K_{15} \sin q_4 \cos q_3 - \rho \cos q_4 \sin q_3 \\ 0 & K_1 K_{15} \sin q_4 \sin q_3 - \rho \cos q_4 \cos q_3 \\ 0 & K_1 \sin q_4 \\ 1 & 0 \\ 0 & 1 \end{bmatrix} \quad \hat{S} = \begin{bmatrix} 0 & -\rho(l_2/l_a \tan q_4 \cos q_3 - \sin q_3) \\ 0 & \rho(-l_2/l_a \tan q_4 \sin q_3 - \cos q_3) \\ 0 & K_1 \sin q_4 \\ 0 & 1/\cos q_4 \\ 1 & 0 \\ 0 & 1 \end{bmatrix} \tag{2}$$

These nonholonomic constraint equations cause the dependence between the defined generalized speeds and decrease the system degrees of freedom (d.o.f.) from five to two for the FWD robots and from six to two for RWD robots. As a result, after some manual simplifications, the e.o.m of the FWD robot becomes :

$$\begin{aligned} I_{C3}\dot{u}_1 - K_4 \sin q_4 \dot{u}_2 - K_4 \cos q_4 u_1 u_2 &= T_{ab} \\ K_4 \sin q_4 \dot{u}_1 + [(K_5 - K_6)\sin^2 q_4 - K_7]\dot{u}_2 - K_8 \sin q_4 \cos q_4 u_1 u_2 &= T_{bc} \end{aligned} \tag{3}$$

and similarly for the RWD robot :

---

[1] Terms with "hat" symbol are reserved for the RWD robot.

$$
\begin{aligned}
I_{C3}\dot{u}_1 - \hat{K}_1 \tan q_4 \dot{u}_2 - \hat{K}_1 (1 - \tan^2 q_4) u_1 u_2 &= T_{ab} \\
\hat{K}_1 \tan q_4 \dot{u}_1 + (\hat{K}_8 - \hat{K}_9 \tan^2 q_4) \dot{u}_2 - \hat{K}_7 \tan q_4 (1 - \tan^2 q_4) u_1 u_2 &= T_{ad}
\end{aligned}
\tag{4}
$$

where

I_{C3} : virtual-tire inertia around unit vector c_3,

ρ : front or rear wheel radius,

K_i, $\hat{K}_i$: constants given in the appendix,

T_{ab} : steering torque input applied from body A to B

T_{bc} : front wheel torque applied from body B to C

T_{ad} : rear wheel torque applied from body A to D

n_i : unit vectors of the Newtonian reference frame N,

a_i : principal axis of inertia of robot main body A,

b_i : unit vectors of the massless body B,

c_i, d_i : principal axis of inertia of virtual-tires C and D respectively.

Defining $\boldsymbol{t} = [T_{ab} \;\; T_{bc}]^T$ and $\hat{\boldsymbol{t}} = [T_{ab} \;\; T_{ad}]^T$ as vectors of input torques, the e.o.m. of the FWD and RWD mobile robots can be written in matrix form as:

$$
\begin{aligned}
\boldsymbol{M}(\boldsymbol{q})\ddot{\boldsymbol{q}} + \boldsymbol{c}^*(\boldsymbol{q},\boldsymbol{u}) &= \boldsymbol{t} \\
\hat{\boldsymbol{M}}(\boldsymbol{q})\ddot{\boldsymbol{q}} + \hat{\boldsymbol{c}}^*(\boldsymbol{q},\boldsymbol{u}) &= \hat{\boldsymbol{t}}
\end{aligned}
\tag{5}
$$

where $M(q)$ and $\hat{M}(q)$ are the mass matrices and $c^*(q,u)$ and $\hat{c}^*(q,u)$ are the vectors of centrifugal and Coriolis forces.

The above second order differential equations (5) can be reformulated as a set of first order differential equations which is more convenient for control design. Defining the state space variables for the FWD robot as: $x_1 = q_4,\ x_2 = \dot{q}_4,\ x_3 = q_5,\ x_4 = \dot{q}_5, x_5 = q_1,\ x_6 = q_2,\ x_7 = q_3$, and for the RWD robot: $x_1 = q_4,\ x_2 = \dot{q}_4,\ x_3 = q_6,\ x_4 = \dot{q}_6, x_5 = q_1,\ x_6 = q_2,\ x_7 = q_3,\ x_8 = q_5$, either of the state-space representation of the system dynamics will be :

$$\dot{x} = f(x) - \Gamma(x)t \tag{6}$$

with f to be one of the following:

$$\begin{aligned} f &= \begin{bmatrix} x_2 & f_1 x_2 x_4 & x_4 & f_2 x_2 x_4 & x_4(K_1 K_{15} s_1 c_7 - \rho c_1 s_7) & x_4(K_1 K_{15} s_1 s_7 - \rho c_1 c_7) & K_1 x_4 s_1 \end{bmatrix}^T \\ \hat{f} &= \begin{bmatrix} x_2 & \hat{f}_1 x_2 x_4 & x_4 & \hat{f}_2 x_2 x_4 & -\rho x_4(l_2/l_a t_1 c_7 - s_7) & \rho x_4(-l_2/l_a t_1 s_7 - c_7) & K_1 x_4 t_1 & x_4/c_1 \end{bmatrix}^T \end{aligned} \tag{7}$$

and Γ to be one of:

$$\Gamma = \begin{bmatrix} 0 & g_1 & 0 & g_2 & 0 & 0 & 0 \\ 0 & g_2 & 0 & g_3 & 0 & 0 & 0 \end{bmatrix}^T, \qquad \hat{\Gamma} = \begin{bmatrix} 0 & \hat{g}_1 & 0 & \hat{g}_2 & 0 & 0 & 0 & 0 \\ 0 & \hat{g}_2 & 0 & \hat{g}_3 & 0 & 0 & 0 & 0 \end{bmatrix}^T \tag{8}$$

where $f_1, f_2, g_1, g_2, g_3, \hat{f}_1, \hat{f}_2, \hat{g}_1, \hat{g}_2, \hat{g}_3$ are nonlinear functions, and c_i, s_i, t_i $(i = 1,7)$ are respectively the cosine, the sine and the tangent of the steering angle x_1 given in the appendix.

Neglecting the tire dynamics may raise a discussion about the validity of the nonholonomic kinematic constraints which depends on the existence of constraint or reaction forces. For a mobile robot, these forces are both lateral friction forces, which prevent tires from skidding, and longitudinal friction forces, which allow acceleration and braking. The existence of these forces [8], results in the nonholonomic constraints and actually without them the system is not controllable. It is also implicitly assumed that the vibrations in tire dynamics are damped enough so that they do not destabilize the proposed path-tracking scheme and the path-tracker will be able to compensate the measured lateral or speed errors arising from tire pneumatic deformations.

3. Control Algorithm

3.1 Choice of a Control-point

In the context of geometric lateral-offset tracking, the instantaneous offset between a vehicle point (*control-point*) and the desired path is defined as the lateral-offset. Most researchers have chosen a control-point attached to the vehicle main body (body A) such as center of gravity (c.g.) Such a point is an appropriate choice for the family of omnidirectional mobile robots. But for a car-like robot, if the angular velocity of the front wheel (around b_1 in Figure 1) is zero, the steering commands will not affect the motion of such control-points and this leads to a singular Jacobian matrix.

This fact can be shown for an arbitrary control-points P* attached to the body A. The position vector of point P* from the vehicle c.g. is $\boldsymbol{p}^* = X_a \boldsymbol{a}_2 - Y_a \boldsymbol{a}_1$, (see figure 1), where X_a and Y_a are any real constant values. In the Newtonian reference frame, N, the derivative of this vector is :

$$\dot{\boldsymbol{p}}^* = \begin{bmatrix} \dot{x}_{p^*} \\ \dot{y}_{p^*} \end{bmatrix} = \begin{bmatrix} \dot{x}_6 \\ \dot{x}_5 \end{bmatrix} - \dot{x}_7 \begin{bmatrix} -s_7 & -c_7 \\ c_7 & -s_7 \end{bmatrix} \begin{bmatrix} X_a \\ Y_a \end{bmatrix} \tag{9}$$

Substituting the appropriate terms of eq. (6) into eq. (9), the steering angular speed x_2 does not appear in the right side of eq. (9), neither for the FWD nor for the RWD robots. Hence, the Jacobian matrix is singular for any point attached to the body A such as P*. The control-point, proposed here, is a steerable point in front of the robot, i.e. the point P in figure 1 with position vector $\boldsymbol{p} = [x_p \; y_p]^T$ which satisfies the necessary condition of having a non-singular decoupling matrix. The idea behind this choice can be visualized by a child pulling a cart. The kinematics of a front steering child-cart is very similar to a car-like mobile robot of figure 1. If the child attaches a rope to any fixed control-point P*(ex. the center of front tire axis c^*), he will have difficulties guiding his cart through a desired path. But, if the pulling rope is attached on a point on the steering handle (visualized by point P), he can run through any desired path and the cart will follow him. The Cartesian coordinates of point P are derived from the vehicle states as:

$$\begin{aligned} x_p &= x_6 - l_1 c_7 - L_p c_{17} \\ y_p &= x_5 - l_1 s_7 - L_p s_{17} \end{aligned} \tag{10}$$

where $c_{ij} = \cos(x_i - x_j)$ and $s_{ij} = \sin(x_i - x_j)$.

The Jacobian matrix J_p which relates the Cartesian velocities of the point P to the joint speeds x_2 and x_4 is then:

$$\dot{\boldsymbol{p}} = J_p \begin{bmatrix} x_2 \\ x_4 \end{bmatrix} = \begin{bmatrix} N_1 & M_1 \\ N_2 & M_2 \end{bmatrix} \begin{bmatrix} x_2 \\ x_4 \end{bmatrix} \tag{11}$$

where N_1, M_1, N_2 and M_2 are given in the appendix. Although, J_p is still configuration dependent, its determinant stays constant, $|J_p| = \rho L_p$, and the matrix inverse exists for any $L_p = 0$. Let us define $L_p^* = L_p/\rho$. For a very small value of L_p^* (less than 0.6) the system is close to singularity and it may result in high traction or steering torques, but simulation shows that with $L_p^* \geq 0.6$ the system is far enough from the singularity and the generated torques are reasonable. At $L_p^* = 0.6$, the point P is close enough to the point c^* and comparing with the vehicle size it can be considered as a pivoting point around c^*.

Compensating the vehicle lateral-offset by using a steerable control-point in front of a car-

like robot is advantageous compared to a vehicle fixed point path tracking. It results in a more robust controller, because perturbations, such as discontinuities in the desired path, are firstly encountered by the steerable point in front of the vehicle. This point requires smaller amount of energy to be returned back on the path. This guidance strategy simplifies the control law development and it is in agreement with human driver behavior, i.e. guiding the vehicle by looking in front of the vehicle.

3.2 Path and Error definition

Figure 2 shows the basic architecture of the proposed scheme in which the inputs are the geometrical characteristics of the desired path and the vehicle desired speed. While the lateral-offset is defined geometrically , the vehicle speed is a step function of time or arc length in order to allow varying the vehicle speed any time and anywhere on the path. The measurement of the instantaneous lateral-offset and speed errors are made in the global or Cartesian reference frame.

A. *Lateral-offset tracking*

The lateral error is defined as *the distance between the control-point P and the nearest point on the desired path.* If the desired path is a general function $y = f(x)$, the nearest point T, is computed by the perpendicular projection of the control-point on the desired path. Then, the lateral-offset will be:

$$e_1 = \pm\sqrt{(x_T - x_P)^2 + (y_T - y_P)^2} \tag{12}$$

where (x_T, y_T) are the results of following differential equations:

$$\frac{d}{dt} f(x_T)[f(x_T) - y_P] - (x_T - x_P) = 0$$
$$y_T = f(x_T) \tag{13}$$

Solving these equations for any general function has some practical limitations which render the generalization of the approach less interesting. First, frequent maneuvers such as U-turn and 270 degree turns on the existing highways cannot be reproduced in the form of smooth functions, i.e. there are more than one $y_T = f(x_T)$ for each x_T. Hence, the desired path must be broken into several functions (segments). Second, the solution to equation (13) must be found numerically for the majority of continuous functions that do not have a constant radius of curvature. Besides, more than one answer is found for x_t.

Since breaking the desired path into different segments is inevitable, the robot pathway through the already-constructed roads can be well approximated by straight line and circular arc segments. These combined paths, with their special characteristic of having constant curvature, appear as the ideal way of modeling the desired path of a car-like robot. This combination is also justified by the fact that a car-like mobile robot has difficulties following any arbitrary paths because of the physical limits on its steering angle and its special kinematics, i.e. restricted mobility. Desaulniers et al. [6] have studied this problem and concluded that the shortest path between two positions is achieved by a combination of line segments and circular arcs of minimal turning radius. This combination is also the optimal

path between each of two arbitrary configurations [14]. Hence, the lateral error is only defined for paths made up of a combination of straight lines and circular arc segments. Choosing this path combination, the radius of the circular arcs are limited to be greater than or equal to the minimal turning radius which is not a restriction. Practically, it is not a restriction on maneuvers because even the radius of a u-turn path is greater than the minimal turning radius.

In figure 3, e_1^A and e_1^B are the lateral-offset errors for the linear and circular arc segments of the desired path, respectively. They are expressed as functions of the control-point position:

$$\begin{aligned} e_1^A &= s_\alpha x_p - c_\alpha (y_p - n) \\ e_1^B &= R - R_c \end{aligned} \tag{14}$$

where $s_\alpha = \sin\alpha$, $c_\alpha = \cos\alpha$, $\Delta x = (x_p - x_B)$, $\Delta y = (y_p - y_B)$ and $R_c = \sqrt{\Delta x^2 - \Delta y^2}$.

The Cartesian coordinates of control-point as functions of the vehicle state-space variables are given in equation (10). As seen in equation (14), the geometric lateral-offsets are only functions of the vehicle position and the characteristics of the desired path. The lateral-offset calculation will switch from e_1^A to e_1^B at the junction point "J". This point is the projection of the circular arc center (x_B, y_B) on the straight line segment.

Since the objective is to design a geometric lateral-offset tracking in which time is involved implicitly, the switching criterion is set to be a distance instead of an instant. To this end, $s(x_p, y_p)$ is computed as the distance that the projected point "T" is traveled while the vehicle is tracking the path:

$$s(x_p, y_p) = c_\alpha x_p - s_\alpha (y_p - n) \tag{15}$$

When the traveling point "T" (figure 3) reaches the junction point J, the traveled distance by the projected point will be $S_J = s(x_B, y_B)$, and the switching criterion becomes $s = S_J$. For the circular arc segments, an arc-length variable (ex. an angle) can be defined similarly as the switching criterion from which the vehicle changes the segment either to another circular arc with different curvature or to a new straight line segment. The lateral-offset definition allows the use of simple geometric criteria to change from one segment to another and its time-independent definition allows the realization of a completely independent speed control strategy.

The major difference between the proposed scheme and the trajectory tracking strategy is in the definition of the lateral error. In trajectory tracking, the error is the instantaneous difference between the actual and desired values which are predefined by the desired trajectories. In the geometric tracking, the lateral-error is the instantaneous geometric offset of the control-point from a given desired path. After that the lateral error is computed, the

control system remains the same for both trajectory and geometric tracking methods. Another difference between the geometric tracking scheme and the trajectory tracking strategy is that the former only uses one output, hence making the independent speed control possible. Anyhow, these two approaches are fundamentally the same, for instance, one may choose $x_P(t)$ and $y_P(t)$ as the linearisable outputs and their desired values as the time parameterized desired trajectories. The major disadvantage of trajectory tracking is that independent speed control is no longer possible.

B. *Longitudinal or Speed Control*

The speed error is defined as be the difference between the vehicle longitudinal speed along a_2 in figure 1 and a desired value. For the FWD and RWD mobile robots, the longitudinal speed errors are defined as follows:

$$\begin{aligned} e_2 &= \rho c_1 x_4 - V_d \\ \hat{e}_2 &= \rho x_4 - V_d \end{aligned} \tag{16}$$

where $V_d \geq 0$ is a multi-step constant speed. For $V_d = 0$ the controller becomes theoretically unstable, but there are only three possible cases: 1) the vehicle has a lateral-offset greater than L_p, 2) the vehicle has a lateral-offset smaller than L_p or 3) the vehicle is on the path. The system is unstable only in the first situation, i.e. if one desires to cancel the lateral-offset without moving the vehicle forward, but this meaningless from practical point of view. In

the second case, $V_d = 0$ does not destabilize the system because the lateral-offset of point P can be canceled only by a steering command without decreasing the real vehicle offset. Still it is meaningless to stop the vehicle before putting it on the path. In the third case, the controller is stable.

The vehicle desired speed represents the driver decision of changing speed which is an abrupt change in most cases. Due to the definition of the geometric lateral-offset, this abrupt change has minor effect on the lateral-offset tracking. It will be verified later by simulation. Although, in most industrial applications of manipulator robots, the trajectory tracking strategy has been successfully implemented, for mobile robots, if the tracking is performed based on trajectory tracking, the system may be destabilize by unpredicted abrupt change of the vehicle speed. For consistency, the lateral and longitudinal errors (our outputs) are grouped into the vector $e = [e_1 \ e_2]^T$. The error e_1 can be either e_1^A or e_1^B depending on the desired path segment and the speed error e_2 is either of the errors defined in equation (16) depending on the vehicle type.

3.3 Controller Design

To realize the lateral-offset tracking and the speed control of a car-like mobile robot, the classical I/OFL method has been chosen among the nonlinear control strategies [15]. As it is shown in figure 2, the true geometric lateral-offset of the vehicle from the desired path,

whatever its speed, is computed in the *Projection* bloc which instantaneously finds the projected point T on the desired path, and computes the vector of errors $\boldsymbol{e}$. The *Linear Controller* produces the linear commands $\nu = [\nu_1 \ \nu_2]^T$ to reduce these errors to zero:

$$\begin{aligned} \nu_1 &= \eta_1 e_1 - \eta_2 \dot{e}_1 \\ \nu_2 &= \eta_3 e_2 \end{aligned} \tag{17}$$

where the gains η_1, η_2, η_3 provides the desired characteristics of system external dynamics, for instance, a settle time of three seconds and a critical damping ratio. Finally, the *Nonlinear Controller* generates an appropriate torque vector to cancel the vehicle dynamic nonlinearities. The torque vector $\boldsymbol{t}$ is either of expressions previously used in equation (5).

As the first step of I/OFL method, equations (14) and (16) must be differentiated until the vehicle input vector $\boldsymbol{t}$ appears explicitly. To avoid the repetition, the process of linearisation is explained using only the FWD terms:

$$\begin{aligned} \ddot{e}_1^A &= \psi_1 - \zeta_1 T_1 - \zeta_2 T_2 \\ \ddot{e}_1^B &= \psi_2 - \zeta_3 T_1 - \zeta_4 T_2 \\ \dot{e}_2 &= \psi_3 - \zeta_5 T_1 - \zeta_6 T_2 \end{aligned} \tag{18}$$

where the terms ψ_k and ζ_m are given in the appendix. The above equations can be written in a compact form:

$$\ddot{e} = \psi - Zt \tag{19}$$

where $\ddot{e} = [\ddot{e}_1 \ \dot{e}_2]^T$, $\psi = [\psi_i \ \psi_3]^T$, ($i = 1$ for $s < S_J$) or ($i = 2$ for $s \geq S_J$), and decoupling matrix $Z = [\zeta_i \ \zeta_j : \zeta_5 \ \zeta_6]$, $(i,j) = (1,2)$ for $s < S_J$ or $(i,j) = (3,4)$ for $s \geq S_J$. A similar equation is found for RWD mobile robot. Then the input torques should be :

$$t = Z^{-1}(\nu - \psi) \tag{20}$$

Substituting it into equation (19), the relationship between the output vector and the new manipulated vector ν becomes simply: $\ddot{e} = \nu$. Since the necessary and sufficient condition of an I/OFL is to have a non-singular matrix Z, for any values of x in the state space, the matrix determinant (ex. $\zeta_1 \zeta_6 - \zeta_2 \zeta_5$ for FWD on the linear segment) is set to zero at both linear and circular arc segments and for both the FWD robots as well as the RWD robots. As a result, both vehicle families require the same restrictions toward a non-singular decoupling matrix :

i) the steering angle must stay in the range of $-\pi/2 < q_4 < \pi/2$. Practically, this is not a restriction and even for severe maneuvers the steering angle value is much smaller than $\pm \pi/2$.

ii) the virtual-tire must never be perpendicular to the desired path. This can be restrictive

if the vehicle initial control-point P is far from the desired path. The theoretical condition is to assume that the lateral-offset is always less than or equal to *Lp*, i.e. small perturbations do not affect the system stability. Nevertheless, simulation results show that if the vehicle desired speed is not zero this condition never takes place even if the lateral-offset is as big as many times of the length of *Lp*. A related discussion is given in the next section.

3.4 Internal Dynamics

To take a formal look at the notion of internal dynamics let us transform the system to the so-called "normal form" by defining the diffeomorphism z as:

$$\begin{aligned} z &= [z_{extr}\ z_{intr}]^T \\ z_{extr} &= [z_1\ z_2\ z_3]^T \\ z_{intr} &= [z_4\ z_5\ z_6\ z_7]^T \end{aligned} \tag{21}$$

For z to be a diffeomorphism, it is sufficient to show that its Jacobian is invertible, i.e. that the gradients ∇z_{extr} and ∇z_{intr} are all linearly independent. The classical approach is to define $z_{extr} = [e_1, L_f e_1, e_2]^T$. Then, choosing $z_{intr} = [x_1, x_3, x_7, ax_5 + bx_6]^T$, with arbitrary *constants* a and b, the Jacobian $\partial z(x)/\partial x$ is invertible. This is true if the determinant is not zero for either of straight line or circular arc segments. After many manipulations, solving $|\partial z(x)/\partial x| = 0$ results in the same restrictions that we had for the decoupling matrix. Besides, the nonzero determinant depends also on the condition $as_\alpha - bc_\alpha = 0$ for the straight line

segment and on the condition $(a\Delta x - b\Delta y)/R_c = 0$ for the circular arc segment. These conditions are not restrictive since a and b are arbitrary, for instance, $a = s_\alpha$, $b = c_\alpha$ for the line segment and $a = b = 1$ for the circular segment result in a nonzero determinant. Using this diffeomorphism, the presentation of internal dynamics, in the normal form, for the straight line segment is :

$$\dot{z}_{intr} = \frac{1}{\rho L_p \tilde{c}_\gamma \tilde{c}_4} \begin{bmatrix} -\rho\tilde{c}_4 & -\rho s_\gamma - K_1 L_p \tilde{c}_\gamma \\ 0 & L_P \tilde{c}_\gamma \\ 0 & K_1 \tilde{s}_4 L_p \tilde{c}_\gamma \\ 0 & L_p \tilde{c}_\gamma [K_1 K_{15} \tilde{s}_4 (a\tilde{c}_6 - b\tilde{s}_6) + \rho\tilde{c}_4 (-a\tilde{s}_6 - b\tilde{c}_6)] \end{bmatrix} \begin{bmatrix} z_2 \\ z_3 + V_d \end{bmatrix}$$

where $\tilde{s}_i = \sin z_i$, $\tilde{c}_i = \cos z_i$ and $\tilde{c}_\gamma = \cos\gamma = \cos(z_4 + z_6 - \alpha)$[2]. Similarly for the circular segment :

$$\dot{z}_{intr} = \frac{1}{\rho L_p \tilde{\delta}_p \tilde{c}_4} \begin{bmatrix} \rho\tilde{c}_4 R_c & \rho(\Delta x \tilde{c}_{46} - \Delta y \tilde{s}_{46}) - K_1 L_p \tilde{s}_4 \tilde{\delta}_p \\ 0 & L_p \tilde{\delta}_p \\ 0 & K_1 L_p \tilde{s}_4 \tilde{\delta}_p \\ 0 & L_p \tilde{\delta}_p [K_1 K_{15} \tilde{s}_4 (a\tilde{c}_6 - b\tilde{s}_6) + \rho\tilde{c}_4 (-a\tilde{s}_6 + b\tilde{c}_6)] \end{bmatrix} \begin{bmatrix} z_2 \\ z_3 + V_d \end{bmatrix}$$

where $\tilde{\delta}_p = \Delta x \tilde{s}_{46} - \Delta y \tilde{c}_{46}$ and $\tilde{c}_{ij} = \cos(z_i + z_j)$, $\tilde{s}_{ij} = \sin(z_i + z_j)$. The $\tilde{\delta}_p = 0$ is the perpendicularity condition of the virtual-tire to circular arc segments. The presented normal form of the

[2] The tilde index is used to distinct the z space from the x space.

internal dynamics, for both linear and circular arc segments, shows that the internal dynamic speeds, i.e. $\dot{z}_{intr} = [\dot{x}_1, \dot{x}_3, \dot{x}_7, a\dot{x}_5 - b\dot{x}_6]^T$, relates to the linearized outputs by bounded trigonometric functions. Since $z_2 = \dot{e}_1$ and $z_3 = e_2 - V_d$ are controlled variables and the terms of the above matrix are all bounded, the stability of internal dynamics becomes dependent on the stability of the external dynamics. Hence, the speeds of the unobservable dynamics stays bounded while the errors are converging to zero. This is valid for both FWD and RWD mobile robots.

4. Simulations

To verify the effectiveness of the proposed control law, simulations have been carried out using Matlab (Simulink). The vehicle parameters given in the appendix have been selected to closely resemble most of today's compact class of FWD and RWD vehicles. Two series of simulations are carried out for FWD and RWD robots to compare their dynamic behavior while the controller tracks the desired path of figure 4 which consists of a straight line followed by a circular arc with a turning radius of about 85 meters. The initial values for vehicle generalized coordinates are all set to zero, i.e. the vehicle is initially far from the desired path and the control-point P is at $[x_p, y_p]^T = [2.6, 0]^T$ meters (figure 5). The desired speed is chosen to keep the lateral acceleration below the critical acceleration, i.e. 3 m/sec.^{2} (0.3 g), to avoid skid in normal road condition.

4.1 lateral-offset tracking with constant speed

In the first simulation, both FWD and RWD robots have to reach and keep the desired speed of 10 m/s during the path following. Figure 4 shows that both robots can nullify the initial position error and can follow the desired path. Figures 5 zooms the initial starting segment to see how the lateral initial error converges to zero in the Cartesian space even for an initial lateral error much larger than *Lp*. The difference between the tracking behavior of the FWD and RWD robots can be explained by the way that the longitudinal controlled speed (vehicle speed along the a_2 axis) is defined for each robot. For the FWD robot, this speed is defined by projecting the velocity of the front wheel on the vehicle longitudinal axis, i.e. $\rho x_4 \cos x_1$.

As a result, the variation of the steering angle affects the *controlled speed*. Since the robot has zero initial velocity, the speed controller tries to keep the steering angle close to zero in order to have the maximum speed projection so as to increase the robot velocity faster. Meanwhile, the lateral-offset tracker wants to increase the absolute value of the steering angle in order to decrease the lateral error.

These opposite requirements, produce a slower increase of the steering angle and a smoother compensation of the lateral-offset deviation for FWD robots. For the RWD robot, the *controlled speed* is simply ρx_4 and steering angle does not affect the speed control, thus there is no such opposite requirements. It seems as if controlling the same parameter ρx_4 for FWD robots, which represents the virtual-tire speed instead of the vehicle longitudinal speed,

removes the conflict and results to an easier and quicker lateral-offset tracking with the inconvenience of higher value of steering angle.

Figure 6 shows the steering angle variation for both FWD and RWD mobile robots. At the beginning of the simulation, the steering angle has smaller values for FWD robots than for RWD vehicles because of the opposite requirement explained previously. At the junction of the path segments, where FWD and RWD robots are both at their desired speed, difference in their steering commands is minor. The variations of the required power for both robots are shown in figure 7 and as it is seen it is more smooth for the FWD robot than for the RWD ones. The reason is partly justified by the above explanation.

Figures 8 and 9 give the time variation of the geometric lateral-offset and the longitudinal speed errors, respectively. Although the second derivative of the desired path is discontinuous at the junction of the two segments, the simulation shows no significant increase on both lateral and longitudinal errors at this point. With the chosen desired speed of 10 m/s, the vehicle reaches this point after eight seconds. The value of Lp has been varied from 0.1 meter to 10 meters to verify its effect on the errors at the junction point but no noticeable change has been observed.

4.2 Effect of discontinuous speed change

As mentioned before, the desired speed can be a function of parameter s or time. In the next set of simulations, the desired speed changes abruptly using a step function of time. The

desired speed is initially set to 15 m/s and it decreases to 10 m/s after 10 seconds. The plot of the lateral-offset tracking (not shown) is quite the same as figures 4 and 5, and no significant difference is recognized, meanwhile figures 10 to 12 show more significant results.

While the vehicle is following the circular arc segment, a sudden change of the desired speed perturbs the lateral offset tracking more than when it is following the straight line segment. This is due to the presence of all nonlinear terms of the system dynamics, i.e. the coupling effect of steering and traction dynamics. Although, no robustness has been considered in the control law development, the controller behaves robust enough in lateral-offset tracking even under the abrupt changes of the desired speed. The opposite requirement on steering commands, explained before for the FWD robots, results in a more robust lateral-offset tracker in the presence of such discontinuous changes in the desired speed, (figure 10 and 12). To ensure the zero-error tracking under perturbations such as parameter uncertainties, the linear commands must be more robust than a simple PD (proportional derivative).

5. CONCLUSION

A method for controlling a FWD and RWD car-like mobile robots under nonholonomic constraints has been developed considering the usually neglected steering dynamics. A control-point in front of the vehicle makes the I/OFL feasible for a geometric lateral error

considering vehicle rigid body dynamics. Unlike the conventional trajectory trackers, the proposed path tracker scheme is designed defining the lateral error as the instantaneous geometric lateral-offset of the mobile robot from the desired path which is composed of straight line and circular arc segments. The nonlinear control law is then developed based on an on-line projection of the steerable control-point P on the desired path. Since the vehicle model is not linearized for small angles, limitations such as low speed or smooth curvature are not imposed on the desired path through the control law development process. In addition, using the lateral-offset as defined and engaging one output to cancel the lateral error , the vehicle speed can be controlled independently from vehicle lateral-offset tracking. The robustness of the scheme under discontinuous variation of the desired speed has been verified by simulation.

For future work; the scheme should be applied on a more complete vehicle model with several degrees of freedoms which includes tire models, a model of aerodynamic and friction forces, and suspension. Also, system robustness under uncertainties of parameters or noise in measurements can be verified toward in order to complete the proposed linear feedback compensator. Another perspective is the path planning problem of point P from the desired path associated to a point fixed on the vehicle main body.

ACKNOWLEDGMENTS

The authors wish to acknowledge our appreciation of the NSERC for their financial support under grant OGP0138153.

Appendix

The mobile robot parameters and the constants used in the dynamic e.o.m.'s, eq. (3), are:

$\rho = 0.33\ m$ $\quad l_1 = 1.41\ m$ $\quad l_a = l_1 - l_2 = 2.82\ m$

$I_{C3} = 0.1455\ kg.m^2$ $\quad I_{C1} = 0.1\ kg.m^2$ $\quad I_{A3} = 2232\ kg.m^2$

$m_A = 1416\ kg$ $\quad m_C = 5\ kg$ $\quad L_p = 1\ m$

$K_1 = \rho / l_a$ $\quad K_2 = l_1^2 - 2 l_a l_1$ $\quad K_3 = K_1^2 K_2$

$K_4 = K_1 I_{C3}$ $\quad K_5 = K_3 m_A$ $\quad K_6 = K_1^2 (I_{C3} - I_{A3})$

$K_7 = I_{C1} + \rho^2 (m_A - m_C)$ $\quad K_8 = K_1^2 m_A l_1 (l_1 - 2 l_a) - K_6$ $\quad K_9 = K_5 - K_6$

$K_{10} = -K_4^2 - K_9 I_{C3}$ $\quad K_{11} = I_{C3} K_7$ $\quad K_{12} = K_4 (K_8 - K_9)$

$K_{13} = -K_4 K_7$ $\quad K_{14} = K_4^2 - K_8 I_{C3}$ $\quad K_{15} = l_1 - la$

$K_{16} = l_1 / la$ $\quad K_{17} = 1 / la$ $\quad \hat{K}_1 = K_1 I_{C3}$

$\hat{K}_2 = K_1^2 (I_{C3} - I_{D3} - I_{A3})$ $\quad \hat{K}_3 = \rho^2 m_C - I_{C1}$ $\quad \hat{K}_4 = \rho^2 m_D - I_{D1}$

$\hat{K}_5 = K_{17}^2$ $\quad \hat{K}_6 = \rho^2 m_A$ $\quad \hat{K}_7 = \rho^2 (m_C + m_A) + I_{C1} + K_2$

$\hat{K}_8 = \hat{K}_3 + \hat{K}_4 + \hat{K}_6$ $\quad \hat{K}_9 = \hat{K}_2 + \hat{K}_3 + \hat{K}_5 \hat{K}_6$ $\quad \hat{K}_{10} = \hat{K}_8 I_{C3}$

$\hat{K}_{11} = I_{C3} \hat{K}_9 + \hat{K}_1^2$ $\quad \hat{K}_{12} = -\hat{K}_1 \hat{K}_8$ $\quad \hat{K}_{13} = -\hat{K}_1 (\hat{K}_9 + \hat{K}_7)$

$\hat{K}_{14} = \hat{K}_1^2 + I_{C3} \hat{K}_7$ $\quad \hat{K}_{15} = K_1 L_p$

The nonlinear functions in equations (6) and (8) are:

$f_1 = (K_{12} \sin^2 x_1 + K_{13}) \cos x_1 / \det M$ $\quad \hat{f}_1 = (\hat{K}_{12} + \hat{K}_{13} \tan^2 x_1)(1 + \tan^2 x_1) / \det \hat{M}$

$f_2 = K_{14} \sin x_1 \cos x_1 / \det M$ $\quad \hat{f}_2 = \hat{K}_{14} \tan x_1 (1 + \tan^2 x_1) / \det \hat{M}$

$g_1 = (K_9 \sin^2 x_1 + K_7) / \det M$ $\quad \hat{g}_1 = (\hat{K}_8 + \hat{K}_9 \tan^2 x_1) / \det \hat{M}$

$g_2 = K_4 \sin x_1 / \det M$ $\quad \hat{g}_2 = \hat{K}_1 \tan x_1 / \det \hat{M}$

$g_3 = I_{C3} / \det M$ $\quad \hat{g}_3 = I_{C3} / \det \hat{M}$

where $\det M = (K_{10}\sin^2 x_1 - K_{11})$ and $\det \hat{M} = (\hat{K}_{11}\tan^2 x_1 - \hat{K}_{10})$ are respectively the mass matrix determinant for FWD and RWD mobile robots. The functions used in the design of the controller are:

$$h_1(\boldsymbol{x}) = K_{17}(1 - \tan^2 x_1)[2x_2^2 \tan x_1 - f_1 x_2 x_4]$$

$$h_2(\boldsymbol{x}) = \rho x_4 x_2 [f_2 \cos x_1 - \sin x_1]$$

$$M_1 = \rho \cos(x_1 - x_7) - L_p K_1 \sin x_1 \sin(x_1 + x_7)$$

$$M_2 = -\rho \sin(x_1 - x_7) - L_p K_1 \sin x_1 \cos(x_1 + x_7)$$

$$\hat{M}_1 = \rho \cos(x_1 - x_7)/\cos x_1 - \hat{K}_{15} \tan x_1 \sin(x_1 - x_7)$$

$$\hat{M}_2 = -\rho \sin(x_1 - x_7)/\cos x_1 - \hat{K}_{15} \tan x_1 \cos(x_1 - x_7)$$

$$N_1 = \hat{N}_1 = -L_p \cos(x_1 - x_7) \qquad N_2 = \hat{N}_2 = -L_p \sin(x_1 - x_7)$$

$$I_{11} = M_1 g_2 + N_1 g_1 \qquad I_{12} = M_1 g_3 - N_1 g_2$$

$$I_{21} = M_2 g_2 + N_2 g_1 \qquad I_{22} = M_2 g_3 - N_2 g_2$$

The terms $\hat{I}_{ij}$ $(i = 1,2\ j = 1,2)$ are exactly the same as the above I_{ij} terms if hat symbol is added to all M, N and g terms. The elements in equation (18) are:

$$\psi_1 = \hat{\psi}_1 = h_1 \sin\alpha - h_2 \cos\alpha$$

$$\psi_2 = \hat{\psi}_2 = -\frac{1}{R_c}(h_1 \Delta x + h_2 \Delta y) - \frac{1}{R_c^3}[\Delta y(N_1 x_2 - M_1 x_4) + \Delta x(N_2 x_2 - M_2 x_4)]^2$$

$$\psi_3 = -\rho(\sin x_1 - f_2) x_2 x_4 \qquad \hat{\psi}_3 = \rho f_2 x_2 x_4$$

$$\zeta_1 = I_{11} \sin\alpha + I_{21} \cos\alpha \qquad \zeta_2 = I_{12} \sin\alpha + I_{22} \cos\alpha$$

$$\zeta_3 = -\frac{1}{R_c}(I_{11} \Delta x + I_{21} \Delta y) \qquad \zeta_4 = -\frac{1}{R_c}(I_{12} \Delta x + I_{22} \Delta y)$$

$$\zeta_5 = \rho g_2 \cos x_1 \qquad \zeta_6 = \rho g_3 \cos x_1$$

where $\Delta x = x_p - x_B$, $\Delta y = y_p - y_B$ and $R_c = \sqrt{\Delta x^2 + \Delta y^2}$

References

[1] A. Astolfi, "Exponential Stabilization of a Car-like Vehicle", IEEE International Conference on Robotics and Automation, 0-7803-1965-6/95, pp.1391-1396, 1995.

[2] G. Campion, G. Bastin and B. Andrea-Novel, "Structural Properties and Classification of Kinematic and Dynamic Models of Wheeled Mobile Robots", IEEE Transactions on Robotics and Automation, vol. 12, no.1, pp. 47-62, 1996 .

[3] B. D'Andréa-Novel, G. Campion And G. Bastin,, "Control of Nonholonomic Wheeled Mobile Robots by State Feedback Linearisation", The International Journal of Robotic Research, vol. 14, no. 6, pp. 543-559, 1995.

[4] Z. Deng, M. Brady, "Dynamic Tracking of a Wheeled Mobile Robot, International Conference on Intelligent Robots and Systems", Part 2, pp. 1295-1298, 1993.

[5] R.M. DeSantis, "Path- tracking for car-like robots with single and double steering", IEEE Transactions on Vehicular Technology vol. 44 no. 2, pp. 366-377, 1995.

[6] G. Desaulniers and F. Soumis, "An Efficient algorithm to find a shortest path for a car-like robot ", IEEE Transactions on Robotics and Automation, vol. 11 no. 6, pp. 819-828., Dec. 1995.

[7] S. Jagannathan, S.Q. Zhu and F.L. lewis, "Path planning and control of a mobile base with nonholonomic constraints", Robotica, vol. 12, pp. 529-539, 1994.

[8] T.R. Kane and D.A. Levinson, "Dynamics Theory and Applications", McGraw-Hill Series in Mechanical Engineering, New York, ISBN 0-07-037846-0, chapters 1-7, 1985.

[9] A. Micaelli, C. Samson "Trajectory Tracking for Two-Steering-Wheeled Mobile Robots " IFAC 1994 Symposium on Robotic Control (SYROCO'94), Capri, Italy, pp. 218-224, 1994.

[10] A. Ollero, And G. Heredia "Stability Analysis of Mobile Robot Path Tracking", proceeding of the IEEE International Conference on Intelligent Robots, vol. 3, pp.461-466, 1995.

[11] C. Samson, "Control of Chained Systems Application to Path Following and Time-varying Point-Stabilization of Mobile Robots", IEEE Transactions on Automatic Control vol. 40, no.1, pp. 64-77, 1995.

[12] N. Sarkar, X. Yun and V. Kumar, "Control of Mechanical Systems with Rolling Constraints: Application to Dynamic Control of Mobile Robots", International Journal of Robotics Research, vol. 13, no. 1, pp. 55-69, 1994.

[13] O.J. Sordalen and C. Canudas de Wit, "Path following and Stabilization of a Mobile Robot, IFAC Nonlinear Control Systems Design, Bordeaux, France, pp. 471-476, 1992.

[14] P. Souères And J.P. Laumond "Shortest Path Synthesis for a Car-like Mobile Robot", IEEE Transaction on Automatic Control, vol. 41, no. 5, pp. 672-689, 1996.

[15] J.J. Slotine and W. Li, "Applied Nonlinear Control", ISBN 0-13-040890-5, Prentice-Hall, 1991.

[16] O.J. Sordalen, C. Canudas de Wit, "Exponential control law for a mobile robot: extension to path following", IEEE Transactions on Robotics and Automation vol. 9, no. 6, pp. 837-842, Dec 1993.

[17] A. Tayebi, M. Tadjine And A. Rachid, "Path Following and Point-Stabilization Control Laws for a Wheeled Mobile Robot", IEEE Proceeding of the 1996 UKACC International Conference on Control, part 2 no. 427/2, 1996.

List of figures:

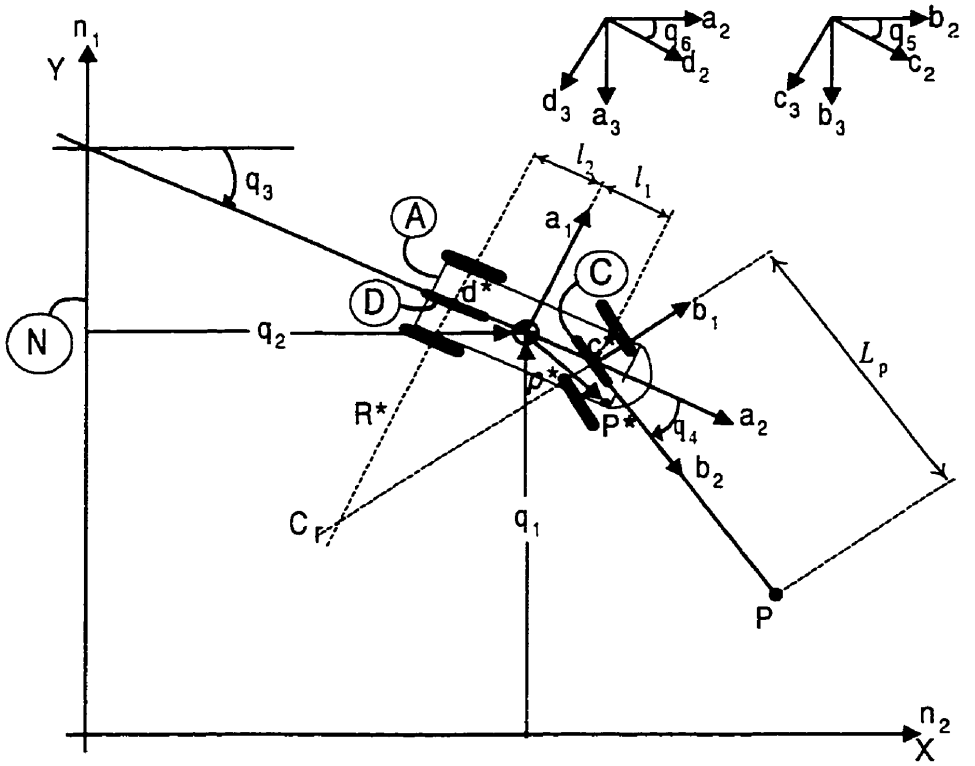

Figure 1 - Planar car-like mobile robot with steerable control-point P.

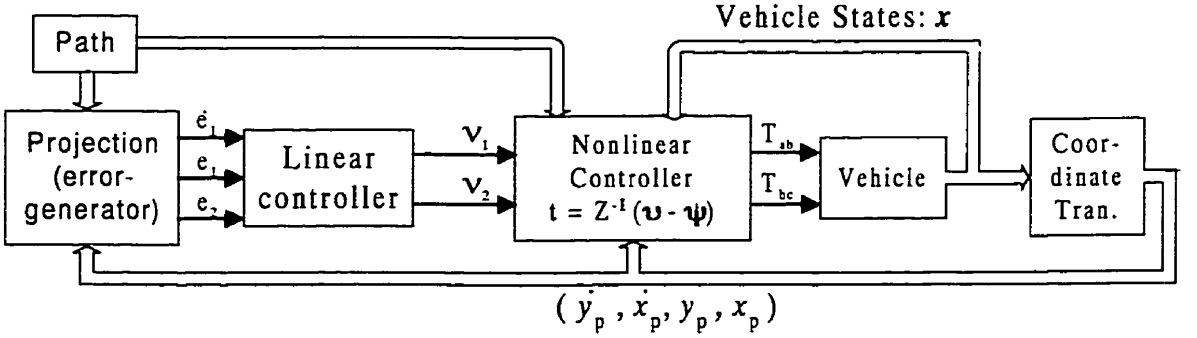

Figure 2 - Architecture of the lateral-offset tracking and speed control algorithm.

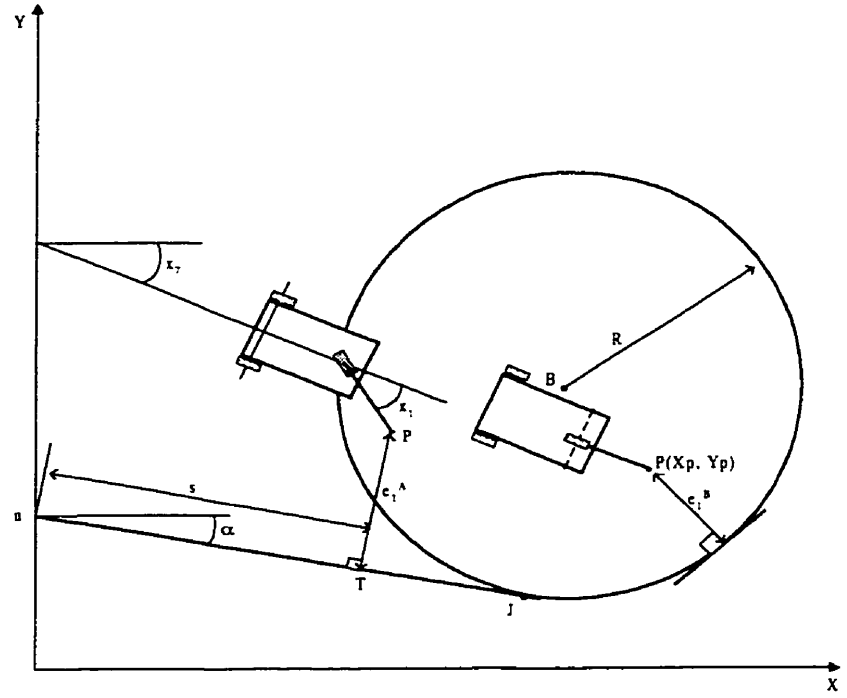

Figure 3 - Geometric lateral error definition for linear and circular arc segments.

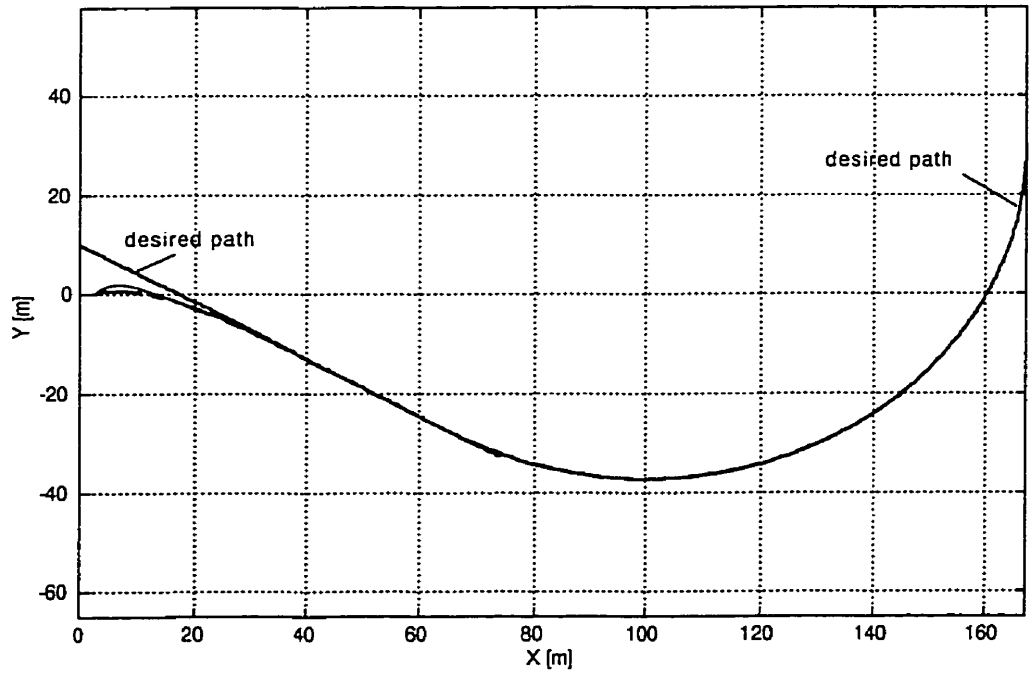

Figure 4 - Lateral-offset tracking of a path with two segments.

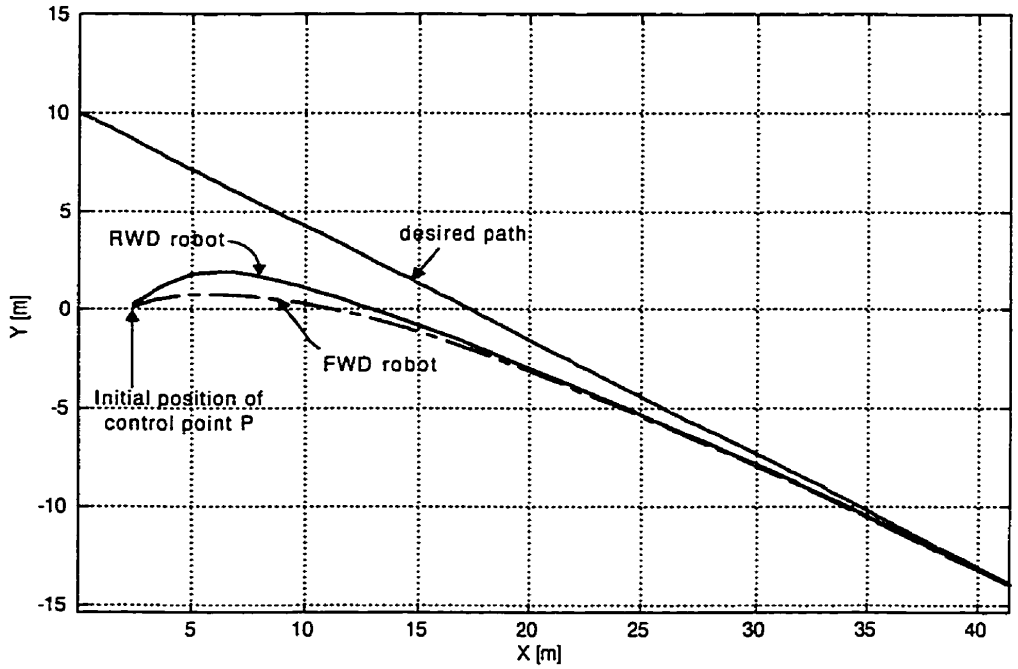

Figure 5 - Zoom of the lateral-offset tracking in the Cartesian space.

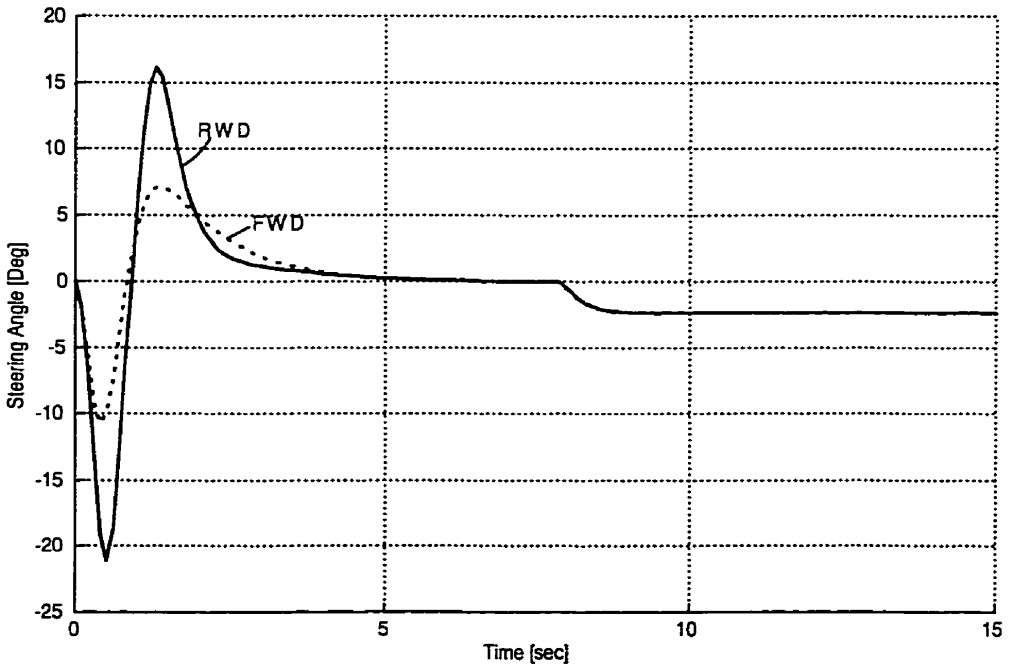

Figure 6 - Time variation of the steering angle.

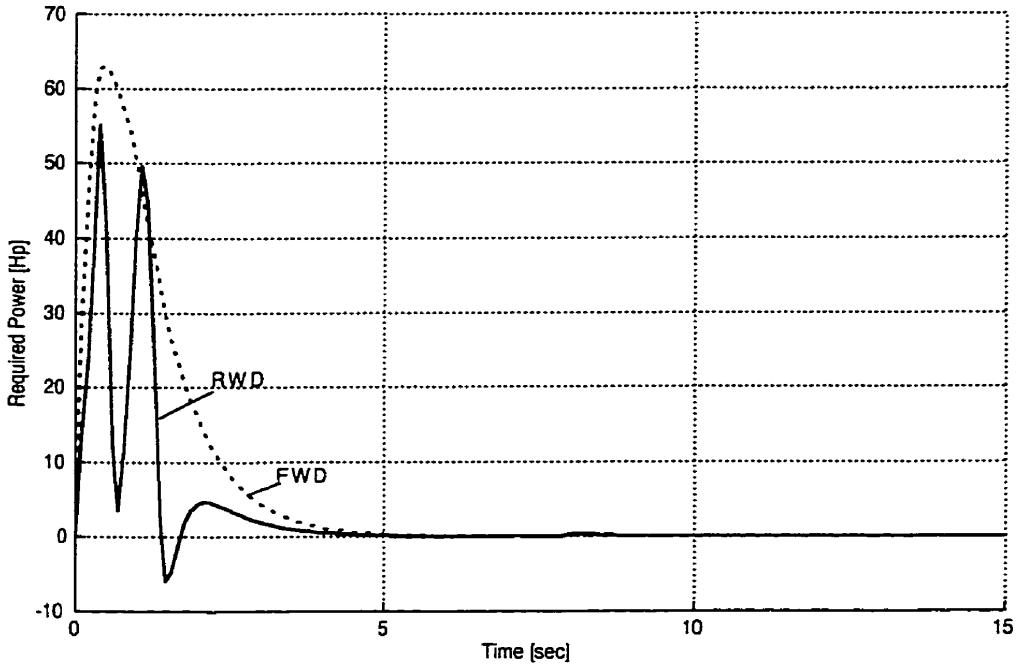

Figure 7 - Time variation of the required power.

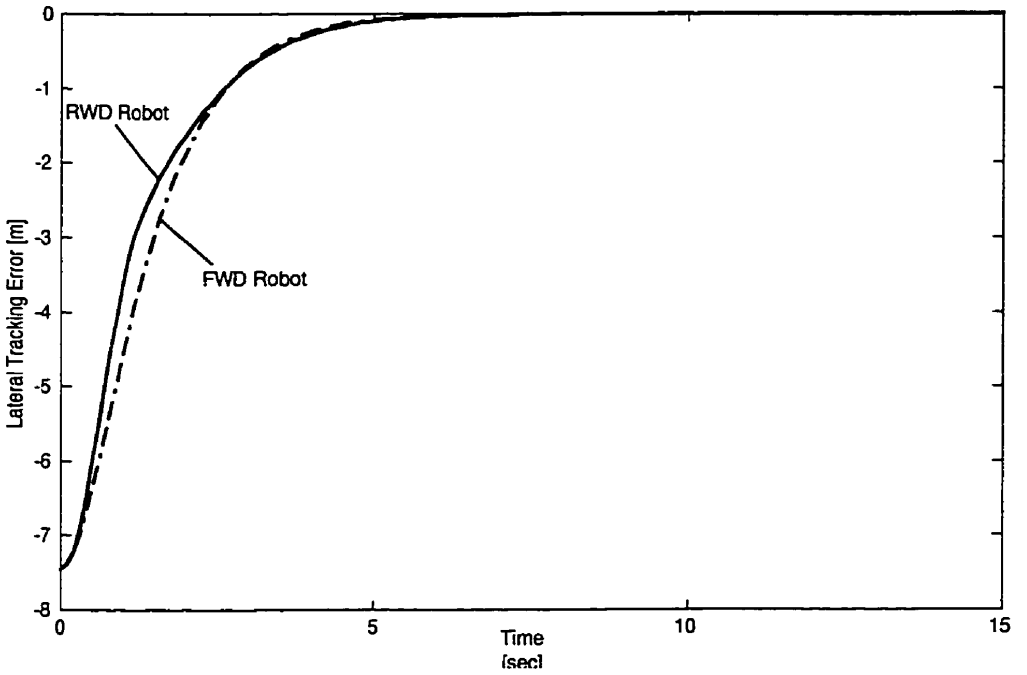

Figure 8 - Variation of the lateral error for both vehicles.

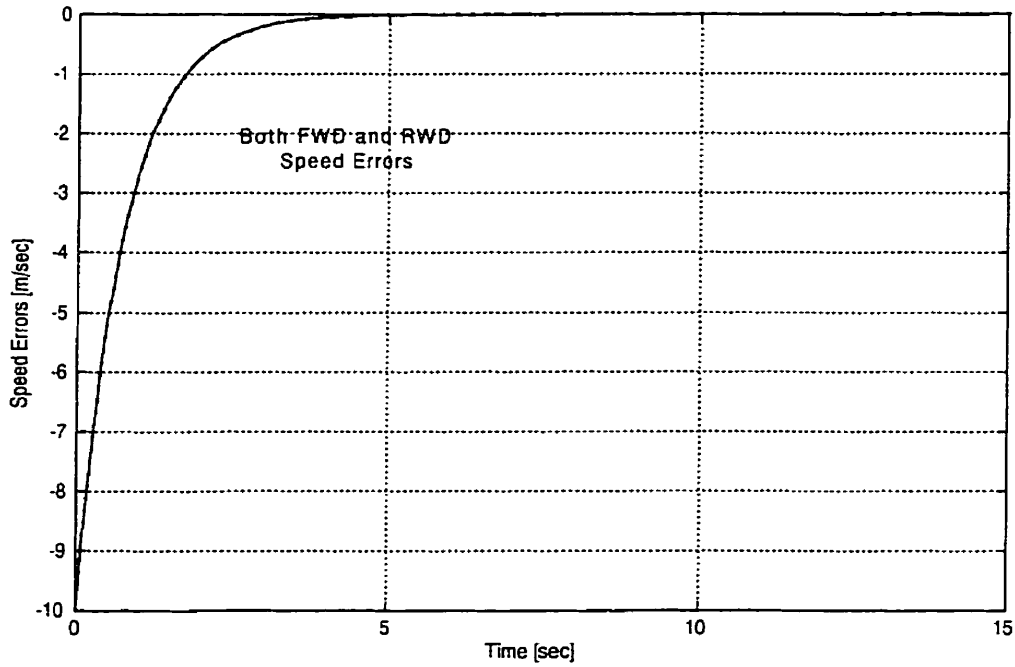

Figure 9 - Time variation of the speed error for both vehicles.

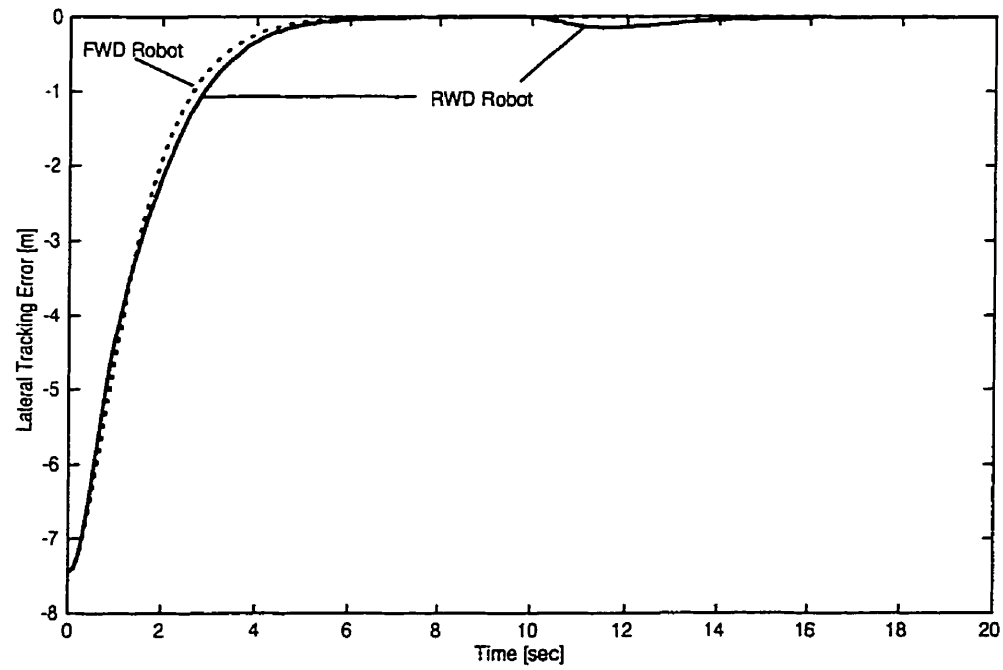

Figure 10 - Lateral error deviation with discontinuous change in desired speed.

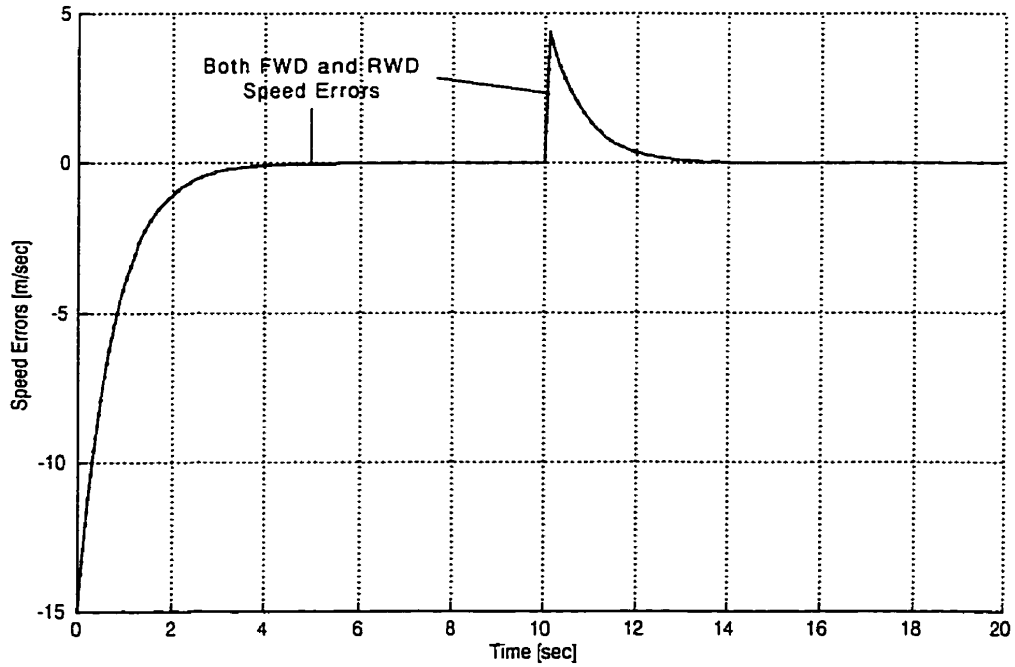

Figure 11 - Time variation of the speed error with discontinuous change in desired speed.

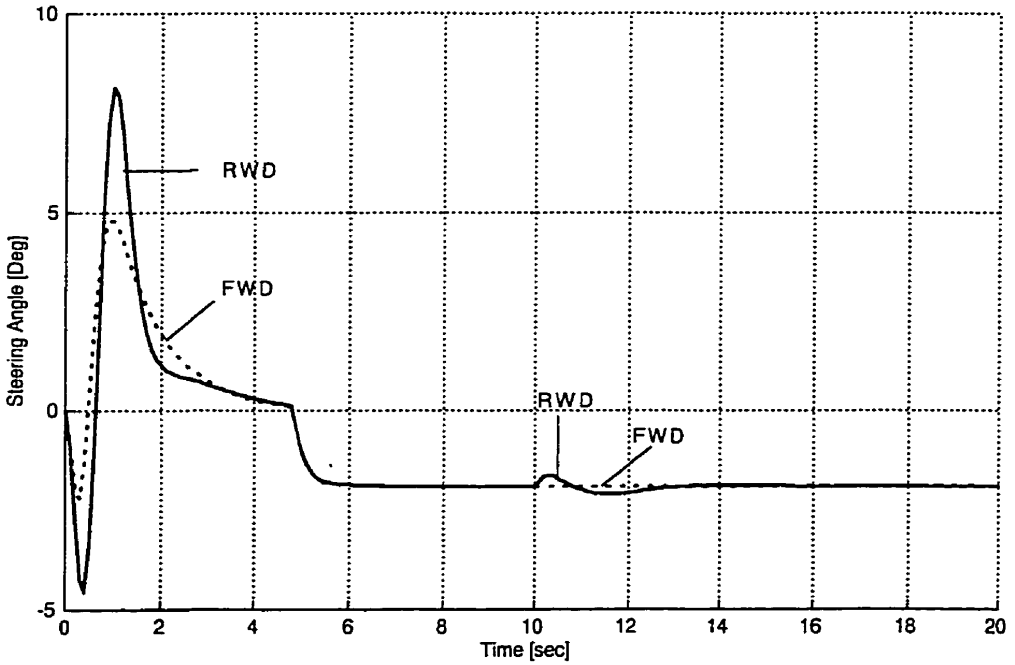

Figure 12 - Time variation of the steering angle for tracking with a discontinuous change in the desired speed.

Appendix D: Equations of Motion of a Car-like Robot using Autolev[2] programing

[2] Autolev is a software based on Dynamics: Theory and Application (Kane, 1985)

Introduction

A step by step development of a dynamic equations of motion (e.o.m) is presented here for a car-like mobile robot. This e.o.m. has been used as the base of the control law developments in all three papers of appendices A, B and C. I address readers, who are not familiar with the Kane method of development, to "Dynamics: Theory and Applications" by Kane and Levinson.

As mentioned in literature survey, enough efforts have been done in modeling the dynamic behavior of ground vehicles. Complete vehicle models with pneumatic and suspension are suitable for the study of vehicle handling, suspension time responses, etc. To study the reactions of a vehicle to different driver commands, or in reverse to develop a controller that reproduces the driver reactions, a dynamic model that only includes concerned DOFs must be in hand. Therefore, it is essential to develop a dynamic vehicle model which has a simple mathematical structure and which includes the planar generalized coordinates, i.e. essential coordinates to model the behavior of the vehicle playing a role in vehicle lateral (steering) and longitudinal (speed) control.

Here, a simple vehicle model is developed to be used as the basic dynamic element of the further control law developments. Some hypothesis are considered to simplify the equations. First assumption is to study car movements in a two dimensional space, here defined as *planar* movements. This assumption is justified easily, first, variations of rolling and pitching angles and vertical movement of the vehicle in most of driving cases are small enough in

comparison with the variation of the vehicle planar configuration, second, the desired path is well generated in two dimension for both lateral and longitudinal control aspects. The second assumption is the kinematic constraint of slippage-free contact between front wheel and road. This condition is true for most of driving cases and is translated to kinematic *nonholonamic constraints*.

Kinematics

Using the generalized coordinates of appendix A, the generalized speeds, i.e. the arbitrary combination of the generalized coordinates derivations, are selected as:

$$
\begin{aligned}
u_1 &= \dot{q}_4 \\
u_2 &= \dot{q}_5 \\
u_3 &= \cos(q_2 - q_3)\dot{q}_1 - q_1 \sin(q_2 - q_3)\dot{q}_2 \\
u_4 &= \sin(q_2 - q_3)\dot{q}_1 - q_1 \cos(q_2 - q_3)\dot{q}_2 \\
u_5 &= \dot{q}_3
\end{aligned}
$$

then, the angular velocity of the vehicle rigid bodies (A, B, C) and the linear velocity of each center of mass A^*, B^*, C^* are:

$$
\begin{aligned}
{}^N\omega^A &= u_5 \bar{a}_3 \\
{}^N\omega^C &= (u_1 - u_5)\bar{a}_3 \\
{}^N v^{A^*} &= u_3 a_1 + u_4 \bar{a}_2 \\
{}^N v^{C^*} &= (-l u_5 + u_3)\bar{a}_1 + u_4 \bar{a}_2 \\
{}^N v^{\hat{C}} &= (-l u_5 + u_3 + \rho \sin\delta u_2)\bar{a}_1 + (u_4 - \rho \cos\delta u_2)\bar{a}_2
\end{aligned}
$$

The slippage free condition, of the point of contact between front wheel and road, in both lateral and longitudinal directions results in three nonholonomic equations of constraint. At

this condition, the angular velocity of the vehicle will become a function of the front wheel speed and the steering angle in an arbitrary Newtonian reference frame *N*, i.e. ${}^{N}\bar{\omega}^{A} = f(u_2, q_4)$, and the velocity of the contact point between front wheel and road becomes zero, i.e. ${}^{N}\bar{v}^{\hat{C}} = 0$. These velocity constraints are equal to the following scalar equations:

$$u_3 = (\frac{l}{L} - 1)\rho u_2 \sin q_4$$
$$u_4 = \rho u_2 \cos q_4$$
$$u_5 = \frac{\rho}{L} u_2 \sin q_4$$

The above velocity constraint equations should replace in the velocity terms and the results should be differentiated in the Newtonian reference frame *N* in order to find the linear and angular acceleration of vehicle bodies. This is a mathematical routine of substitution and derivation that can be done by Atolev software. The following step by step computer program is written to this end:! The model has five generalized coordinates and three equations of constraints:

DOF(2,5)

N is a the default frame that moves on the road and which is our local Newtonian reference frame for the vehicle motions. *A* is the car main body frame, *B* is a massless frame fixed on the front wheel center of rotation and *C* is the wheel reference frame:

FRAMES(A,B,C)

MASSLESS(B)

MASS(A,MA,C,MC)

```
POINTS(CHAT)
```

An assumption here is that all frames coincide the principal inertial axis of bodies:

```
PRINCIPAL(A,C)

CONST(L1,L2,RO,La)

VAR(Q1,Q2,Q3,Q4,Q5)

SPECIFIED(S23,C23,S4,C4)

S3=SIN(Q3)

C3=COS(Q3)

S4=SIN(Q4)

C4=COS(Q4)

S5=SIN(Q5)

C5=COS(Q5)

SIMPROT(N,A,3,Q3)

DIRCOS(N,A,C3,-S3,0,S3,C3,0,0,0,1)

SIMPROT(A,B,3,Q4)

DIRCOS(A,B,C4,-S4,0,S4,C4,0,0,0,1)

SIMPROT(B,C,1,Q5)

DIRCOS(B,C,1,0,0,0,C5,-S5,0,S5,C5)

DIRCOS(A,C)

DIRCOS(N,B)

DIRCOS(N,C)

Q1'=COS(Q3)*U3-SIN(Q3)*U4
```

```
Q2'=SIN(Q3)*U3+COS(Q3)*U4

Q3'=U5

Q5'=U2

Q4'=U1

WAN=Q3'*A3

WBA=Q4'*A3

WCB=Q5'*B1

WBN=ADD(WAN,WBA)

WCA=ADD(WBA,WCB)

WCN=ADD(WBN,WCB)

VASTARN=U3*A1+U4*A2

VCSTARA=-L1*Q3'*A1

VCSTARN=ADD(VASTARN,VCSTARA)

VCHATB=-RO*Q5'*(-S4*A1+C4*A2)

VCHATA=ADD(VCSTARA,VCHATB)

VCHATN=ADD(VASTARN,VCHATA)
```

The equations of constraints are come from having no lateral or longitudinal slippage. The angular velocity of body *A* in the reference frame *A* is calculated and the first equation of constraint is extracted:

```
U5=RO*Sd*U2/La
```

Also the velocity of CHAT in reference frame N is zero in both directions :

```
U4=RO*Cd*U2
```

U3=L1*RO*SD*U2/LA-RO*SD*U2

CONSTRAIN

Dynamics

The objective of the dynamic analyses is to find the e.o.m. of the car-like robot. This is a very straight forward but time consuming step toward a unique solution which justifies the use of the computer code generator Autolev. The rest of commands are then:

ALFAN=DERIV(WAN,T,N)

ALFBN=DERIV(WBN,T,N)

ALFCN=DERIV(WCN,T,N)

AASTARN=DERIV(VASTARN,T,N)

ACSTARN=DERIV(VCSTARN,T,N)

ACHATN=DERIV(VCHATN,T,N)

FRSTAR

TORQUE(B/C)=TBC*B1

TORQUE(A/B)=TAB*B3

FR

KANE

The final result of this program are two dynamic e.o.m.. The derived equations of motion are manually simplified as far as it was possible and they represented in the matrix form of:

$$\boldsymbol{M\ddot{Q}} - \boldsymbol{C^*} = \boldsymbol{T}$$

with

$$M = \begin{bmatrix} Ic_\delta & k_4 \sin q_4 \\ k_4 \sin q_4 & k_5 \sin^2 q_4 - k_6 \sin q_4 - k_7 \end{bmatrix} \quad C^* = \begin{bmatrix} k_4 \cos q_4 \\ k_8 \sin q_4 \cos q_4 \end{bmatrix} \dot{q}_4 \dot{q}_5 \quad T = \begin{bmatrix} T_{AB} \\ T_{BC} \end{bmatrix}$$

where K_1 to K_8 are the constants representing the vehicle characteristics. This compact equation has the vector of torque inputs at right and the rigid body dynamics of the system at left. This is the conventional form of representing dynamics of manipulator robots.

Finally, these equations have been transformed to the state space for the control purpose. The final state equations of motion are given as:

$$\dot{x}_i = f(x_k) + g(x_1) T_{ab} + h(x_1) T_{bc}$$
$$\dot{x}_j = f(x_m)$$

The first series of the state equations with (i = 1,2,3,4) are the equations of motion of the rested two DOFs after applying the motion constraints and the second series with (j = 1,2,3) are the velocity constraints transformed to the state space. In these equations (k = 1,2,3,4) and (m = 1,2,3) are the floating state variables. The state space representation is given because it facilitates the understanding of the steps made toward the control law design and it is the normal form seen in the literature.